ISSN 1881-7831 Online ISSN 1881-784X

DD&T

Drug Discoveries & Therapeutics

Volume 9, Number 4
August, 2015

IRCA BSSA

IACMHR

www.ddtjournal.com

DD&T
Drug Discoveries & Therapeutics

ISSN: 1881-7831
Online ISSN: 1881-784X
CODEN: DDTRBX
Issues/Year: 6
Language: English
Publisher: IACMHR Co., Ltd.

Drug Discoveries & Therapeutics is one of a series of peer-reviewed journals of the International Research and Cooperation Association for Bio & Socio-Sciences Advancement (IRCA-BSSA) Group and is published bimonthly by the International Advancement Center for Medicine & Health Research Co., Ltd. (IACMHR Co., Ltd.) and supported by the IRCA-BSSA and Shandong University China-Japan Cooperation Center for Drug Discovery & Screening (SDU-DDSC).

Drug Discoveries & Therapeutics publishes contributions in all fields of pharmaceutical and therapeutic research such as medicinal chemistry, pharmacology, pharmaceutical analysis, pharmaceutics, pharmaceutical administration, and experimental and clinical studies of effects, mechanisms, or uses of various treatments. Studies in drug-related fields such as biology, biochemistry, physiology, microbiology, and immunology are also within the scope of this journal.

Drug Discoveries & Therapeutics publishes Original Articles, Brief Reports, Reviews, Policy Forum articles, Case Reports, News, and Letters on all aspects of the field of pharmaceutical research. All contributions should seek to promote international collaboration in pharmaceutical science.

Editorial Board

Editorial and Head Office:

Pearl City Koishikawa 603,
2-4-5 Kasuga, Bunkyo-ku,
Tokyo 112-0003, Japan
Tel.: +81-3-5840-9697
Fax: +81-3-5840-9698
E-mail: office@ddtjournal.com

Drug Discoveries & Therapeutics

Editorial and Head Office

Pearl City Koishikawa 603, 2-4-5 Kasuga, Bunkyo-ku,
Tokyo 112-0003, Japan

Tel: +81-3-5840-9697, Fax: +81-3-5840-9698
E-mail: office@ddtjournal.com
URL: www.ddtjournal.com

Editorial Board Members

CONTENTS

Volume 9, Number 4, 2015

Reviews

Original Articles

Mini-Review

DOI: 10.5582/ddt.2015.01052

Usefulness of silkworm as a model animal for understanding the molecular mechanisms of fungal pathogenicity

Masaki Ishii, Yasuhiko Matsumoto, Kazuhisa Sekimizu*

Laboratory of Microbiology, Graduate School of Pharmaceutical Sciences, The University of Tokyo, Tokyo, Japan.

Summary ***Candida albicans*, *Candida tropicalis*, *Candida grabrata*, and *Cryptococcus neoformans* are causative pathogens of opportunistic diseases in immunocompromised human patients. Silkworms are killed by injection of these pathogenic fungi into their hemolymph. In this paper, we describe recent results by our laboratory and other researchers using gene-deficient strains of these pathogenic fungi. The silkworm is considered to be a useful model animal for understanding the pathogenicity of these fungi. Silkworms are also beneficial for evaluating therapeutically active anti-fungal reagents.**

Keywords: Fungi, silkworm, infectious disease

1. Introduction

Pathogenic fungi cause serious infectious diseases, such as pneumonia, in humans. Older persons, HIV-infected patients, and patients undergoing treatment with immunosuppressive therapies are particularly susceptible to fungal infections. Pathogenic fungi have various virulence factors that are required for their survival in host environments. The expression of virulence factors in fungi seems to be regulated in response to the host environments. Understanding the molecular mechanisms of pathogenicity by fungi will help to establish effective therapeutic strategies for fungal infection.

In general, animal models mimicking human infectious diseases are used to identify virulence factors in pathogens. Mice are widely used as a model animal for fungal infections (*1*). The use of large numbers of mammalian animals, however, is costly and associated with ethical issues regarding animal welfare. To address these problems, we propose the use of silkworms as an animal model to study human pathogens (*2-4*). The cost to purchase and rear silkworms is much lower than that of mice, and the use of silkworms avoids the ethical problems of killing mammals. We previously reported silkworm-infection model of *Staphylococcus aureus*, which causes opportunistic diseases in humans (*5-9*). We recently demonstrated that the silkworm *S. aureus* infection model was useful for discovering novel antibiotics effective in a mouse model (*5,6*). Moreover, disruption mutants of *S. aureus* with attenuated killing abilities in silkworms exhibited less pathogenicity than wild-type strains in mice (*7-9*). Silkworms are killed by injection of *Candida albicans* (*10,11*), *Candida tropicalis* (*10*), *Candida grabrata* (*12*), or *Cryptococcus neoformans* (*13*). Therefore, the silkworm seems to be a suitable animal model for identifying genes of bacteria and fungi responsible for the expression of pathogenicity. In this mini review, we describe recent findings in silkworm infection models of each pathogenic fungus.

2. Silkworm-fungal infection models

2.1. *Candida albicans*

C. albicans is frequently isolated from patients with fungal infection. We previously reported that injection of *C. albicans* kills silkworms and that administration of anti-fungal drugs has therapeutic effects (*10*). The regulatory mechanisms of the pathogenesis of *C. albicans* mediated by protein kinases in *C. albicans* have been reported (*14,15*). Important roles for type 2B serine/threonine protein kinases, called the calcineurin complex CMP1 (also known as CNA1), in the pathogenicity of *C. albicans* have been demonstrated (*15*). Protein kinase SIT4 and YVH1 are also involved in the pathogenicity (*16,17*). Hanaoka *et al*. screened

**Address correspondence to:*
Dr. Kazuhisa Sekimizu, Laboratory of Microbiology, Graduate School of Pharmaceutical Sciences, The University of Tokyo, Hongo 7-3-1, Bunkyo-ku, Tokyo 113-0033, Japan.
E-mail: sekimizu@mol.f.y-tokyo.ac.jp

virulence factors among protein kinases in *C. albicans* using the silkworm infection model (*11*). They injected 21 gene-disrupted mutants of genes encoding protein kinases into the hemolymph of silkworms, and found four gene mutants (*cmp1*, *sit4*, *yvh1*, and *ptc1*) with attenuated killing ability in silkworms (*11*). Among these genes, the pathogenicity of the *ptc1* gene had not been previously reported. Thus, this gene was first identified as a virulence gene of fungi in a study using silkworms. The *ptc1* gene-disrupted mutant exhibited low hyphae formation activity and low protease activity. Moreover, the mutant also exhibited attenuated pathogenicity in mice (*11*). The other three genes were previously shown to be associated with pathogenicity by altered expression of virulence genes in a mouse infection model (*16-18*). These findings suggest that the silkworm-*C. albicans* infection model is useful for identifying the virulence factors of *C. albicans*.

2.2. *Candida tropicalis*

C. tropicalis is a pathogenic fungus that is frequently isolated from human patients. We demonstrated that antifungal reagents have therapeutic effects in a silkworm infection model with *C. tropicalis* (*10*). *C. tropicalis* is a fungus closely related to *C. albicans*. Thus, future experiments with *C. tropicalis* gene-disrupted mutants using the silkworm fungal infection model may allow us to identify the virulence genes of the fungus.

2.3. *Candida grabrata*

C. grabrata resides in the human intestinal tract. This fungus causes opportunistic infections in patients with the metabolic diseases, such as diabetes (*19*). Ueno *et al*. screened *C. grabrata* mutants with low pathogenicity in hyperglycemic silkworms, created by feeding a high glucose diet (*20*). They demonstrated that the *cyb2* gene of *C. grabrata* is required for the pathogenicity of *C. grabrata* against hyperglycemic silkworms (*12*). In addition, a *hap2* gene mutant and *hap5* gene mutant in which the RNA level of the *cyb2* gene is decreased, exhibit less virulence in the hyperglycemic silkworm. The *cyb2* gene encodes a protein with 65% homology to lactate dehydrogenase in *Saccharomyces cerevisiae* (*12*). A *C. grabrata cyb2* deficiency mutant exhibits decreased colonization ability in the gastrointestinal tract based on a mouse model of diabetes (*12*). These findings indicate the usefulness of the silkworm infection model with *C. grabrata* for searching for virulence factors of *C. grabrata*.

2.4. *Cryptococcus neoformans*

C. neoformans is a causal microbial of severe fungal infections, such as pneumonia and encephalitis. Antifungal agents have therapeutic effects in silkworms infected with *C. neoformans* (*13*). *C. neoformans* has a characteristic capsular structure on the cell surface. The capsular structure is suggested to be required for the pathogenicity of *C. neoformans*. *C. neoformans* has at least two serotypes, serotype A and serotype D. Serotype A of the fungus has higher capsule-forming ability and higher pathogenicity in mammals than the serotype D (*21*). As in mammalian infection experiments, the *C. neoformans* serotype A exhibits higher pathogenicity in the silkworm infection model than *C. neoformans* serotype D (*13*). Furthermore, mutants of the *can*, *gpa1*, and *pka1* genes, which are required for *C. neoformans* pathogenicity in mammals, also exhibit lower virulence in silkworms. The protein encoded the cna gene is suggested to contribute to the pathogenicity *via* calcineurin signaling (*22*).

The *gpa1* gene encodes a G-protein α-subunit that contributes to the capsular formation (*23*). Protein kinase A acts downstream of Gpa1 and contributes to capsule formation (*24*). We also demonstrated that the pathogenicity of *C. neoformans* is significantly altered

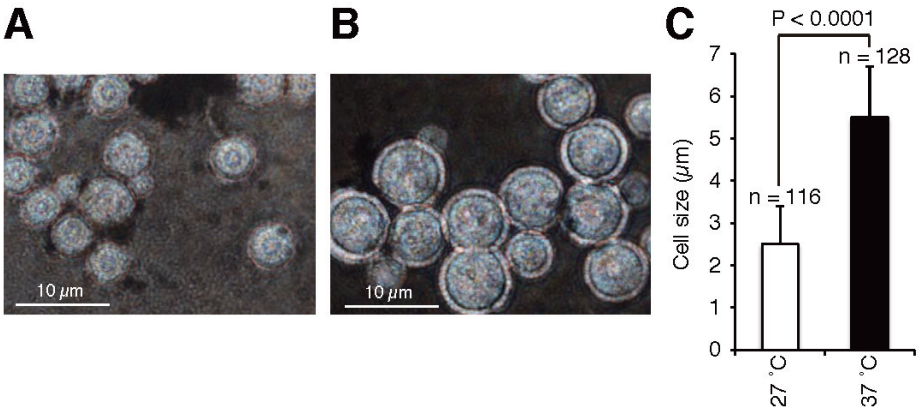

Figure 1. Effect of temperature on the capsular formation of *C. neoformans* in the hemolymph of live silkworms. Cells of *C. neoformans* were injected into the silkworm hemolymph. Twenty-four hours after injection, *C. neoformans* cells were harvested from the silkworm hemolymph, stained with Indian ink, and observed under a microscope. **(A)** Cells of *C. neoformans* in the hemolymph of silkworms reared at 27°C. **(B)** Cells of *C. neoformans* in the hemolymph of silkworms reared at 37°C. **(C)** Mean diameters of *C. neoformans* cells at 27°C and 37°C. Figures were taken from Matsumoto *et al*. (*13*).

Table 1. Virulence genes tested in the silkworm-fungal infection-model

Species	Genes	Conditions	*Ref.*
Candida albicans	*cmp1*	27°C	(*11*)
	syt4	27°C	(*11*)
	yvh1	27°C	(*11*)
	PTC1	27°C	(*11*)
Candida grabrata	*cyb2*	37°C, Diabetic	(*12*)
	hap2	37°C, Diabetic	(*12*)
	hap5	37°C, Diabetic	(*12*)
Cryptococcus neoformans	*gpa1*	37°C	(*13*)
	pka1	37°C	(*13*)
	cna1	37°C	(*13*)

by temperature; the pathogenicity of the fungi against silkworms is much stronger at 37°C than at 27°C. The capsule size and cell size of *C. neoformans* at 37°C in the silkworm hemolymph is significantly greater than that at 27°C condition (Figure 1). This finding suggests that capsule formation is required for the pathogenicity of *C. neoformans* in both silkworms and mammals. Taken together, these findings suggest that the silkworm is a suitable animal model for evaluation of the pathogenicity of *C. neoformans*.

3. Conclusions

The silkworm fungal infection model was used to evaluate the pathogenicities of four different species of fungi, *C. albicans*, *C. tropicalis*, *C. grabrata*, and *C. neoformans*. Among these pathogenic fungi, gene-disrupted mutants of pathogenic genes in *C. albicans*, *C. grabrata*, and *C. neoformans* exhibited less pathogenicity in silkworms (Table 1). In particular, strains deficient in genes encoding the intracellular signaling proteins such as protein kinases and G proteins had decreased killing ability in silkworms. In *C. albicans* and *C. grabrata*, pathogenic genes identified by screening in silkworm infection models are required for pathogenicity in mammals. Therefore, we suggest that the silkworm fungal infection model is useful for identifying the genes necessary for fungal pathogenicity in mammals.

Fungal infections, which cause opportunistic diseases, are anticipated to become a serious problem in future along with advances in medical care and increasing number of aged people in our society. Identification of virulence factors in fungi using silkworm infection models will help to elucidate the molecular mechanisms of fungal pathogenesis and facilitate the development of strategies for preventing and treating fungal infections.

References

1. Hohl TM. Overview of vertebrate animal models of fungal infection. Immunol Methods. 2014; 410:100-112.
2. Kaito C, Sekimizu K. A silkworm model of pathogenic bacterial infection. Drug Discov Ther. 2007; 1:89-93.
3. Fujiyuki T, Imamura K, Hamamoto H, Sekimizu K. Evaluation of therapeutic effects and pharmacokinetics of antibacterial chromogenic agents in a silkworm model of *Staphylococcus aureus* infection. Drug Discov Ther. 2010; 4:349-354.
4. Kaito C, Usui K, Kyuma T, Sekimizu K. Isolation of mammalian pathogenic bacteria using silkworms. Drug Discov Ther. 2011; 5:66-70.
5. Hamamoto H, Urai M, Ishii K, *et al*. Lysocin E is a new antibiotic that targets menaquinone in the bacterial membrane. Nat Chem Biol. 2015; 11:127-133.
6. Nwibo DD, Hamamoto H, Matsumoto Y, Kaito C, Sekimizu K. Current use of silkworm larvae (*Bombyx mori*) as an animal model in pharmaco-medical research. Drug Discov Ther. 2015; 9:133-135.
7. Kaito C, Kurokawa K, Matsumoto Y, Terao Y, Kawabata S, Hamada S, Sekimizu K. Silkworm pathogenic bacteria infection model for identification of novel virulence genes. Mol Microbiol. 2005; 56:934-944.
8. Kaito C, Morishita D, Matsumoto Y, Kurokawa K, Sekimizu K. Novel DNA binding protein SarZ contributes to virulence in *Staphylococcus aureus*. Mol Microbiol. 2006; 62:1601-1617.
9. Matsumoto Y, Kaito C, Morishita D, Kurokawa K, Sekimizu K. Regulation of exoprotein gene expression by the *Staphylococcus aureus cvfB* gene. Infect Immun. 2007; 75:1964-1972.
10. Hamamoto H, Kurokawa K, Kaito C, Kamura K, Manitra Razanajatovo I, Kusuhara H, Santa T, Sekimizu K. Quantitative evaluation of the therapeutic effects of antibiotics using silkworms infected with human pathogenic microorganisms. Antimicrob Agents Chemother. 2004; 48:774-779.
11. Hanaoka N, Takano Y, Shibuya K, Fugo H, Uehara Y, Niimi M. Identification of the putative protein phosphatase gene PTC1 as a virulence-related gene using a silkworm model of *Candida albicans* infection. Eukaryot Cell. 2008; 7:1640-1648.
12. Ueno K, Matsumoto Y, Uno J, Sasamoto K, Sekimizu K, Kinjo Y, Chibana H. Intestinal resident yeast *Candida glabrata* requires Cyb2p-mediated lactate assimilation to adapt in mouse intestine. PLoS One. 2011; 6:e24759.
13. Matsumoto Y, Miyazaki S, Fukunaga DH, Shimizu K, Kawamoto S, Sekimizu K. Quantitative evaluation of cryptococcal pathogenesis and antifungal drugs using a silkworm infection model with *Cryptococcus neoformans*. J Appl Microbiol. 2012; 112:138-146.
14. Yu SJ, Chang YL, Chen YL. Calcineurin signaling: lessons from Candida species. FEMS Yeast Res. 2015; 15:fov016.
15. Blankenship JR, Wormley FL, Boyce MK, Schell WA, Filler SG, Perfect JR, Heitman J. Calcineurin is essential for *Candida albicans* survival in serum and virulence. Eukaryot Cell. 2003; 2:422-430.
16. Lee CM, Nantel A, Jiang L, Whiteway M, Shen SH. The serine/threonine protein phosphatase SIT4 modulates yeast-to-hypha morphogenesis and virulence in *Candida albicans*. Mol Microbiol. 2004; 51:691-709.
17. Hanaoka N, Umeyama T, Ueno K, Ueda K, Beppu T, Fugo H, Uehara Y, Niimi M. A putative dual-specific protein phosphatase encoded by YVH1 controls growth, filamentation and virulence in *Candida albicans*. Microbiology. 2005; 151(Pt 7):2223-2232.

18. Bader T, Schröppel K, Bentink S, Agabian N, Köhler G, Morschhäuser J. Role of calcineurin in stress resistance, morphogenesis, and virulence of a *Candida albicans* wild-type strain. Infect Immun. 2006; 74:4366-4369.
19. Segireddy M, Johnson LB, Szpunar SM, Khatib R. Differences in patient risk factors and source of candidaemia caused by *Candida albicans* and *Candida glabrata*. Mycoses. 2011; 54:e39-43.
20. Matsumoto Y, Sumiya E, Sugita T, Sekimizu K. An invertebrate hyperglycemic model for the identification of anti-diabetic drugs. PLoS One. 2011; 6:e18292.
21. Lin X, Nielsen K, Patel S, Heitman J. Impact of mating type, serotype, and ploidy on the virulence of *Cryptococcus neoformans*. Infect Immun. 2008; 76:2923-2938.
22. Odom A, Muir S, Lim E, Toffaletti DL, Perfect J, Heitman J. Calcineurin is required for virulence of *Cryptococcus neoformans*. EMBO J. 1997; 16:2576-2589.
23. Alspaugh JA, Perfect JR, Heitman J. *Cryptococcus neoformans* mating and virulence are regulated by the G-protein alpha subunit GPA1 and cAMP. Genes Dev. 1997; 11:3206-3217.
24. Kozubowski L, Lee SC, Heitman J. Signalling pathways in the pathogenesis of Cryptococcus. Cell Microbiol. 2009; 11:370-380.

(Received August 6, 2015; Accepted August 11, 2015)

Review

DOI: 10.5582/ddt.2015.01015

Studies of host-pathogen interactions and immune-related drug development using the silkworm: interdisciplinary immunology, microbiology, and pharmacology studies

Kenichi Ishii[1], Hiroshi Hamamoto[2], Kazuhisa Sekimizu[2,*]

[1] *Department of Biological Sciences, Graduate School of Science, The University of Tokyo, Tokyo, Japan;*
[2] *Laboratory of Microbiology, Graduate School of Pharmaceutical Sciences, The University of Tokyo, Tokyo, Japan.*

Summary **Innate immunity acts as a front-line barrier against invading pathogens, and the majority of the components are widely conserved among species. Regulation of innate immunity is important for overcoming infections and preventing self-damaging sepsis. Using the silkworm (*Bombyx mori*) as an animal model, we elucidated the activation processes of innate immunity with emphasis on a multifunctional insect cytokine called paralytic peptide. Moreover, we established an ex vivo system using silkworm larval specimens to quantitatively evaluate the immunostimulatory activity of natural compounds. We observed that overactivation of innate immunity in silkworms induces tissue damage followed by host death, resembling sepsis-induced multi-organ failure in humans. Here, we summarize our recent findings and propose the usefulness of the silkworm as an animal model for studying immune regulation and for evaluating compounds with the potential to regulate innate immunity.**

Keywords: Innate immunity, insect cytokine, sepsis, virulence factors, antibiotics

1. Insect innate immunity

Animals continuously encounter pathogenic microorganisms throughout life. The immune system has thus evolved to overcome infection and maintain health. The immune system in higher animals is categorized as either innate or acquired. Innate immunity acts as the first-line barrier at an early stage of infection and sends signals to alert the acquired immune system, which produces specific antibodies. Rapid and coordinated activation of innate immunity is vital to prevent the growth of microorganisms. Therefore, understanding the regulatory mechanisms underlying innate immunity is crucial in terms of medical treatment and drug development for infectious diseases in humans.

Released online in J-STAGE as advance publication April 10, 2015.

*Address correspondence to:
Dr. Kazuhisa Sekimizu, Laboratory of Microbiology, Graduate School of Pharmaceutical Sciences, The University of Tokyo. 7-3-1 Hongo, Bunkyo-ku, Tokyo 113-0033, Japan.
E-mail: sekimizu@mol.f.u-tokyo.ac.jp

Recent studies revealed that most components of innate immunity are widely conserved from mammals to insects (*1*). Insects possess relatively simple physiologic systems and, because they lack antibody-producing organs, rely solely on innate immunity. This makes insects a suitable model for studying the basis of innate immunity. A representative insect-oriented immunologic study is the discovery of Toll in *Drosophila*, which led to the identification of mammalian Toll-like receptors. Insect Toll functions as a receptor for an endogenous ligand called Spaetzle and relays signals to transcription factors that produce antimicrobial peptides (AMPs) (*2*). Genomic studies revealed that insects possess several isotypes of the toll gene, and the repertoire and activation pattern varies among species. The silkworm (*Bombyx mori*) has 12 toll isotypes, some of which are expressed several hours after pathogen infection (*3,4*). Batteries of signaling molecules mediate the Toll pathway, which are also self-induced together with AMPs (*5-9*). In addition, infectious stimuli activate other innate immune pathways, such as IMD (*10*), JNK (*11*), and JAK/STAT (*12*), to act in concert with the Toll pathway (*13*). The production processes of AMPs and other toxic substances in the cell-free system (*e.g.*,

melanization) are referred to as humoral immunity, whereas immunosurveillence hemocytes are involved in cellular immunity, such as engulfment and clearance of non-self agents (*e.g.*, phagocytosis and encapsulation) (*14*). Appropriate regulation of the time and degree of immunoactivation is crucial to achieve efficient host protection against infectious pathogens. Our understanding of the regulatory mechanisms in insect innate immunity, however, remains insufficient at the molecular level, relative to that of individual responses.

2. Activation of innate immunity by the insect cytokine, paralytic peptide, in silkworms

As described below, we established an alternative infection model using the silkworm as a host animal to evaluate the effectiveness of antibiotics (*15*) and to analyze the virulence mechanisms of pathogenic bacteria (*16*). In the course of our studies using the silkworm infection model, we observed that bacteria-infected larvae were paralyzed, accompanied by slow muscle contraction (*17*). This paralysis was apparently different from the rapid and direct stimulation of muscle contraction by neurotransmitter-like substances (*18*), but very similar to that caused by an endogenous cytokine-like factor named paralytic peptide (PP). PP was originally identified as the factor responsible for paralysis caused by "blood donation" between silkworms; larvae injected with hemolymph isolated from another silkworm exhibit slow paralysis (*19*). PP was initially transcribed as a 14-kDa inactive precursor, and the N-terminus 23 amino acid residues are cleaved by proteolysis to generate the active form of PP in the stimulated hemolymph (*20*). Although the physiologic relevance of PP-induced paralysis was unknown at that time, we considered that PP was involved in bacteria-induced paralysis in silkworms (Figure 1A).

To test the above hypothesis, we first established an *ex vivo* assay system to quantitate the degree of paralysis by measuring the length of the larval muscle specimen after sample injection (Figure 1B). We confirmed using this system that injecting both heat-killed bacteria and a chemically synthesized active form of PP induces slow muscle contraction, which reaches a maximum after 5 to 10 min and then recovers to the basal level within 30 min (*17*). Among the microorganism-derived components, we found that peptidoglycan (PG) and beta-glucan (BG), major cell wall components of bacteria and fungi respectively, induce muscle contraction in a dose-dependent manner (*17*). In contrast, lipopolysaccharide (LPS), another bacterial component that is a potent immunostimulant, is ineffective even at high concentrations (*21*), suggesting ligand specificity. When the specimens were treated with anti-PP serum that specifically binds to PP and inhibits its biologic activities (*22*), muscle contraction caused by the bacterial PG and BG, as well as that induced by active PP, is completely suppressed (*17*). Moreover, we observed the rapid generation of active PP in the hemolymph of silkworms injected with PG and BG (*17*). These findings suggest a causative relationship between pathogen-induced paralysis and PP activation in silkworm hemolymph (Figure 1A).

The findings that bacterial and fungal cell wall components induce PP activation raise the following questions: *1*) how is PP activated? *2*) what happens after PP activation? and *3*) what is the biologic significance of the bacteria-induced PP activation? In the following

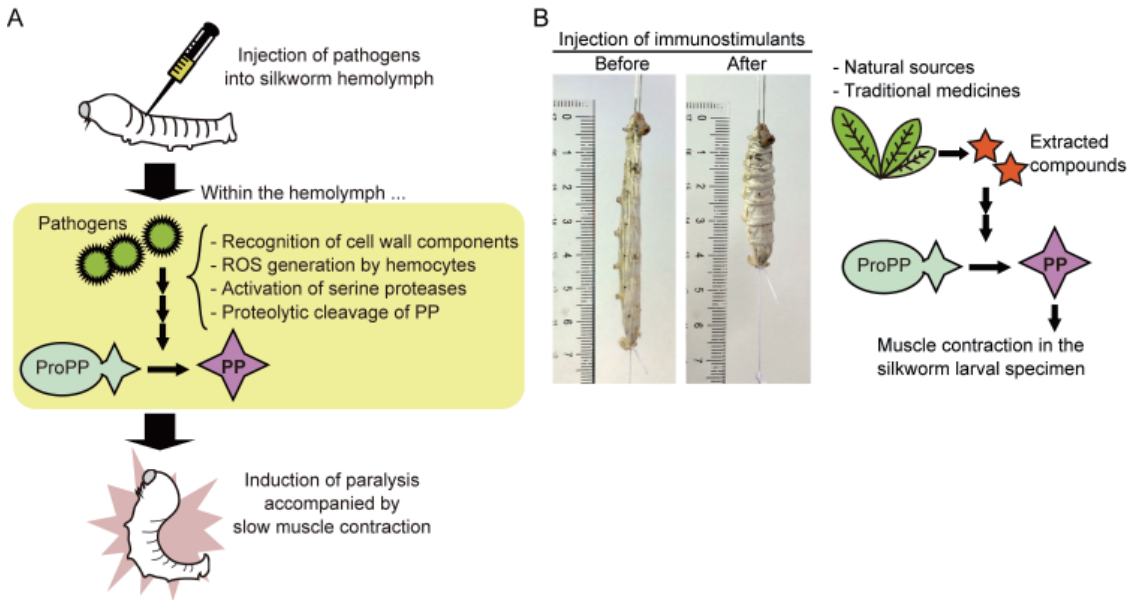

Figure 1. Activation of the insect cytokine paralytic peptide (PP) induced by pathogens. (A) PP activation processes induced by pathogens in the silkworm hemolymph. **(B)** Silkworm larval muscle contraction assay and its application for evaluation of immune-activating compounds. Abbreviations: AMP, antimicrobial peptides; MAPK, mitogen-activated protein kinase; NO, nitric oxide; ROS, reactive oxygen species.

subsections, we summarize our recent findings regarding these issues.

2.1. *Upstream processes of PP activation*

For the upstream processes of PP activation, we focused on reactive oxygen species (ROS). Using specific pharmacologic inhibitors, we found that the presence of live hemocytes, ROS, and activated serine proteases are required for pathogen-induced PP activation (*17*). We considered that live hemocytes recognize the pathogen-derived components and generate ROS (*i.e.*, a process called oxidative burst), followed by the onset of a putative serine-protease cascade that cleaves the PP precursor (Figure 1A). Specification of ROS types, hemocyte populations, pathogen-recognition receptors, and proteases will be examined in future studies. As serine proteases are involved in other immune responses, such as melanization (*23-25*) and Spaeztle activation (*26-28*), their crosstalk and role in PP activation will be interesting to evaluate in future studies.

2.2. *Downstream processes induced by active paralytic peptide*

Based on our findings that PP activation is triggered by pathogen components, PP might mediate defensive responses against infectious pathogens. To gain insight into the downstream events induced by PP, we performed a genome-wide microarray analysis of the hemocytes and fat body, the main immune organs in the silkworm larvae. Among a number of genes with altered expression patterns after PP injection, several genes encoding cytokine-like factors were upregulated, suggesting the existence of a complex network of insect cytokines (*29*).

We further studied the effect of PP on defensive responses in each organ. Active PP induced the expression of phagocytosis-related genes in hemocytes and promoted the engulfment of bacteria (Figure 2). In addition, the amount of AMP mRNA expressed in the fat body increased after PP injection, and activation of p38 mitogen-activated protein kinase (MAPK) mediated this PP-dependent AMP production (Figure 2). In addition to the well-known role of p38 MAPK in stress responses, recent studies demonstrated its contribution to insect immunity (*30*). Moreover, we found that PP induces the expression of nitric oxide (NO) synthase in the fat body, and NO production is required for both p38 MAPK activation and AMP expression (*31*). Although previous reports revealed that NO functions as a messenger molecule in insect immunity (*32*), but the pathway responsible for NO production has remained unknown (*33*). Our findings are thus the first to reveal a regulatory axis comprising insect cytokine PP, NO, and p38 MAPK. Further studies

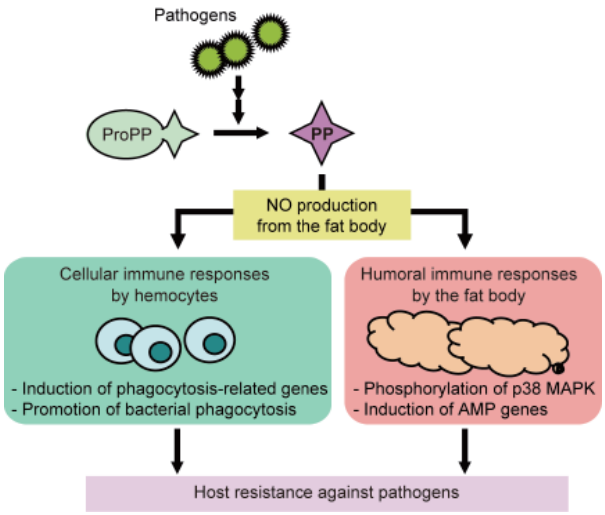

Figure 2. Immune responses induced by active paralytic peptide (PP). Abbreviations: LPS, lipopolysaccharides.

of signal mediators may reveal the connection between the extracellular cytokine network and intracellular signaling matrices that lead to regulated immune-gene expression.

PP and its Lepidoptera homologs belong to the ENF peptide family (*34*), named after their conserved C-terminal amino acid residues (glutamic acid, asparagine, and phenylalanine). The PP homologs have various biologic activities, which are reflected by the names given to these homologs in other Lepidoptera species: growth-blocking peptide, plasmatocyte-spreading peptide, and cardioactive peptide (*34*). We demonstrated that the C-terminus ENF residues are required for the immunostimulating activity of PP (*31*), as observed in PP homologs with other activities (*35,36*). The above signaling pathways mediating the PP-dependent immune responses might also be involved in different biologic events, such as development, downstream of other PP homologs. In addition to Lepidoptera insects, a *Drosophila* ENF peptide regulates the switching of humoral and cellular immunity (*37,38*). Moreover, PP homologs share similarity in their tertiary structure with mammalian epidermal growth factor and interact with mammalian epidermal growth factor receptors (*39*). We expect that conserved counterparts of the PP pathway exist in vertebrates and that studies of insect cytokines will shed light on the basis of innate immune regulation.

2.3. *Biologic relevance of paralytic peptide activation in host-pathogen interactions*

The biologic significance of PP activation has been demonstrated in the silkworm infection model using several pathogenic bacteria. Given that PP activation is triggered by pathogen components and that the active form of PP induces gene expression in immune tissues, we examined the protective role of PP in

infected host insects. The death of silkworms infected with *Staphylococcus aureus*, a human opportunistic pathogen, is delayed by injecting an excess amount of active PP. In contrast, the bacteria-dependent silkworm killing effects are accelerated when the larvae are treated with an anti-PP serum that specifically inhibits the biologic functions of PP. These findings suggest that PP acts as an insect cytokine that confers host protection against pathogens (*17*).

Using the silkworm infection model, we demonstrated that most human pathogens have silkworm-killing effects (*40,41*). Among them, *Serratia marcescens*, another pathogenic bacterium that infects infants and immunocompromised patients, kills silkworms with an extremely small number of cells (*42,43*). Silkworms infected with *S. marcescens* have unique phenotypes that are not induced by other pathogens, reduced hemocyte viability (*42*) and an increased number of freely circulating hemocytes in the hemolymph (*44*). While the hemocyte killing effects are induced by live *S. marcescens* cells and not the culture supernatant, the hemocyte number is increased by injecting either live bacteria or the supernatant, suggesting that the two phenotypes are caused by different mechanisms.

By screening the *S. marcescens* transposon mutant library, we found that mutants defective in the biosynthesis of LPS O-antigen and flagella, cell surface components required for bacterial motility, exhibit attenuated hemocyte-killing ability (*42*). This LPS- and flagella-dependent hemocyte killing by *S. marcescens* impairs glucan-induced muscle contraction in the muscle contraction assay (*42*), further supporting our previous notion that the presence of live hemocytes is required for PP activation (*17*). Isolated LPS and flagella proteins themselves, however, fail to kill hemocytes; thus, it is likely that other uncharacterized factors are directly involved in the apoptosis induction. Nevertheless, mutants lacking LPS O-antigen and flagella have much lower virulence in silkworm larvae compared with the parent strain (*42*), suggesting that suppression of host immunity *via* hemocyte killing largely contributes to *S. marcescens* pathogenicity (Figure 3A).

Another phenotype observed in silkworms injected with the culture supernatant of *S. marcescens*, but not other bacterial species, is the transient increase in the number of freely circulating hemocytes. We purified the factor responsible for the hemocyte-increasing activity of the culture supernatant through biochemical approaches and identified serralysin metalloprotease (*44*). We demonstrated that serralysin degrades the adhesive molecules at the hemocyte surface, resulting in cell detachment from the internal body cavity and an increase in freely circulating cells. Consistent with previous reports, PP induces adhesive molecules in hemocytes thereby increasing cell adhesiveness (*29*). On the other hand, the PP-dependent increase in hemocyte adhesiveness is blocked by serralysin treatment, without

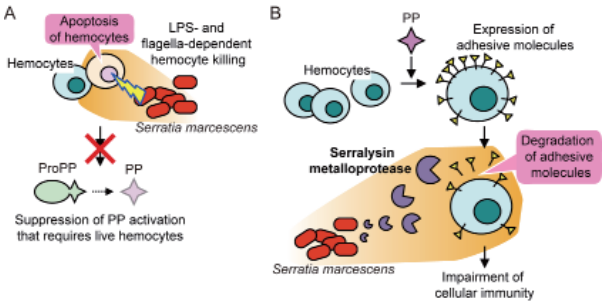

Figure 3. Immune-evading mechanisms of the pathogenic bacterium *S. marcescens*. (A) Suppression of paralytic peptide (PP) activation *via* hemocyte killing by *S. marcescens*. **(B)** Impairment of cellular immunity *via* production of serralysin metalloprotease by *S. marcescens*. Abbreviations: LPS, lipopolysaccharides; ROS, reactive oxygen species.

direct degradation of PP itself. Moreover, serralysin suppresses immunologic activities, such as phagocytosis, by hemocytes and bacterial clearance within the silkworm hemolymph (*44*). Together, these findings suggest that *S. marcescens* impairs host immunity, including the PP pathway, *via* two distinct mechanisms: direct hemocyte-killing mediated by bacterial surface components (Figure 3A), and degradation of adhesive molecules by the secretion of serralysin metalloprotease (Figure 3B). The significance of PP in self-defense is highlighted through analyses of these battles between host animals and pathogens.

3. Evaluation of immunostimulatory compounds using silkworms

As described above, the silkworm muscle contraction assay is suitable for evaluating stimulatory effects of test samples on the PP pathway (Figure 1). The silkworm *ex vivo* system has several advantages compared to other immunologic assays, such as interleukin production using mammalian macrophages. Because bacterial LPS, a contaminant frequently present in natural sources, fails to trigger PP activation (*21*), the activity measured by the silkworm contraction assay is free from false-positives due to environmental LPS. This is presumably due to the presence of LPS-absorbing proteins in the silkworm hemolymph (*45*). Moreover, samples injected into the hemolymph of the larval specimen are subjected to drug-metabolic processes. Therefore, we consider that the silkworm muscle contraction assay is applicable for evaluating the immunostimulatory effects of compounds. In this section, we present the practical use of the silkworm muscle contraction assay.

3.1. *Purification of immunostimulatory polysaccharides from green tea leaves*

Tea leaves contain various compounds, such as polyphenol, that affect human health. The factors responsible for the bioactivities reported in tea remain largely unknown at the molecular level. A hot water

extract of green tea (*Camellia sinensis*) leaves exhibits potent activity in the silkworm muscle contraction assay (*46*). On the other hand, known components of green tea leaves, such as catechin, polyphenon, and cellulose, fail to induce muscle contraction, suggesting that the leaves contain uncharacterized substances that stimulate innate immunity. We purified the active component from the tea extract by successive chromatography steps. Based on the physical properties of the active fraction, we assumed that it contained polysaccharides. Monosaccharide analysis and nuclear magnetic resonance revealed that the polysaccharide structure contains D-galacturonic acid and methyl ester residues (*46*). Moreover, the activity of the purified fraction is sensitive to enzymatic treatment by beta-glucanase, suggesting the presence of a beta-glucan structure connected with a polygalacturonic acid backbone (*46*). We further verified the immunostimulatory effect of this polysaccharide in a conventional interleukin-6 production assay using mouse peritoneal macrophages (*46*). These findings support our statement that the silkworm muscle contraction assay is useful for identifying novel substances with immunostimulatory activity.

3.2. *Characterization of immunostimulatory glucans from rock tripe*

Rock tripe, a group of lichens that grow on rocks, is used as a traditional medicine in Eastern countries (called "iwatake" in Japanese and "seogi" in Korea). These lichens produce various polysaccharides, some of which have stimulatory effects on mammalian immune cells (*47*). By using the silkworm contraction assay, we evaluated the immunostimulatory effects of these rock tripe-derived polysaccharides. We found that GE-3, a beta-1,6 glucan from *Gyrophora esculenta*, induces muscle contraction in larval specimens (*21*). Moreover, GE-3 promotes PP activation within the silkworm hemolymph in a dose-dependent manner (21). A previous microarray analysis revealed that PP injection upregulates immune genes that are also induced in virus-infected insects (*48,49*). Using the *Bombyx mori* nucleopolyhedrosis virus silkworm infection model (*50*), we demonstrated that GE-3 has a host protective effect (*21*).

In contrast to GE-3, some of the plant-derived beta-glucans (*e.g.*, laminaran, lentinan, schizophyllan, and ukonan) fail to induce muscle contraction (*21*), suggesting that the host system recognizes specific structural patterns of beta-glucans that lead to PP activation and host protection. The precise mechanism of ligand recognition and the downstream anti-viral immune reactions, however, require further studies.

4. Overactivation of innate immunity in silkworms

The immune system is a "double-edged sword", and overactivation of immune reactions damages the host animal itself. In humans, severe inflammatory states are due mainly to the dysregulation of innate immunity, rather than acquired immunity, and are related to numerous diseases; either local or systemic, acute or chronic. In mammals, pathogen-recognizing receptors such as Toll-like receptors trigger exaggerated responses called cytokine storms, in which overproduced cytokines amplify the inflammatory signal. A striking example is Toll-like receptor 4-dependent septic shock in mice injected with bacterial LPS; death caused by LPS treatment is clearly suppressed in *tlr4* gene-knock out mice (*51*). In this sense, studies of the mechanisms that modulate immune responses are crucial to understand and overcome the "negative" side of immunity. Regardless of the basic conservation in innate immunity, however, there has been no reported model of sepsis in invertebrates that includes immune system overactivation.

Among the human pathogens with lethal effects in silkworms, we focused on *Porphyromonas gingivalis*, a Gram-negative bacterium causative for periodontal disease. Larval death caused by this specific bacterium has distinct features not observed in silkworms infected with other model pathogens. First, the silkworms infected with *P. gingivalis* are not cured by antibiotic administration, despite inhibition of the *in vitro* growth of *P. gingivalis* and the finding of therapeutic effects on other pathogenic bacteria. While viable bacterial cells within the silkworm hemolymph decrease soon after infection, *P. gingivalis* continues to kill silkworms after several days. Moreover, heat-killed *P. gingivalis* cells are as toxic to silkworms as live bacteria. Second, the hemolymph of *P. gingivalis*-infected larvae show intense blackening, a defensive reaction called melanization, several hours after injection. The degree of hemolymph blackening is much higher after *P. gingivalis* infection than infection by other pathogens. We considered from these findings that *P. gingivalis* surface components kill silkworms by excess activation of melanization (*52*).

We further assessed the killing mechanism by *P. gingivalis*. Both hemolymph blackening and host-killing by *P. gingivalis* are suppressed by 1-phenyl-2-thiourea and serine protease inhibitors, agents that inhibit insect melanization. As melanin itself is not toxic to silkworms, we shifted our focus to ROS generated as side-products during melanin polymerization. ROS are a well-known trigger of cell-death signals and are thus implicated in a wide range of stress-related diseases and inflammation. We found that radical scavengers and pharmacologic inhibitors of cell-death signals exhibited therapeutic effects in silkworms infected with *P. gingivalis* (Figure 4). Although *P. gingivalis* also induced potent muscle contraction, inhibition of the PP pathway by PP-antiserum did not affect silkworm killing, suggesting that melanization is specifically involved in the host damaging process. Together, these

findings suggest that *P. gingivalis*-induced excess ROS production during melanization is followed by activation of cell death signals and organ failure. We proposed this as the first insect model of bacteria-induced immune overactivation causing severe damage against the host (*52*).

How does *P. gingivalis* induce excess melanization? We only know that PG, a major cell wall component in bacteria, is responsible for the onset of melanization. The composition and structure of PG vary among bacterial species. In general, Gram-negative or Gram-positive bacteria possess either diaminopimelic acid - or Lys-type PG, followed by more detailed classifications. Comparison with the toxic effects of PG from other bacteria, however, fails to reveal a clear relationship between the PG type and immunoreactivity (*52*). Furthermore, *P. gingivalis* PG-induced host killing is not observed in two Diptera species (*D. melanogaster* and *Sarcophaga peregrina*), whereas other Lepidopteran and Coleopteran insects are killed and their hemolymph blackened (*52*). Identification of the precise PG structure and the host PG-receptor involved in the excess melanization may provide reasonable explanations for the above comparative study, and further elucidate the evolutionary diversification of immunomodulation.

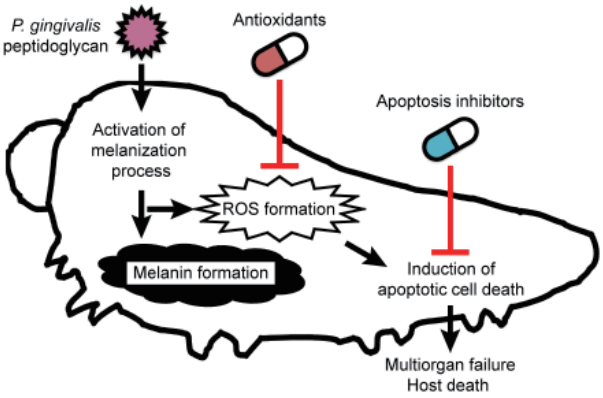

Figure 4. Overactivation of immune responses by *P. gingivalis* peptidoglycan in silkworms.

5. Perspectives for using silkworms as a model animal for the development of immuno-regulatory drugs

As mentioned above, we initially established a pathogen infection model using the silkworm as a host animal. The lower rearing costs and fewer ethical issues associated with using a large number of silkworms for drug screening and development are advantageous compared with mammalian models. The pharmacokinetic parameters and toxicity of most drugs evaluated in silkworms are comparable to those reported in mammals, suggesting that both models possess similar drug metabolism systems (*15,53,54*). Using the *S. aureus*-silkworm infection model, we recently identified a novel antibiotic named lysocin E (*55*). During the purification procedure of therapeutically active substances from the *Lysobacter* culture supernatant, we observed that the *in vitro* antibacterial activity does not increase in proportion with the *in vivo* therapeutic activity (*55*), indicating the importance of evaluating *in vivo* activity using the whole animal, and not only in *in vitro* assays, to screen and identify therapeutically active compounds (Figure 5).

As exemplified by the antibiotic lysocin E, this silkworm infection model allows us to determine compounds that modulate the immune system using silkworms. As presented in the above sections, the silkworm muscle contraction assay is suitable for screening substances, such as polysaccharides, contained in natural sources that stimulate innate immunity. The combination of an *ex vivo* muscle contraction assay and the silkworm infection model may lead to the identification of compounds with therapeutic effects through immune system activation rather than direct toxicity to pathogens. Because these compounds recruit host immune systems to suppress pathogen activity, the development of drug resistance may be limited, as discussed in the case of host AMPs used for infection control (*56*). In addition, these compounds could be effective against a wide range of pathogens, and may also be applicable for cancer therapy (*56*).

On the other hand, the *P. gingivalis*-silkworm

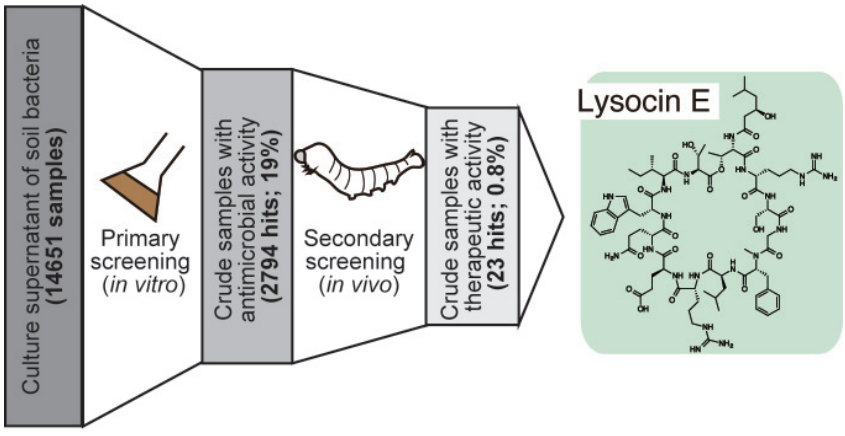

Figure 5. Identification of a novel antibiotic, lysocin E, through *in vivo* drug screening using the silkworm infection model.

infection model could be used to evaluate compounds that attenuate the overactivated state of the host immune system. Because excess ROS production is widely considered to cause cell death, radical scavengers and apoptosis inhibitors are expected to prevent tissue damage at the inflammatory site. We demonstrated that *N*-acetyl-L-cysteine and glutathione, antioxidants with therapeutic effects in mammalian sepsis (*57*), suppress silkworm killing by the *P. gingivalis* peptidoglycan (*52*). While antioxidant activity is reported in a number of natural origins and traditional medicines, such as ginseng (*58*), in most cases the active substances responsible for the activity are yet to be determined. We consider that the silkworm model is suitable for searching for compounds from these potential sources with protective effects against sepsis that accompanies immune overactivation.

6. Concluding remarks

Insects are simple and useful models for analyzing the basis of regulatory mechanisms in innate immunity. Recent findings regarding the multifunctional insect cytokine PP in silkworms provide novel insights into the communication network among immune tissues and host-pathogen interactions. In contrast to mammalian models, insects are currently rarely applied to human drug development. The established silkworm assays evaluating both "positive" (cytokine activation) and "negative" (excess inflammation) aspects of immunity have potential applications in the development of therapeutic agents that affect host immunologic states. The silkworm is thus revolutionizing basic science by opening new fields of interdisciplinary research that include immunology, microbiology, and pharmacology.

References

1. Hoffmann JA, Reichhart JM. *Drosophila* innate immunity: An evolutionary perspective. Nat Immunol. 2002; 3:121-126.
2. Lemaitre B, Nicolas E, Michaut L, Reichhart JM, Hoffmann JA. The dorsoventral regulatory gene cassette spatzle/Toll/cactus controls the potent antifungal response in *Drosophila* adults. Cell. 1996; 86:973-983.
3. Tanaka H, Ishibashi J, Fujita K, Nakajima Y, Sagisaka A, Tomimoto K, Suzuki N, Yoshiyama M, Kaneko Y, Iwasaki T, Sunagawa T, Yamaji K, Asaoka A, Mita K, Yamakawa M. A genome-wide analysis of genes and gene families involved in innate immunity of *Bombyx mori*. Insect Biochem Mol Biol. 2008; 38:1087-1110.
4. Cheng TC, Zhang YL, Liu C, Xu PZ, Gao ZH, Xia QY, Xiang ZH. Identification and analysis of Toll-related genes in the domesticated silkworm, *Bombyx mori*. Dev Comp Immunol. 2008; 32:464-475.
5. Meng X, Khanuja BS, Ip YT. Toll receptor-mediated *Drosophila* immune response requires Dif, an NF-kappaB factor. Genes Dev. 1999; 13:792-797.
6. Rutschmann S, Jung AC, Zhou R, Silverman N, Hoffmann JA, Ferrandon D. Role of *Drosophila* IKK gamma in a toll-independent antibacterial immune response. Nature Immunol. 2000; 1:342-347.
7. Silverman N, Zhou R, Stoven S, Pandey N, Hultmark D, Maniatis T. A *Drosophila* IkappaB kinase complex required for Relish cleavage and antibacterial immunity. Genes Dev. 2000; 14:2461-2471.
8. Irving P, Troxler L, Heuer TS, Belvin M, Kopczynski C, Reichhart JM, Hoffmann JA, Hetru C. A genome-wide analysis of immune responses in *Drosophila*. Proc Natl Acad Sci U S A. 2001; 98:15119-15124.
9. Tauszig-Delamasure S, Bilak H, Capovilla M, Hoffmann JA, Imler JL. *Drosophila* MyD88 is required for the response to fungal and Gram-positive bacterial infections. Nature Immunol. 2002; 3:91-97.
10. Lemaitre B, Kromer-Metzger E, Michaut L, Nicolas E, Meister M, Georgel P, Reichhart JM, Hoffmann JA. A recessive mutation, immune deficiency (imd), defines two distinct control pathways in the *Drosophila* host defense. Proc Natl Acad Sci U S A. 1995; 92:9465-9469.
11. Sluss HK, Han Z, Barrett T, Goberdhan DC, Wilson C, Davis RJ, Ip YT. A JNK signal transduction pathway that mediates morphogenesis and an immune response in *Drosophila*. Genes Dev. 1996; 10:2745-2758.
12. Agaisse H, Petersen UM, Boutros M, Mathey-Prevot B, Perrimon N. Signaling role of hemocytes in *Drosophila* JAK/STAT-dependent response to septic injury. Dev Cell. 2003; 5:441-450.
13. Boutros M, Agaisse H, Perrimon N. Sequential activation of signaling pathways during innate immune responses in *Drosophila*. Dev Cell. 2002; 3:711-722.
14. Lavine MD, Strand MR. Insect hemocytes and their role in immunity. Insect Biochem Mol Biol. 2002; 32:1295-1309.
15. Hamamoto H, Kurokawa K, Kaito C, Kamura K, Manitra Razanajatovo I, Kusuhara H, Santa T, Sekimizu K. Quantitative evaluation of the therapeutic effects of antibiotics using silkworms infected with human pathogenic microorganisms. Antimicrob Agents Chemother. 2004; 48:774-779.
16. Kaito C, Kurokawa K, Matsumoto Y, Terao Y, Kawabata S, Hamada S, Sekimizu K. Silkworm pathogenic bacteria infection model for identification of novel virulence genes. Mol Microbiol. 2005; 56:934-944.
17. Ishii K, Hamamoto H, Kamimura M, Sekimizu K. Activation of the silkworm cytokine by bacterial and fungal cell wall components *via* a reactive oxygen species-triggered mechanism. J Biol Chem. 2008; 283:2185-2191.
18. Sekimizu K, Larranaga J, Hamamoto H, Sekine M, Furuchi T, Katane M, Homma H, Matsuki N. D-Glutamic acid-induced muscle contraction in the silkworm, *Bombyx mori*. J Biochem. 2005; 137:199-203.
19. Ha SD, Nagata S, Suzuki A, Kataoka H. Isolation and structure determination of a paralytic peptide from the hemolymph of the silkworm, *Bombyx mori*. Peptides. 1999; 20:561-568.
20. Kamimura M, Nakahara Y, Kanamori Y, Tsuzuki S, Hayakawa Y, Kiuchi M. Molecular cloning of silkworm paralytic peptide and its developmental regulation. Biochem Biophys Res Commun. 2001; 286:67-73.
21. Fujiyuki T, Hamamoto H, Ishii K, Urai M, Kataoka K, Takeda T, Shibata S, Sekimizu K. Evaluation of innate immune stimulating activity of polysaccharides using a silkworm (*Bombyx mori*) muscle contraction assay. Drug Discov Ther. 2012; 6:88-93.

22. Nakahara Y, Kanamori Y, Kiuchi M, Kamimura M. Effects of silkworm paralytic peptide on *in vitro* hematopoiesis and plasmatocyte spreading. Arch Insect Biochem Physiol. 2003; 52:163-174.
23. Ashida M, Ishizaki Y, Iwahana H. Activation of pro-phenoloxidase by bacterial cell walls or beta-1,3-glucans in plasma of the silkworm, *Bombyx mori*. Biochem Biophys Res Commun. 1983; 113:562-568.
24. Katsumi Y, Kihara H, Ochiai M, Ashida M. A serine protease zymogen in insect plasma. Purification and activation by microbial cell wall components. Eur J Biochem. 1995; 228:870-877.
25. Kan H, Kim CH, Kwon HM, Park JW, Roh KB, Lee H, Park BJ, Zhang R, Zhang J, Soderhall K, Ha NC, Lee BL. Molecular control of phenoloxidase-induced melanin synthesis in an insect. J Biol Chem. 2008; 283:25316-25323.
26. Ligoxygakis P, Pelte N, Hoffmann JA, Reichhart JM. Activation of *Drosophila* Toll during fungal infection by a blood serine protease. Science. 2002; 297:114-116.
27. Kim CH, Kim SJ, Kan H, Kwon HM, Roh KB, Jiang R, Yang Y, Park JW, Lee HH, Ha NC, Kang HJ, Nonaka M, Soderhall K, Lee BL. A three-step proteolytic cascade mediates the activation of the peptidoglycan-induced toll pathway in an insect. J Biol Chem. 2008; 283:7599-7607.
28. Roh KB, Kim CH, Lee H, Kwon HM, Park JW, Ryu JH, Kurokawa K, Ha NC, Lee WJ, Lemaitre B, Soderhall K, Lee BL. Proteolytic cascade for the activation of the insect toll pathway induced by the fungal cell wall component. J Biol Chem. 2009; 284:19474-19481.
29. Ishii K, Hamamoto H, Kamimura M, Nakamura Y, Noda H, Imamura K, Mita K, Sekimizu K. Insect cytokine paralytic peptide (PP) induces cellular and humoral immune responses in the silkworm *Bombyx mori*. J Biol Chem. 2010; 285:28635-28642.
30. Shinzawa N, Nelson B, Aonuma H, Okado K, Fukumoto S, Miura M, Kanuka H. p38 MAPK-dependent phagocytic encapsulation confers infection tolerance in *Drosophila*. Cell Host Microbe. 2009; 6:244-252.
31. Ishii K, Adachi T, Hamamoto H, Oonishi T, Kamimura M, Imamura K, Sekimizu K. Insect cytokine paralytic peptide activates innate immunity *via* nitric oxide production in the silkworm *Bombyx mori*. Dev Comp Immunol. 2013; 39:147-153.
32. Foley E, O'Farrell PH. Nitric oxide contributes to induction of innate immune responses to gram-negative bacteria in *Drosophila*. Genes Dev. 2003; 17:115-125.
33. Rivero A. Nitric oxide: An antiparasitic molecule of invertebrates. Trends Parasitol. 2006; 22:219-225.
34. Strand MR, Hayakawa Y, Clark KD. Plasmatocyte spreading peptide (PSP1) and growth blocking peptide (GBP) are multifunctional homologs. J Insect Physiol. 2000; 46:817-824.
35. Clark KD, Volkman BF, Thoetkiattikul H, Hayakawa Y, Strand MR. N-terminal residues of plasmatocyte-spreading peptide possess specific determinants required for biological activity. J Biol Chem. 2001; 276:37431-37435.
36. Tada M, Aizawa T, Shinohara Y, Matsubara K, Miura K, Yoshida M, Shitara K, Kouno T, Mizuguchi M, Nitta K, Hayakawa Y, Kawano K. Roles of aromatic residues in the structure and biological activity of the small cytokine, growth-blocking peptide (GBP). J Biol Chem. 2003; 278:10778-10783.
37. Tsuzuki S, Ochiai M, Matsumoto H, Kurata S, Ohnishi A, Hayakawa Y. *Drosophila* growth-blocking peptide-like factor mediates acute immune reactions during infectious and non-infectious stress. Sci Rep. 2012; 2:210.
38. Tsuzuki S, Matsumoto H, Furihata S, Ryuda M, Tanaka H, Sung EJ, Bird GS, Zhou Y, Shears SB, Hayakawa Y. Switching between humoral and cellular immune responses in *Drosophila* is guided by the cytokine GBP. Nat Commun. 2014; 5:4628.
39. Aizawa T, Hayakawa Y, Nitta K, Kawano K. Structure and activity of insect cytokine GBP which stimulates the EGF receptor. Mol Cells. 2002; 14:1-8.
40. Kaito C, Usui K, Kyuma T, Sekimizu K. Isolation of mammalian pathogenic bacteria using silkworms. Drug Discov Ther. 2011; 5:66-70.
41. Kaito C, Akimitsu N, Watanabe H, Sekimizu K. Silkworm larvae as an animal model of bacterial infection pathogenic to humans. Microb Pathog. 2002; 32:183-190.
42. Ishii K, Adachi T, Imamura K, Takano S, Usui K, Suzuki K, Hamamoto H, Watanabe T, Sekimizu K. Serratia marcescens induces apoptotic cell death in host immune cells *via* a lipopolysaccharide- and flagella-dependent mechanism. J Biol Chem. 2012; 287:36582-36592.
43. Ishii K, Adachi T, Hara T, Hamamoto H, Sekimizu K. Identification of a Serratia marcescens virulence factor that promotes hemolymph bleeding in the silkworm, *Bombyx mori*. J Invertebr Pathol. 2014; 117:61-67.
44. Ishii K, Adachi T, Hamamoto H, Sekimizu K. Serratia marcescens suppresses host cellular immunity *via* the production of an adhesion-inhibitory factor against immunosurveillance cells. J Biol Chem. 2014; 289:5876-5888.
45. Kato Y, Motoi Y, Taniai K, Kadono-Okuda K, Yamamoto M, Higashino Y, Shimabukuro M, Chowdhury S, Xu J, Sugiyama M, *et al*. Lipopolysaccharide-lipophorin complex formation in insect hemolymph: A common pathway of lipopolysaccharide detoxification both in insects and in mammals. Insect Biochem Mol Biol. 1994; 24:547-555.
46. Dhital S, Hamamoto H, Urai M, Ishii K, Sekimizu K. Purification of innate immunostimulant from green tea using a silkworm muscle contraction assay. Drug Discov Ther. 2011; 5:18-25.
47. Adachi Y, Okazaki M, Ohno N, Yadomae T. Leukocyte activation by (1-->3)-beta-D glucans. Mediators Inflamm. 1997; 6:251-256.
48. Sagisaka A, Fujita K, Nakamura Y, Ishibashi J, Noda H, Imanishi S, Mita K, Yamakawa M, Tanaka H. Genome-wide analysis of host gene expression in the silkworm cells infected with *Bombyx mori* nucleopolyhedrovirus. Virus Res. 2010; 147:166-175.
49. Bao YY, Tang XD, Lv ZY, Wang XY, Tian CH, Xu YP, Zhang CX. Gene expression profiling of resistant and susceptible *Bombyx mori* strains reveals nucleopolyhedrovirus-associated variations in host gene transcript levels. Genomics. 2009; 94:138-145.
50. Orihara Y, Hamamoto H, Kasuga H, Shimada T, Kawaguchi Y, Sekimizu K. A silkworm baculovirus model for assessing the therapeutic effects of antiviral compounds: Characterization and application to the isolation of antivirals from traditional medicines. J Gen Virol. 2008; 89:188-194.
51. Poltorak A, He X, Smirnova I, Liu MY, Van Huffel C, Du X, Birdwell D, Alejos E, Silva M, Galanos C, Freudenberg M, Ricciardi-Castagnoli P, Layton B, Beutler B. Defective

LPS signaling in C3H/HeJ and C57BL/10ScCr mice: Mutations in Tlr4 gene. Science. 1998; 282:2085-2088.
52. Ishii K, Hamamoto H, Imamura K, Adachi T, Shoji M, Nakayama K, Sekimizu K. Porphyromonas gingivalis peptidoglycans induce excessive activation of the innate immune system in silkworm larvae. J Biol Chem. 2010; 285:33338-33347.
53. Asami Y, Horie R, Hamamoto H, Sekimizu K. Use of silkworms for identification of drug candidates having appropriate pharmacokinetics from plant sources. BMC Pharmacol. 2010; 10:7.
54. Hamamoto H, Tonoike A, Narushima K, Horie R, Sekimizu K. Silkworm as a model animal to evaluate drug candidate toxicity and metabolism. Comp Biochem Physiol C Toxicol Pharmacol. 2009; 149:334-339.
55. Hamamoto H, Urai M, Ishii K, *et al*. Lysocin E is a new antibiotic that targets menaquinone in the bacterial membrane. Nat Chem Biol. 2015; 11:127-133.
56. Baltzer SA, Brown MH. Antimicrobial peptides: Promising alternatives to conventional antibiotics. J Mol Microbiol Biotechnol. 2011; 20:228-235.
57. Ortolani O, Conti A, De Gaudio AR, Moraldi E, Cantini Q, Novelli G. The effect of glutathione and *N*-acetylcysteine on lipoperoxidative damage in patients with early septic shock. Am J Respir Crit Care Med. 2000; 161:1907-1911.
58. Dong GZ, Jang EJ, Kang SH, Cho IJ, Park SD, Kim SC, Kim YW. Red ginseng abrogates oxidative stress *via* mitochondria protection mediated by LKB1-AMPK pathway. BMC Complement Altern Med. 2013; 13:64.

(Received March 19, 2015; Revised April 3, 2015; Accepted April 4, 2015)

Review

DOI: 10.5582/ddt.2015.01042

Oesophageal squamous cell carcinoma (ESCC): Advances through omics technologies, towards ESCC salivaomics

Juan José González-Plaza[1,2,*], Nataša Hulak[3], Eduardo García Fuentes[4,5], Lourdes Garrido-Sánchez[5,6], Zhaxybay Zhumadilov[1], Ainur Akilzhanova[1]

[1] *Laboratory of Genomic and Personalized Medicine, Center for Life Sciences, PI "National Laboratory Astana", AOE "Nazarbayev University", Astana, Kazakhstan;*
[2] *Research Department, University Hospital for Infectious Diseases "Dr. Fran Mihaljević", Zagreb, Croatia;*
[3] *Department of Microbiology, Faculty of Agriculture, University of Zagreb, Zagreb, Croatia;*
[4] *Unidad de Gestión Clínica de Endocrinologíay Nutrición, Instituto de Investigación Biomédica de Málaga (IBIMA), Hospital Regional Universitario, Málaga, Spain;*
[5] *CIBER Fisiología de la Obesidad y Nutrición (CIBEROBN), Málaga, Spain;*
[6] *Unidad de Gestión Clínica de Endocrinología y Nutrición, Instituto de Investigación Biomédica de Málaga (IBIMA), Hospital Clínico Virgen de la Victoria, Málaga, Spain.*

Summary **Oesophageal Squamous Cell Carcinoma (ESCC) is one of the two main subtypes of oesophageal cancer, affecting mainly populations in Asia. Though there have been great efforts to develop methods for a better prognosis, there is still a limitation in the staging of this affection. As a result, ESCC is detected at advances stages, when the interventions on the patient do not have such a positive outcome, leading in many cases to recurrence and to a very low 5-year survival rate, causing high mortality. A way to decrease the number of deaths is the use of biomarkers that can trace the advance of the disease at early stages, when surgical or chemotherapeutic methodologies would have a greater effect on the evolution of the subject. The new high throughput omics technologies offer an unprecedented chance to screen for thousands of molecules at the same time, from which a new set of biomarkers could be developed. One of the most convenient types of samples is saliva, an accessible body fluid that has the advantage of being non-invasive for the patient, being easy to store or to process. This review will focus on the current status of the new omics technologies regarding salivaomics in ESCC, or when not evaluated yet, the achievements in related diseases.**

Keywords: Oesophageal squamous cell carcinoma, saliva, salivaomics, transcriptomics, proteomics, metabolomics

1. Introduction

Oesophageal Cancer (EC) has two main subtypes with different pathological features, Adenocarcinoma (EAC) and ESCC (*1,2*), representing between them more than 90% of the detected cases (*3*). There is also a different trend in the geographical distribution for both EC subtypes, being that of EAC in the Western world (*4*), while ESCC is especially present in Asia, for example in China (*5-7*), Iran (*8,9*), Japan (*10*), or Kazakhstan (*11*). In this last country, ESCC is the 6th major type of diagnosed cancer, with high mortality rates among women (9th place) and men (5th place) (*11*). Early detection of ESCC and subsequent treatment would be crucial in order to decrease mortality (*12*), but as indicated by several authors (*4,13-15*) lack of early stage diagnostic tools is one of the biggest problems in ESCC diagnostics, especially because ESCC is manifested as asymptomatic lesions at first stages. Some of the current techniques used for diagnosis are non-invasive imaging methods, as well as more conventional ones that include computed tomography (CT) scan, or endoscopic ultrasound (EUS). Some of the difficulties that these techniques face are in the case of EUS the limitation that tumour enlargement pose for the passage of endoscope in advanced cases, or for

**Address correspondence to:*
Dr. Juan José González Plaza, University Hospital for Infectious Diseases "Dr. Fran Mihaljević" Research Department Mirogojska 8, 10 000 Zagreb, Croatia.
E-mail: plaza@bfm.hr

CT the lower sensitivity displayed in comparison to a combination of PET (Positron Emission Tomography) and the use of 2-deoxy-2-(^{18}F)fluoro-D-glucose (^{18}F-FDG) (*16*). As previously indicated by Takeshita (*15*) there have been advances in the use of several techniques as those mentioned above, but still a late detection happens at very advanced stages (*17,18*), when surgical interventions are not effective and lead to recurrence and low survival rates (*19*).

Besides, an additional problem for ESCC is the multifactorial nature of its occurrence (*20*), and the influence that different habits would have over the risk of developing this disease, as it has been associated with heavy smoking, drinking, or low intake of vegetables or fruits (*21-23*). The increased risk factor in this case as indicated by Cheng and Day (*22*) may come as a consequence from a direct contact of the potential carcinogen with the epithelium, some existing transport facilitating mechanism, or derived from compounds that increase the cell turnover in the epithelial cells. Albeit yet a controversial topic, there have been also studies trying to correlate the occurrence of HPV infections and ESCC, though results showed an elevated degree of variation that did not yield a clear association between the viral infection and the development of the disease (*24-26*).

A molecular feature that could be associated to the development of this disease would serve as an indicator for a more effective treatment. In this scenario, the discovery of biomarkers would become a great advantage for clinicians allowing an early diagnosis of ESCC, as it has been for many other diseases, *e.g.* level of serum creatinine as indicator of renal function. The term biomarker (biological marker) can be defined as "a characteristic that is objectively measured and evaluated as an indicator of normal biological processes, pathogenic processes, or pharmacologic responses to a therapeutic intervention", definition that was proposed at the 1998 National Institutes of Health Biomarkers Definitions Working Group (*27,28*). Biomarkers can aid in diagnosis, and an efficient way to discover them is the use of available omics technologies. Transcriptomics, Proteomics, or Metabolomics (TPM) are relatively new high throughput techniques that allow performing massive screenings of different molecules. Each of them refer to the complete set of transcripts/proteins/metabolites (respectively) and their quantity, for a given cell with a given genotype, under certain environmental conditions (including developmental or physiological stage, as well as being under influence of bioregulators) (*29-32*). After this definition, it comes as a logic consequence that physiological changes that accompany the development of a disease in humans lead to changes in the TPM profile, that can be observed and measured in a tissue, or indirectly measured/observed in human fluids, *e.g.* urine, sweat, saliva. Currently due to the development of omics technologies, these profile changes can be detected and analysed (*29-32*). The advantage of using TMP "expression" biomarkers is that they are closely related to the disease, as they are usually by-products of its development. Metabolites are for example end-points of all the system, being the final products of metabolic pathways (*33*) and a reflection of the phenotype (*34*). Therefore, this approach would yield biomarkers that are potentially specific for the studied disease, and have a potentially direct application (*35*). The use of a combination of this new technologies (*36*), can largely contribute in the understanding of each disease, their evolution, and molecular mechanisms.

A very important point in studies concerning cancer or other diseases, is the validation of the model through testing in an independent set of samples (*36*). This would be, for example, a set of individuals with the same features as the control (healthy), and another set of independent affected ones, which were not used in the original screening. It will mean that the found biomarkers have the power to potentially predict or be associated with the disease in any given set of samples that fulfil the disease conditions. Otherwise, this would be (the necessary) technical validation of the study. Biomarkers that are validated in this way can be promising targets for further clinical testing assays.

Considering the final aim of developing biomarkers to routinely use them for ESCC testing in clinical settings, one of the most accessible and interesting types of human samples is saliva (*35*). It has numerous advantages, being easily accessible for clinicians, and non-invasive for patients (*37-39*). Compared to imaging techniques, saliva collection is methodologically less demanding than a ^{18}F-FDG PET assay (*16*), allowing to scale up the number of patients to sample. Compared with other identification techniques as EUS, its advantage is that saliva collection avoids the anxiety that an endoscopy may cause to the patient, or the potential disturbances afterwards. Other interesting features of saliva in comparison to blood, is that saliva does not need dedicated precautions for storage or biosecurity, besides it does not clot (*14*). Thus, its handling is very convenient for any hospital facility worldwide, especially in depressed or impoverished areas.

Saliva is a human fluid that is originated mostly in three salivary glands (*parotis*, *submandibularis* and *sublingualis*), as well as a number of minor glands, and the fluid from gingival crevice (*37,40*). It is a complex mixture of exudates derived from mucosa, plasma, microflora (or what we will refer as oral metabiome/microbiome), epithelial cells, small metabolites and different transcripts, among other minor compounds (*41-44*). This complexity must be considered as a very important feature for its study. Regarding the protein content, some studies reported that approximately 20%-30% of the proteins that can be found in blood plasma are present in saliva (*45,46*). According to

Castagnola *et al.*, most of the proteins (more than 90% of representation) are not from gland secretory origin, but common to other body fluids or tissues. However, despite this abundance, common proteins account only for 15% w/w of the salivary proteome, something that has to be considered as a potential drawback for biomarker discovery studies (*41*). An aspect of saliva that cannot be forgotten, of importance because it can affect the results, is the human oral microbiome (*47,48*). It can be defined as the population of different bacterial species that inhabit the oral cavity, while they form part of the whole human microbiota. Taking in account all of the above mentioned features from saliva, there is room for discovery of different biomarkers associated to the development of ESCC.

In conditions of disease, human saliva can reflect the physiological state as occurs in blood (*49,50*). This has been demonstrated in the work of Asatsuma *et al*. (*51*) (Table 1), in which they found significant differences in a protein between the healthy patients compared with the ones affected by primary Sjögren's syndrome (pSS). Nevertheless, this disease affects salivary and lachrymal glands (*52*), and it could be thought that these type of alterations are easier to trace in saliva than other conditions, for which could not be possible the discovery of useful biomarkers. Then it is important to address here the important findings in a disease that is not directly related with the oral cavity, Breast Cancer (BC), where saliva was the sample of choice. A successful example is the study of Zhang and collaborators (*53*) (Table 1), where they discovered and validated eight mRNA biomarkers and a protein biomarker, having a 92% accuracy in the tested sample set.

It is then clear that saliva diagnostics is a powerful tool and at the same time a promising biofluid. The current status regarding ESCC salivaomics will be reviewed when available in the following sections for the three main current high throughput technologies: transcriptomics, proteomics, and metabolomics. For clarity, the most promising results in salivary biomarker discovery have been briefly resumed in Table 1.

2. Transcriptomics

Transcriptomics studies and quantifies the set of RNA molecules produced by the genome as a result of the environmental influences, or the developmental stage. A major question that has to be addressed is the stability of RNA in saliva. It is a common presumption that RNA cannot be stable in saliva (*54*) due to its labile nature and the presence of RNases in the oral cavity (*55*). A further complication for cancer studies is the reported higher activity of RNases in gastric cancer patients (*56*), leading to a higher degradation of total RNA in the oral cavity of affected subjects. If that described situation applies for other types of cancer, being ESCC of our interest, chances to find intact RNA are lower and thus the capability to discovery useful potential biomarkers will decrease vastly. There have been successful studies focusing on saliva as the sample material for oral squamous cell carcinoma (OSCC), for example the work of Li and collaborators (*55*) (Table 1), where they found more than 1,600 differentially expressed genes. However some other studies (*54*) have described that the observed signalling molecule was in fact DNA, not RNA, what complicates the analysis. Notwithstanding, Li and colleagues were the first ones to observe more than 3,000 different RNA transcripts in human saliva (*44*) (Table 1), according to what they report in a more recent study from their laboratory, in which Park and colleagues (*57*) (Table 1) further characterized the stability of RNA in saliva. This latter study tested whether informative RNA molecules exist in saliva or not through different molecular biology assays. As reported (*57*) , until 2004 most of the detected RNA had a viral or bacterial origin. In this study Park and colleagues (*57*) used a 22,283 cDNA probes microarray (Agilent Affymetrix Human Genome U133A) to test the complexity of several oral saliva samples in terms of number of distinct transcripts that could be detected, having found more than 6,000 in the whole saliva. Regarding stability, one of the possibilities that they indicate for the stability of RNA in saliva is the association with mucin, protein that would protect from degradation, as well as other type of macromolecules. Are there additional sources of cell free circulating RNA in saliva? Amidst the possible origins some authors have indicated apoptotic processes (*58*), while other studies report the presence of exosomes (*59,60*). In keeping with this last possibility, Ogawa and collaborators (*59*) (Table 1) found for the first time the presence of exosomal vesicles in whole saliva samples from humans.

For efficient biomarker discovery, the release of RNA from the apoptotic cells has to occur in a quantity that allows an early identification and efficient tracking of the disease. The appearance of RNAs in latter stages of the disease will not have such a clinical value for ESCC, as there are other available techniques that were mentioned in the previous section, and because of the current critical need for early markers. In that way, the presence of exosomes and their nature as a communication mean between distant cell types (*61-64*), can be a key point to exploit biomarker discovery. That would be of a great interest in the case of ESCC, as the chances for detecting apoptotic derived RNA may not be so big during early stages than in advanced ones, but still tumorigenic cells may be starting to derive RNA containing exosomes for communication while the lesion is not yet detectable.

More interesting developments related with saliva that focused on studying BC and their potential salivary biomarkers, were achieved by Zhang and collaborators

Table 1. Most promising advances regarding biomarker discovery in saliva

Methodology	Model of study	Discovery	Importance	*Ref.*
ELISA; sandwich EIA	pSS	Significantly increased levels of MMP-9/TIMP-1 and MMP-9 in pSS patients	Use of saliva to study differences between affected patients and healthy ones	Asatsuma *et al*. (*51*)
Affymetrix Human Genome U133A Array	Healthy subjects	3,000 different RNA transcripts in human saliva	Large scale methodology to study transcriptomics in saliva	Li *et al*. (*44*)
Affymetrix Human Genome U133A Array	OSCC	1,600 differentially expressed genes	Differentially expressed genes between affected patients and healthy ones through large scale approach	Li *et al*. (*55*)
Affymetrix microarray platform/2D-DIGE	BC	Discovery and validation of eight mRNA, and a protein biomarker (92% accuracy)	Salivary biomarkers in a disease not related with oral cavity, broadening the field	Zhang *et al*. (*53*)
Affymetrix Human Genome U133A Array	Healthy subjects	Characterization of RNA stability in saliva	Observation of the association with mucin and other macromolecules, for protection against degradation	Park *et al*. (*57*)
Peptide sequencing/MALDI-TOF-MS	Healthy subjects	Exosomes in saliva samples	First time report of exosomal vesicles in whole saliva samples from humans	Ogawa *et al*. (*59*)
miRNA microarray	EC	Different miRNA profiles in saliva derived from healthy patients and affected ones	Four validated miRNA biomarkers in EC	Xie *et al*. (*70*)
RNAseq	Healthy subjects	20-25% of sequenced reads that align to the human genome, while another 30% aligns to HOMD	First whole RNAseq in saliva samples from healthy human subjects, methodology to differentiate microbiota from human moiety	Spielmann *et al*. (*43*)
RNAseq	Healthy subjects	Human oral and gut microbiome and transcriptome differences	Establishment of patient self-collection of samples	Franzosa *et al*. (*72*)
RNAseq	PD	Oral metabiome differences between healthy microbiome and disease microbiome	Found differences in the diversity of the community between disease and healthy states	Jorth *et al*. (*73*)
RNAseq	Healthy subjects	exRNAs as micro RNA, Piwi-interacting RNA, and circular RNA	Characterization of diverse RNA species from saliva.	Bahn *et al*. (*74*)
Peptide sequencing/MS	Healthy subjects	Characterization of the salivary metaproteome	First catalogue of metaproteome, serving as a reference for future studies	Jagtap *et al*. (*76*)
Subtractive proteomics approach, combination of separation techniques: LC, LC-MS/MS, QqTOF MS	OSCC	Differential levels of proteins between healthy and affected patients	Verification of results in independent set of patients and healthy subjects, promising biomarkers	Hu *et al*. (*81*)
CE-TOF-MS	BC, OC, PC, PD	57 metabolites for accurate prediction of the probability of each disease	Shows the feasibility to obtain valuable information and biomarkers from saliva, in a variety of cancer diseases	Sugimoto *et al*. (*85*)

ELISA: enzyme-linked immunosorbent assay; EIA: enzyme immunoassay; pSS: primary Sjögren's syndrome; MMP-9: metalloproteinase-9 ; TIMP-1: tissue inhibitor of metalloproteinase-1; 2D-DIGE: two-dimensional difference gel electrophoresis; BC: Breast Cancer; OSCC: Oral Squamous Cell Carcinoma; MALDI-TOF-MS: matrix-assisted laser desorption/ionization time-of-flight mass spectrometry; EC: Oesophageal Cancer; PD: periodontal disease; HOMD: Human Oral Microbiome Database; exRNAs: extracellular RNAs; LC: liquid chromatography; MS: mass spectrometry; QqTOF: quadrupole-quadrupole-time-of-flight; CE: Capillary Electrophoresis; OC: oral cancer; PC: pancreatic cancer.

(*53*) (Table 1) through a microarray platform. Amidst their results, it was found that 1,402 genes had > 2 fold up-regulation, while 2,447 > 2 fold down-regulation in their saliva samples. Their findings indicate that saliva is a relatively good source of transcripts for biomarker discovery when comparing affected subjects to healthy ones. A further selection of the 27 top up-regulated candidates based on p-value and fold-change ($p < 0.01$, fold change > 10) allowed them to select potential candidates, that in the next stage of their

study were validated through RT-PCR. This last assay rendered 11 positive genes out of 27 genes. To be able to complete their study, the 11 candidates were tested in an independent sample (30 BC patients, 63 controls), having found 8 pre-validated markers (*53*).

Microarray is a platform that despite its limitations or a lower resolution compared with RNAseq, the new high throughput platform for transcriptomics, can be still very useful for studies in saliva, as it has been demonstrated in the reviewed papers using this approach in miRNA ESCC profiles. If a search over the studies that focused on ESCC and microarrays is performed directly in Gene Expression Omnibus (GEO) using the keywords "ESCC" and "array", the outcome gives back more than 300 results. However, up to date and to our knowledge, no study in the salivary ESCC transcriptome has been performed using this platform yet, according to the last bibliographic searches performed using keywords as "saliva", "microarray", and "ESCC" or "oesophageal squamous cell carcinoma". The exception to that comes from several studies that focused in miRNA characterization and identification using salivary samples (as well as tissues).

In one of those studies, Ishibashi and colleagues (*65*) used a microarray platform to analyse ESCC expression profiles between normal and cancer affected samples from 12 individuals. The 24 paired samples come either from the tumour area with more than 80% of tumour cells, or from normal tissue at least 4 cm away from the affected zone. An interesting option for microarray analysis in ESCC, has been the comparison of tumour cells with cell lines overexpressing an important gene for tumour progression (*66*), or a different splice variant (*67*), as it can aid to clear many questions about the development of the disease. Both of these studies have been carried out in the same laboratory, and show the potential of transcriptomics, as well as other type of complementary technologies, to address fundamental questions in molecular biology being an alternative for obtaining a higher resolution profile than classic approaches.

Identification of miRNAs in ESCC has been a promising research area with a number of studies published in the field. Matushima *et al*. (*68*) have studied ESCC cell lines that were moderate and well differentiated, as well as a control squamous epithelial oesophageal line, through a microarray platform for miRNA. Besides, they have performed functional studies increasing or decreasing the expression of miR-205, a miRNA overexpressed exclusively in ESCC cell lines. Additional assays included estimation of wound healing, cellular invasion and migration, or evaluation of the regulation target, that in this case was zinc finger E-box binding homeobox 2 (*ZEB2*). An important feature of the work of Guo and collaborators (*69*), is that they obtained the distinct miRNA profiles for ESCC tumour samples in frozen archival tissues, having obtained 46 differentially expressed ones. They established a minimum set of 7 that can differentiate between cancer and normal tissues. Despite the degradation, miRNA profiles in these stored samples were displaying similar values to that of fresh tissues, enlightening the use of the extensive tissue archives to gain better understanding of the disease. Some significant examples with saliva samples can be found in the recent work of Xie and collaborators (*70*), where they found different miRNA profiles in saliva derived from healthy patients and Oesophageal Cancer (EC) affected individuals, with four of them validated in a set of independent individuals, through a miRNA microarray. According to them, their work has been the first to assess the miRNA content in EC. Comparing both of the above mentioned studies, it seems that saliva renders less information, though is still valuable resource for biomarker discovery in terms of miRNAs. As it was pointed out by Xie (*70*), saliva can be considered an end point of blood circulation, having a certain degree of representation of the molecules in blood, stating that it serves for diagnostic purposes. Further broadening this point, Wang and collaborators (*71*) carried out a meta-analysis in several papers studying ESCC miRNA profiles in Asian populations, including that of Xie *et al.* (*70*). They observed that miRNA profiles in blood have a bigger diagnostic accuracy than those derived from saliva. Despite this observation, miRNA based diagnostics is a promising field in saliva (as well as blood), due to the higher stability, reproducibility, correlated concentrations to some types of cancers, or ease of detection through RT-qPCR (*71*).

Within the new RNAseq methodologies there have been promising discoveries focusing on saliva, as the work of Spielmann and colleagues (*43*) (Table 1), in which they highlight the power of salivary transcriptome as a diagnostic tool for human diseases using a massive RNA sequencing approach. With a similar methodological approach, Franzosa (*72*) (Table 1) revealed the importance of RNA studies in related locations to ESCC within human body by studying human oral and gut microbiome and transcriptome. The work of Spielmann and collaborators (*43*) is the first whole RNAseq in saliva samples from healthy human subjects, broadening to new studies in the field that will focus on the differences between healthy and affected samples. Both types of approaches have not been used in ESCC yet, and could therefore pose a great source of different biomarker tools. As it was mentioned above, the oral microbiome is an important part to consider when studying saliva. Spielmann and collaborators (*43*) report a 20-25% of sequenced reads that align to the human genome, while another 30% aligns to the Human Oral Microbiome Database (HOMD). They have detected more than 4,000 genes (coding and non-coding), while

structural integrity of the transcripts was conserved (*43*). Considering the potential of the metabiome as a diagnostic tool, there has been a close study in the oral metabiome between healthy and affected patients of periodontal disease (*73*) (Table 1), having found differences in the diversity of the community in both cases. A very interesting suggestion was that metabolic pathways are conserved while there are geographical, ethnical, and food consuming factors that may alter the species presence. If this gets demonstrated, we may expect that microbiome in ESCC affected patients displays different expression patterns to that one observed in healthy subjects, and this could serve as a prognostic marker for the development of the disease. Another study using RNAseq in salivary samples was performed afterwards by Bahn and colleagues (*74*) (Table 1). They carried out a similar massive study on the cell free component of salivary samples than that of Spielmann (*43*), but focused on extracellular RNAs (exRNAs) as micro RNA, Piwi-interacting RNA, and circular RNA.

3. Proteomics

The development of proteomics has been notable in different body fluids as urine, blood and saliva, as Amado and colleagues (*75*) have indicated. One of the features that they highlighted was the convenience of adding proteases inhibitors, due to the presence of proteases from bacteria and saliva which may affect the downstream procedure. As it has been already mentioned in the introduction, most of the proteins in saliva (90%) are shared with blood, but they represent only 15% w/w (*41*), while there have been studies reporting that 20-30% of the proteins in saliva can be found also in plasma (*45,46*). An interesting question that arises in here, and in agreement with Amado (*75*), is about how many of those proteins belong to the human moiety, or to the metabiome. An answer to that question was obtained by Jagtap and collaborators (*76*) (Table 1), in a deep study of the salivary metaproteome of healthy subjects, where they found that most of the detected proteins had a human origin, being non-human peptides present in much lower quantities. Additionally they determined over 200 different bacterial species. Their focus was the salivary supernatant, which largely remains free of bacterial component, as the pellet fraction collects the bacteria present in the oral cavity after the initial centrifugation. Even though, by using pooled samples from 6 individuals, they were able to find bacterial peptides in this fraction. Besides these significant discoveries, their study can serve as a reference for future studies that will focus on the differences between healthy subjects and those affected by a disease, especially ESCC. An extensive review on the topic was written by Uemura and collaborators (*77*), which focuses on the proteomics advances regarding EC in its two main forms, ESCC and EAC. This thorough revision of the bibliography, gives a precise idea of the status until 2014 of the usage of proteomics for different downstream applications, such as early detection, prediction of lymph node metastasis, therapy response prediction, prognostic prediction, as well as the applications in the development of novel therapeutics, or the elucidation of molecular mechanisms of action. Although all of those studies reviewed by Uemura are focused mainly on serum or biopsy samples from ESCC or EAC tissues, they give a complete perspective on what has been done until date using the available proteomic approaches. Equally as interesting, is the review written in 2012 by Qi *et al*. (*78*) which focused exclusively on ESCC proteomics, yet there were no reported studies using saliva as the source for proteins.

One of the included studies in the paper from Qi, was a proteomic profiling of cancer tissues from Chinese ESCC subjects, carried out by Du and collaborators (*79*), who found differential expression of 22 proteins (17 up- and 5 down-regulated) through MALDI-TOF (Matrix-Assisted Laser Desorption/ ionization- Time of Flight) or LC-ESIT-IT MS (Liquid Chromatography-Electrospray/Ionization Ion Trap) approaches. According to Uemura (*77*), this work can be classified into the group of prognostic prediction biomarkers, considering that one of their findings was a correlation between poor prognosis and the expression levels of calreticunin, and 78-kDA glucose-regulated protein (GRP78) (*79*). The biological functions that were represented in the differentially expressed proteins are related with terms as glycolysis, regulation of transcription, cell proliferation, cell motility or cell signal transduction among others, what is related with the kind of processes that occur within a group of malignant cells, for example the Warburg effect (*80*).

But coming back to the field of salivaomics, one interesting approach was followed by Hu and colleagues, who used saliva as the source material to study the proteome of 64 healthy subjects compared with another group of 64 affected patients, although the disease in this case was OSCC (*81*) (Table 1). The methodology included a subtractive proteomics approach for their in-depth study, through a combination of separation techniques such as LC and LC-MS/MS, together with a QqTOF MS. About the methodologies, further explanation of the techniques can be consulted in the two above mentioned reviews from Uemura (*77*) and Qi (*78*). In their study Hu and colleagues concluded with a verification of their experimental results, being promising targets for biomarker discovery in OSCC. Regarding saliva and ESCC, we were not able to find studies relating both, only the reported ones using saliva in related affections as OSCC. This situation makes proteomic biomarker discovery in ESCC a promising and unexplored field of research.

4. Metabolomics

A remarkable review about the application of metabolomics for biomarker discovery can be found in the work of Armitage and Barbas (*82*). They have highlighted a variety of key pathways that are altered in cases of cancer, but considering all the potentially involved metabolites there is no current platform that can detect all of them at the same time. The choice of analytical platform can range between the two main techniques used in metabolomics analysis, one of them being MS (Mass Spectrometry) based approaches, with a deep profiling capacity; and NMR (Nuclear Magnetic Resonance). The latter has the advantage of being fast and reproducible (*83*), while there is no need to disrupt the tissues or samples, a feature that can be used for *in vivo* studies as showed by Morvan and Demidem (*84*), where they analysed the response of tumours to a chemotherapy treatment in tissues and mice. Albeit these advantages, it shows lower resolution than MS based choices, for which there have been advances in separation techniques with the coupling of MS to different complementary methodologies, for example CE-MS (Capillary Electrophoresis), GC-MS (Gas Chromatography), or LC-MS (Liquid Chromatography) (*82*).

Unfortunately, up to date there have been no published studies on metabolite analysis in saliva of ESCC patients. However some works as that of Sugimoto *et al*. (*85*) (Table 1), used the saliva of subjects affected in breast (30 subjects), oral (69 subjects), and pancreatic cancers (18 subjects), as well as periodontal disease (11 subjects), compared with a set of 87 healthy ones. In their approach they used a combination of CE-TOF-MS methodologies, having found a set of 57 metabolites for accurate prediction of the probability of each disease. Moreover, they show that it is possible to obtain valuable metabolomic information and biomarkers from saliva, in a variety of cancer diseases that affect other areas of the human body than oral cavity. One of the important metabolites discovered, choline, is relevant because choline-containing metabolites participate in phospholipid metabolism of cell membranes, and that has been associated to malignancy, as it has been reported by other authors that is a reflection of the increased proliferation state of tumorigenic cells.

A recent review has been published by Abbassi Ghadi (*86*) focused on studies using any type of sample in gastric and oesophageal cancers, being the most interesting studies for ESCC salivaomics, those performed in biofluids as serum or urine. The variety of analytical platforms from the studies included in this review range from GC-MS, High Resolution-Magic Angle Spinning-NMR, CE-MS, LC-MS, and Selected Ion Flow Tube-Mass Spectrometry. Due to the inherent differences in each platform, sensitivity, sample preparation, or type of sample source, there was a notable variability among the reviewed references, having found that glutamine is the most consistent biomarker for both cancers across many studies. An interesting idea highlighted by these authors is that potentially useful biomarkers should be further tested in other analytical platforms, and using different statistical approaches, to lower as much as possible the false positives discovery.

Wu and colleagues (*87*) focused on the screening of 20 paired samples from the same patients affected by EC (18 ESCC and 2 EAC), including both non-affected tissue and tumour samples (with at least 90% cancer cells), resulting in the identification of 20 metabolites through GC-MS. Other metabolomics studies focusing exclusively on ESCC as the disease model, include the one from Yang and collaborators (*88*), where they have studied the profile changes in ESCC tumours at different stages derived from tissue samples using a NMR based approach. They have addressed, according to their results, the possibility that some metabolic changes arises before any morphological alterations could be detected, and that is precisely what could pose an advantage in the early screening of this disease. Jin and collaborators (*89*) have pointed out that ESCC metastasis advances primarily through the lymphatic system, acting as well as a key prognostic factor. In their study they used GC-MS to elucidate the possible alterations in a set of ESCC serum samples (including metastatic and non-metastatic ones), versus healthy controls. One of the key elements of their study was the evaluation of the metabolomics differences in those subjects with lymph node metastasis. They have found a marked Warburg effect (*80*) on ESCC cells due to the enhanced glycolysis, which leads to decreased levels of glucose and glutamine in blood, as well as a notably higher content of lactic acid. This last metabolite was found in higher quantities in those patients with lymph node metastasis than non-metastatic ESCC subjects. Some other metabolites usually associated with tumour cells, are for example the observed increased levels of certain long chain fatty acids, that could be derived from a stronger *de novo* fatty acid biosynthesis, with some fatty acids being up-regulated in the metastatic samples compared with non-metastatic ones. Glutamine is another metabolite that was found to be decreased in metastatic cells, at its lowest levels from the three groups. They demonstrated that a combination of altered metabolites in cancer cases, could be used as a metabolomic signature for discrimination between patients in different stages.

Xu and collaborators (*90*) studied the metabolomics differences in ESCC, through a RR-LC-MS (Rapid Resolution) platform. They analysed different blood samples from healthy and affected patients, as well as other samples derived from ESCC patients that underwent a chemoradiotherapy treatment, being

divided in two groups, Overall Responders and non-Overall Responders. Among their results, 11 of the discovered metabolites were classified as tentatively potential biomarkers, while another set of 18 metabolites were classified in other group that potentially will serve as biomarkers for the diagnosis of ESCC. In keeping with the results from the study of Jin, there was an observation of an abnormality in the levels of several fatty acids. A similar finding was reported by Liu *et al*. (91), who used peripheral blood in order to isolate cell-free plasma through a UPLC-ESI-TOF-MS (ultraperformance liquid chromatography-electrospray ionization-accurate time-of-flight) platform, having found 6 metabolites related with the phospholipids metabolism, out of 11 potential metabolite biomarkers.

5. Conclusion

Despite the potential drawbacks that saliva may have, as lower representation of molecules that could be used as biomarkers in comparison with other body fluids, a higher degree of degradation of its components due to the exposure of the oral cavity to the open environment, or an enhanced RNase activity as reported for some cancer types, it has been demonstrated by many authors that it is possible to use saliva as a sample source, as it has been reviewed through this text.

Amidst its many advantages, it is an easily accessible biofluid, that fulfil the requirements for fast and efficient collection for many hospital settings all over the world, with minimum storage and biosecurity measurements, while it represents a non-invasive way to test patients, increasing their well-being. Once that the biomarkers have been validated and approved for their clinical use, the type of analysis that can be carried out to test for the different molecules as metabolites, proteins, or transcripts are relatively easy performed with minimum technical requirements. It is only for the discovery of those biomarkers when sophisticated and dedicated technologies must be applied.

For example, the transcription levels for given expression biomarkers can be carried out through RT-qPCR an accurate and quick method available at any diagnostic facility nowadays. In the case of proteins or metabolites, a targeted approach can be followed as well, what makes analyses more affordable. In agreement with the reviewed bibliography, we can conclude that a panel of biomarkers that cover the three main omics will have more discriminating power than focusing on measuring separately gene or miRNA expression, proteins, or metabolites.

There has not been a great development of salivaomics in ESCC patients despite the successful stories from other type of cancers, except for those efforts in miRNA analysis of saliva. Thus, it is a promising field for ESCC biomarker discovery with enough room for improvement.

Acknowledgements

This work has been funded by the Ministry of Education and Science of the Republic of Kazakhstan.

References

1. McCabe ML, Dlamini Z. The molecular mechanisms of oesophageal cancer. Int Immunopharmacol. 2005; 5:1113-1130.
2. Greenawalt DM, Duong C, Smyth GK, Ciavarella ML, Thompson NJ, Tiang T, Murray WK, Thomas RJS, Phillips WA. Gene expression profiling of esophageal cancer: Comparative analysis of Barrett's esophagus, adenocarcinoma, and squamous cell carcinoma. Int J Cancer. 2007; 120:1914-1921.
3. Daly JM, Fry WA, Little AG, Winchester DP, McKee RF, Stewart AK, Fremgen AM. Esophageal cancer: Results of an American College of Surgeons patient care evaluation study. J Am Coll Surg. 2000; 190:562-572.
4. Vaughan TL. From genomics to diagnostics of esophageal adenocarcinoma. Nat Genet. 2014; 46:806-807.
5. Hu YC, Lam KY, Law S, Ying Chuan Hu, King Yin Lam, Law S, Wong J, Srivastava G. Identification of differentially expressed genes in esophageal squamous cell carcinoma (ESCC) by cDNA expression array: Overexpression of Fra-1, Neogenin, Id-1, and CDC25B genes in ESCC. Clin Cancer Res. 2001; 7:2213-2221.
6. Jiang Y, Li Q, Zhao J, Lv J. Identification of a novel fusion gene (HLA-E and HLA-B) by RNA-seq analysis in esophageal squamous cell carcinoma. Asian Pac J Cancer Prev. 2014; 15:2309-2312.
7. Takikita M, Hu NAN, Shou JZ, Giffen C, Wang QH, Wang C, Hewitt SM, Taylor PR. Fascin and CK4 as biomarkers for esophageal squamous cell carcinoma. Anticancer Res. 2011; 31:945-952.
8. Moghanibashi M, Jazii FR, Soheili ZS, Zare M, Karkhane A, Parivar K, Mohamadynejad P. Proteomics of a new esophageal cancer cell line established from Persian patient. Gene. 2012; 500:124-133.
9. Noori S, Monabati A, Ghaderi A. The prevalence of human papilloma virus in esophageal squamous cell carcinoma. Iran J Med Sci. 2012; 37:126-133.
10. Lin Y, Totsuka Y, He Y, Kikuchi S, Qiao Y, Ueda J, Wei W, Inoue M, Tanaka H. Epidemiology of esophageal cancer in Japan and China. J Epidemiol. 2013; 23:233-242.
11. Rakhimova S, Akilzhanova A, Zhukov Y, Omarov M, Zhumadilov Z. Esophageal cancer in Kazakhstan: Multi-omic research challenges. Cent Asian J Glob Heal. 2014; 3:3-4.
12. Su H, Hu N, Yang HH, Wang C, Takikita M, Wang Q-H, Giffen C, Clifford R, Hewitt SM, Shou JZ, Goldstein AM, Lee MP, Taylor PR. Global gene expression profiling and validation in esophageal squamous cell carcinoma and its association with clinical phenotypes. Clin Cancer Res. 2011; 17:2955-2966.
13. Xie GX, Chen TL, Qiu YP, Shi P, Zheng XJ, Su MM, Zhao AH, Zhou ZT, Jia W. Urine metabolite profiling offers potential early diagnosis of oral cancer. Metabolomics. 2012; 8:220-231.
14. Zhang A, Sun H, Wang P, Wang X. Salivary proteomics in biomedical research. Clin Chim Acta. 2013; 415:261-

265.
15. Takeshita N, Hoshino I, Mori M, Akutsu Y, Hanari N, Yoneyama Y, Ikeda N, Isozaki Y, Maruyama T, Akanuma N, Komatsu A, Jitsukawa M, Matsubara H. Serum microRNA expression profile: miR-1246 as a novel diagnostic and prognostic biomarker for oesophageal squamous cell carcinoma. Br J Cancer. 2013; 108:644-652.
16. Barber TW, Duong CP, Leong T, Bressel M, Drummond EG, Hicks RJ. ^{18}F-FDG PET/CT has a high impact on patient management and provides powerful prognostic stratification in the primary staging of esophageal cancer: A prospective study with mature survival data. J Nucl Med. 2012; 53:864-871.
17. Li Y, Zhang Q, Peng B, Shao Q, Qian W. Identification of glutathione S-transferase omega 1 (GSTO1) protein as a novel tumor-associated antigen and its autoantibody in human esophageal squamous cell carcinoma. Tumor Biol. 2014; 1:10871-10877.
18. Chen B, Fang WK, Wu ZY, Xu XE, Wu J, Fu JH, Yao XD, Huang JH, Chen JX, Shen JH, Zheng CP, Wang SH, Li EM, Xu LY. The prognostic implications of microvascular density and lymphatic vessel density in esophageal squamous cell carcinoma: Comparative analysis between the traditional whole sections and the tissue microarray. Acta Histochem. 2014; 116:646-653.
19. Mariette C, Balon JM, Piessen G, Fabre S, Van Seuningen I, Triboulet JP. Pattern of recurrence following complete resection of esophageal carcinoma and factors predictive of recurrent disease. Cancer. 2003; 97:1616-1623.
20. Zhang X, Lin P, Zhu ZH, Long H, Wen J, Yang H, Zhang X, Wang DF, Fu JH, Fang Y, Rong TH. Expression profiles of early esophageal squamous cell carcinoma by cDNA microarray. Cancer Genet Cytogenet. 2009; 194:23-29.
21. Yokoyama A, Omori T, Yokoyama T. Risk appraisal and endoscopic screening for esophageal squamous cell carcinoma in Japanese populations. Esophagus. 2007; 4:135-143.
22. Cheng KK, Day NE. Nutrition and esophageal cancer. Cancer Causes Control. 1996; 7:33-40.
23. Takezaki T, Shinoda M, Hatooka S, Hasegawa Y, Nakamura S, Hirose K, Inoue M, Hamajima N, Kuroishi T, Matsuura H, Tajima K. Subsite-specific risk factors for hypopharyngeal and esophageal cancer (Japan). Cancer Causes Control. 2000; 11:597-608.
24. Cao F, Han H, Zhang F, Wang B, Ma W, Wang Y, Sun G, Shi M, Ren Y, Cheng Y. HPV infection in esophageal squamous cell carcinoma and its relationship to the prognosis of patients in northern China. Sci World J. 2014; 2014:804738.
25. Hu JM, Li L, Chen YZ, Pang LJ, Yang L, Liu CX, Zhao J, Chang B, Zou H, Qi Y, Liang WH, Li F. Human papillomavirus type 16 infection may be involved in esophageal squamous cell carcinoma carcinogenesis in Chinese Kazakh patients. Dis Esophagus. 2013; 26:703-707.
26. Liyanage SS, Li Q, Zheng Y, *et al*. The relationship between Human Papillomavirus and oesophageal squamous cell carcinoma in China – A review of the evidence. AID. 2013; 3:17-34.
27. Atkinson AJJ, Colburn WA, DeGruttola VG, DeMets DL, Downing GJ, Hoth DF, Oates JA, Peck CC, Schooley RT, Spilker BA, Woodcock J, Zeger SL. Biomarkers and surrogate endpoints: Preferred definitions and conceptual framework. Clin. Pharmacol Ther. 2001; 69:89-95.
28. Strimbu K, Tavel JA. What are biomarkers? Curr Opin HIV AIDS. 2010; 5:463-466.
29. Fernie AR, Trethewey RN, Krotzky AJ, Willmitzer L. Metabolite profiling: From diagnostics to systems biology. Nat Rev Mol Cell Biol. 2004; 5:763-769.
30. Han X, Aslanian A, Yates JR. Mass spectrometry for proteomics. Curr Opin Chem Biol. 2008; 12:483-490.
31. Baye TM, Abebe T, Wilke RA. Genotype-environment interactions and their translational implications. Per Med. 2011; 8:59-70.
32. Wang Z, Gerstein M, Snyder M. RNA-Seq: A revolutionary tool for transcriptomics. Nat Rev Genet. 2009; 10:57-63.
33. Holmes E, Wilson ID, Nicholson JK. Metabolic phenotyping in health and disease. Cell. 2008; 134:714-717.
34. Zhang A, Sun H, Yan G, Wang P, Wang X. Metabolomics for biomarker discovery: Moving to the clinic. Biomed Res Int. 2015. DOI:10.1155/2015/354671.
35. Zhang A, Sun H, Wang P, Han Y, Wang X. Recent and potential developments of biofluid analyses in metabolomics. J Proteomics. 2012; 75:1079-1088.
36. Cowin PA, Anglesio M, Etemadmoghadam D, Bowtell DDL. Profiling the cancer genome. Annu Rev Genomics Hum Genet. 2010; 11:133-159.
37. Bonne NJ, Wong DT. Salivary biomarker development using genomic, proteomic and metabolomic approaches. Genome Med. 2012; 4:82.
38. Zhang Y, Sun J, Lin C-C, Abemayor E, Wang MB, Wong DT. The emerging landscape of salivary diagnostics. Oral Health Dent Manag. 2014; 13:200-210.
39. Romano-Keeler J, Wynn JL, Maron JL. Great expectorations: The potential of salivary "omic" approaches in neonatal intensive care. J Perinatol. 2014; 34:169-173.
40. Aps JKM, Martens LC. The physiology of saliva and transfer of drugs into saliva. Forensic Sci Int. 2005; 150:119-131.
41. Castagnola M, Cabras T, Vitali A, Sanna MT, Messana I. Biotechnological implications of the salivary proteome. Trends Biotechnol. 2011; 29:409-418.
42. Takeda I, Stretch C, Barnaby P, Bhatnager K, Rankin K, Fub H, Weljie A, Jha N, Slupsky C. Understanding the human salivary metabolome. NMR Biomed. 2009; 22:577-584.
43. Spielmann N, Ilsley D, Gu J, Lea K, Brockman J, Heater S, Setterquist R, Wong DTW. The human salivary RNA transcriptome revealed by massively parallel sequencing. Clin Chem. 2012; 58:1314-1321.
44. Li Y, Zhou X, St. John MAR, Wong DTW. RNA profiling of cell-free saliva using microarray technology. J Dent Res. 2004; 83:199-203.
45. Yan W, Apweiler R, Balgley BM, *et al*. Systematic comparison of the human saliva and plasma proteomes. Proteomics Clin Appl. 2009; 3:116-134.
46. Bandhakavi S, Stone MD, Onsongo G, Van Riper SK, Griffin TJ. A dynamic range compression and three-dimensional peptide fractionation analysis platform expands proteome coverage and the diagnostic potential of whole saliva. J Proteome Res. 2009; 8:5590-5600.
47. Dewhirst FE, Chen T, Izard J, Paster BJ, Tanner ACR, Yu W-H, Lakshmanan A, Wade WG. The human oral microbiome. J Bacteriol. 2010; 192:5002-5017.
48. Turnbaugh PJ, Turnbaugh PJ, Ley RE, Ley RE, Hamady

M, Hamady M, Fraser-Liggett CM, Fraser-Liggett CM, Knight R, Knight R, Gordon JI, Gordon JI. The human microbiome project. Nature. 2007; 449:804-810.
49. Walsh RJ, Sek WK, Yao Y, Jallal B, Kiener PA, Pinkus JL, Beggs AH, Amato AA, Greenberg SA. Type I interferon-inducible gene expression in blood is present and reflects disease activity in dermatomyositis and polymyositis. Arthritis Rheum. 2007; 56:3784-3792.
50. Wakugawa M, Nakamura K, Kakinuma T, Onai N, Matsushima K, Tamaki K. CC chemokine receptor 4 expression on peripheral blood CD4+ T cells reflects disease activity of atopic dermatitis. J Invest Dermatol. 2001; 117:188-196.
51. Asatsuma M, Ito S, Watanabe M, Takeishi H, Nomura S, Wada Y, Nakano M, Gejyo F, Igarashi A. Increase in the ratio of matrix metalloproteinase-9 to tissue inhibitor of metalloproteinase-1 in saliva from patients with primary Sjögren's syndrome. Clin Chim Acta. 2004; 345:99-104.
52. Borchers AT, Naguwa SM, Keen CL, Gershwin ME. Immunopathogenesis of Sjögren's syndrome. Clin Rev Allergy Immunol. 2003; 25:89-104.
53. Zhang L, Xiao H, Karlan S, Zhou H, Gross J, Elashoff D, Akin D, Yan X, Chia D, Karlan B, Wong DT. Discovery and preclinical validation of salivary transcriptomic and proteomic biomarkers for the non-invasive detection of breast cancer. PLoS One. 2010; 5:1-7.
54. Kumar S V, Hurteau GJ, Spivack SD. Validity of messenger RNA expression analyses of human saliva. Clin Cancer Res. 2006; 12:5033-5039.
55. Li Y, St John MA, Zhou X, Kim Y, Sinha U, Jordan RC, Eisele D, Abemayor E, Elashoff D, Park NH, Wong DT. Salivary transcriptome diagnostics for oral cancer detection. Clin Cancer Res. 2004; 10:8442-8450.
56. Kharchenko SV, Shpakov AA. Regulation of the RNAse activity of the saliva in healthy subjects and in stomach cancer. Izv Akad Nauk SSSR Biol. 1989; 1:58-63.
57. Park NJ, Li Y, Yu T, Brinkman BMN, Wong DT. Characterization of RNA in saliva. Clin Chem. 2006; 52:988-94.
58. Tzimagiorgis G, Michailidou EZ, Kritis A, Markopoulos AK, Kouidou S. Recovering circulating extracellular or cell-free RNA from bodily fluids. Cancer Epidemiol. 2011; 35:580-589.
59. Ogawa Y, Kanai-Azuma M, Akimoto Y, Kawakami H, Yanoshita R. Exosome-like vesicles with dipeptidyl peptidase IV in human saliva. Biol Pharm Bull. 2008; 31:1059-1062.
60. Palanisamy V, Sharma S, Deshpande A, Zhou H, Gimzewski J, Wong DT. Nanostructural and transcriptomic analyses of human saliva derived exosomes. PLoS One. 2010; 5:e8577.
61. Mathivanan S, Ji H, Simpson RJ. Exosomes: Extracellular organelles important in intercellular communication. J Proteomics. 2010; 73:1907-1920.
62. Braicu C, Tomuleasa C, Monroig P, Cucuianu A, Berindan-Neagoe I, Calin GA. Exosomes as divine messengers: Are they the Hermes of modern molecular oncology? Cell Death Differ. 2014; 22:34-45.
63. Liao J, Liu R, Yin L, Pu Y. Expression profiling of exosomal miRNAs derived from human esophageal cancer cells by solexa high-throughput sequencing. Int J Mol Sci. 2014; 15:15530-15551.
64. Raposo G, Stoorvogel W. Extracellular vesicles: Exosomes, microvesicles, and friends. J Cell Biol. 2013; 200:373-383.
65. Ishibashi Y, Hanyu N, Nakada K, Suzuki Y, Yamamoto T, Yanaga K, Ohkawa K, Hashimoto N, Nakajima T, Saito H, Matsushima M, Urashima M. Profiling gene expression ratios of paired cancerous and normal tissue predicts relapse of esophageal squamous cell carcinoma. Cancer Res. 2003; 63:5159-5164.
66. Wu B, Li C, Du Z, Zhou FEI, Xie J. Functional analysis of the mRNA profile of neutrophil gelatinase-associated lipocalin overexpression in esophageal squamous cell carcinoma using multiple bioinformatic tools. Mol Med Rep. 2014; 10:1800-1812.
67. Wu B, Lv G, Zou H, Du Z, Wu J. Exploration of potential roles of a new LOXL2 splicing variant using network knowledge in esophageal squamous cell carcinoma. The Scientific World Journal. 2014; 2014:431792.
68. Matsushima K, Isomoto H, Yamaguchi N, *et al*. MiRNA-205 modulates cellular invasion and migration *via* regulating zinc finger E-box binding homeobox 2 expression in esophageal squamous cell carcinoma cells. J Transl Med. 2011; 9:30.
69. Guo Y, Chen Z, Zhang L, *et al*. Distinctive microRNA profiles relating to patient survival in esophageal squamous cell carcinoma. Cancer Res. 2008; 68:26-33.
70. Xie Z, Chen G, Zhang X, Li D, Huang J, Yang C, Zhang P, Qin Y, Duan Y, Gong B, Li Z. Salivary MicroRNAs as Promising Biomarkers for Detection of Esophageal Cancer. PLoS One. 2013; 8:e57502.
71. Wang Y, Wang Q, Zhang N, Ma H, Gu Y, Tang H, Xu Z, Gao Y. Identification of microRNAs as novel biomarkers for detecting esophageal squamous cell carcinoma in Asians: A meta-analysis. Tumor Biol. 2014; 35:11595-11604.
72. Franzosa EA, Morgan XC, Segata N, Waldron L, Reyes J, Earl AM, Giannoukos G, Boylan MR, Ciulla D, Gevers D, Izard J, Garrett WS, Chan AT, Huttenhower C. Relating the metatranscriptome and metagenome of the human gut. Proc Natl Acad Sci U S A. 2014; 111:E2329-2338.
73. Jorth P, Turner KH, Gumus P, Nizam N, Buduneli N, Whiteley M. Metatranscriptomics of the human oral microbiome during health and disease. MBio. 2014; 5:1-10.
74. Bahn JH, Zhang Q, Li F, Chan T, Lin X, Kim Y, Wong DTW, Xiao X. The landscape of MicroRNA, Piwi-Interacting RNA, and Circular RNA in human saliva. Clin Chem. 2014; 230:221-230.
75. Amado FML, Ferreira RP, Vitorino R. One decade of salivary proteomics: Current approaches and outstanding challenges. Clin Biochem. 2013; 46:506-517.
76. Jagtap P, Mcgowan T, Bandhakavi S, Tu ZJ, Seymour S, Griffin TJ, Rudney JD. Deep metaproteomic analysis of human salivary supernatant. Proteomics. 2012; 12:992-1001.
77. Uemura N, Kondo T. Current advances in esophageal cancer proteomics. Biochim Biophys Acta (BBA)-Proteins Proteomics. 2014; 1584:687-695.
78. Qi YJ, Chao WX, Chiu JF. An overview of esophageal squamous cell carcinoma proteomics. J Proteomics. 2012; 75:3129-3137.
79. Du XL, Hu H, Lin DC, Xia SH, Shen XM, Zhang Y, Luo ML, Feng Y Bin, Cai Y, Xu X, Han YL, Zhan QM, Wang MR. Proteomic profiling of proteins dysregulated in Chinese esophageal squamous cell carcinoma. J Mol Med. 2007; 85:863-875.
80. Kim JW, Dang CV. Cancer's molecular sweet tooth and the Warburg Effect. Cancer Res. 2006; 66:8927-8930.

81. Hu S, Arellano M, Boontheung P, Wang J, Zhou H, Jiang J, Elashoff D, Wei R, Loo J, Wong DT. Salivary proteomics for oral cancer biomarker discovery. Clin Cancer Res. 2008; 14:6246-6252.
82. Armitage EG, Barbas C. Metabolomics in cancer biomarker discovery: Current trends and future perspectives. J Pharm Biomed Anal. 2014; 87:1-11.
83. Emwas AHM, Salek RM, Griffin JL, Merzaban J. NMR-based metabolomics in human disease diagnosis: Applications, limitations, and recommendations. Metabolomics. 2013; 9:1048-1072.
84. Morvan D, Demidem A. Metabolomics by proton nuclear magnetic resonance spectroscopy of the response to chloroethylnitrosourea reveals drug efficacy and tumor adaptive metabolic pathways. Cancer Res. 2007; 67:2150-2159.
85. Sugimoto M, Wong DT, Hirayama A, Soga T, Tomita M. Capillary electrophoresis mass spectrometry-based saliva metabolomics identified oral, breast and pancreatic cancer-specific profiles. Metabolomics. 2010; 6:78-95.
86. Abbassi-Ghadi N, Kumar S, Huang J, Goldin R, Takats Z, Hanna GB. Metabolomic profiling of oesophago-gastric cancer: A systematic review. Eur J Cancer. 2013; 49:3625-3637.
87. Wu H, Xue R, Lu C, Deng C, Liu T, Zeng H, Wang Q, Shen X. Metabolomic study for diagnostic model of oesophageal cancer using gas chromatography/mass spectrometry. J. Chromatogr. B Anal. Technol. Biomed. Life Sci. 2009; 877:3111-3117.
88. Yang Y, Wang L, Wang S, Liang S, Chen A, Tang H, Chen L, Deng F. Study of metabonomic profiles of human esophageal carcinoma by use of high-resolution magic-angle spinning 1H NMR spectroscopy and multivariate data analysis. Anal Bioanal Chem. 2013; 405:3381-3389.
89. Jin H, Qiao F, Chen L, Lu C, Xu L, Gao X. Serum metabolomic signatures of lymph node metastasis of esophageal squamous cell carcinoma. J Proteome Res. 2014; 13:4091-4103.
90. Xu J, Chen Y, Zhang R, Song Y, Cao J, Bi N, Wang J, He J, Bai J, Dong L, Wang L, Zhan Q, Abliz Z. Global and targeted metabolomics of esophageal squamous cell carcinoma discovers potential diagnostic and therapeutic biomarkers. Mol Cell Proteomics. 2013; 12:1306-1318.
91. Liu R, Peng Y, Li X, Wang Y, Pan E, Guo W, Pu Y, Yin L. Identification of plasma metabolomic profiling for diagnosis of esophageal squamous-cell carcinoma using an UPLC/TOF/MS platform. Int J Mol Sci. 2013; 14:8899-8911.

(Received July 3, 2015; Revised August 1, 2015; Accepted August 25, 2015)

Review

DOI: 10.5582/ddt.2015.01043

Evaluation of antithrombotic effect: Importance of testing components and methodologies

Junichiro Yamamoto[1,*], Yukinori Tamura[2], Yoshinobu Ijiri[3], Masahiro Iwasaki[4], Masahiro Murakami[5], Osamu Matsuo[6]

[1] *Laboratory of Physiology, Faculty of Nutrition, Kobe Gakuin University, Kobe, Japan;*
[2] *Department of Physiology and Regenerative Medicine, Faculty of Medicine, Kinki University, Osakasayama, Japan;*
[3] *Department of Health and Nutrition, Faculty of Health and Nutrition, Osaka Shoin Women's University, Osaka, Japan;*
[4] *Division of Metabolism and Clinical Nutrition, Kansai Electric Power Hospital, Fukushima-ku, Osaka, Japan;*
[5] *Laboratory of Pharmaceutics, Faculty of Pharmacy, Osaka Ohtani University, Osaka, Japan;*
[6] *Faculty of Medicine, Kinki University, Osakasayama, Japan.*

Summary **The beneficial antithrombotic effect of some dietary components may offer the most promising approach of prevention of cardiovascular diseases and arterial thrombosis. The major stumbling block in finding effective dietary components is the lack of physiologically relevant techniques which can detect potential antithrombotic effect in humans. The presently used platelet function and coagulation tests do not allow the assessment of global thrombotic status and their value in screening dietary components for antithrombotic effect is questionable. Most of these *in vitro* tests ignore the effect of flow and shear stress, thrombin generation and vascular endothelium, the major contributors to arterial thrombogenesis in humans. As a gold standard, we employed the helium-neon (He-Ne) laser-induced thrombosis test in murine carotid artery and mesenteric microvessels, as the pathomechanism of this test closely reflects arterial thrombogenesis in humans. Results obtained with laser thrombosis test were compared with various shear-induced *in vitro* platelet function tests which use native blood (Haemostatometry, Thrombotic Status Analyser, Global Thrombosis Test-GTT). Contribution of vascular endothelium to thrombogenesis was assessed by measuring flow-mediated vasodilation (FMV) *in vivo*. The combination of the two shear-induced ex vivo thrombosis tests (Haemostatometry and GTT) with FMV correlated most closely with the laser-thrombosis test. Our findings suggest that combining the commercially available point-of-care GTT with the FMV test could provide a better assessment of the overall thrombotic status than either of the two tests alone.**

Keywords: Global Thrombosis Test, shear-induced thrombosis, flow-mediated vasodilation, helium-neon laser-induced thrombosis, nutrients, traditional kampo medicine

1. Introduction

Prevention and treatment of arterial thrombotic disorders are very important socioeconomic challenges. Compared to the Western-type diet, the Mediterranean-style and the Vegetarian diets reduced the risk of arterial thrombosis and death from coronary heart disease in patients in secondary myocardial infarction prevention trials (*1-3*). Several nutrients (omega-3 fatty acids; red wine; onion, garlic, kiwi; chocolate, etc.) were shown to inhibit platelet function *in vitro* (*4*).

In finding dietary components with potential antithrombotic effect, the use of physiologically relevant techniques is of crucial importance. Only such test(s) which proved to be useful in clinical practice in detecting overall thrombotic status, predicting major adverse thrombotic events should be used for screening diet components and nutrients for antithrombotic effect.

**Address correspondence to:*
Dr. Junichiro Yamamoto, Laboratory of Physiology, Faculty of Nutrition, Kobe Gakuin University, 518 Arise, Igawadani-cho, Nishi-ku, Kobe 651-2180, Japan.
Present address: Emeritus Professor, Kobe Gakuin University, Kobe, Japan.
E-mail: yamamoto@nutr.kobegakuin.ac.jp

Despite platelets play a pivotal role in thrombosis, point-of-care platelet function tests failed to materialize clinical expectations. Tailoring antithrombotic medication based on monitoring platelet function by these tests did not improve clinical outcome (*5*). Numerous nutrients inhibited platelet aggregation induced *in vitro* by various soluble agonists but such effect did not manifest in antithrombotic effect in humans. Therefore, there is still a need to identify tests which accurately reflect the overall thrombotic status in humans. At present, prothrombotic status is assessed by measuring platelet aggregation to various soluble agonists (adenosine diphosphate, collagen, arachidonic acid, thrombin), and by using various biomarkers of coagulation and fibrinolysis and extrapolating the results. All these tests are carried out from anticoagulated blood samples, in which platelet activation do not generate thrombin. This approach has been much less rewarding than it was originally expected. Most of the platelet function tests in clinical use which measure platelet aggregation to various soluble agonists failed in cardiac patients guiding antithrombotic medication (*6*). It has been shown that only those tests, which take the high shear and flow conditions and the generation of thrombin by platelets into account, have relevance to the pathomechanism of occlusive arterial thrombosis *in vivo*. Here we compare results obtained by commonly-used platelet function tests performed from anticoagulated blood and those obtained using shear-induced thrombosis and thrombolysis test performed from non-anticoagulated blood. Numerous inconsistencies exist between the commonly used tests and also between these and the shear-induced thrombosis tests. Our findings show that the commonly used platelet function tests performed at low shear conditions and from anticoagulated blood do not reflect the overall thrombotic status, whilst the innovative shear-induced thrombosis tests performed from non-anticoagulated blood do (*7,8*).

In addition to referring those findings which were obtained by conventional platelet function tests and showed antiplatelet effect of various nutrients, here we focus on the techniques which enabled us to screen large number of fruits, vegetables and nutrients and identified those varieties, which had significant antithrombotic effect. This would provide better understanding of those technologies for assessment of antithrombotic status, leading to efficient discovery and development of an effective antithrombotic medicament.

2. Methodology

2.1. *Light transmittance aggregometry*

The technique has been described in details elsewhere (*9*). In citrate-anticoagulated blood sample, platelet activation and aggregation is induced by various soluble agonists, such as adenosine diphosphate, collagen, arachidonic acid, adrenalin, and thrombin. The following nutrients inhibited platelet aggregation to various agonists: berries, cocoa and dark chocolate, coffee, garlic, ginger, kiwi fruit, omega-3 fatty acids, onion, purple grape juice, red vine, white vine, tomato (*4*).

2.2. *PFA-100*

PFA-100 is a global test for primary haemostasis, performed from citrate-anticoagulated blood. The principle and the test details are described (*9*). The measured "closure time" was increased (platelet inhibition) by berries, cocoa and dark chocolate (*4*).

2.3. *Laser-induced thrombosis in the microcirculation and in the carotid artery*

Formation of platelet-rich thrombi and their embolization was initiated in the mouse carotid artery or the rat mesenteric microvessels using the He-Ne laser-induced thrombosis technique (*10,11*). He-Ne laser-induced thrombosis method has been previously described in detail (*12*). In brief, the mesenteric or pial microvessels of anaesthetized rats or the left femoral artery of anaesthetized mice, was exposed and Evans blue dye was injected through the jugular vein (rat) or tail vein (mice). The centre of the mesenteric or pial microvessel or the carotid artery was irradiated with laser, and the formation of a thrombus at the site of irradiation was monitored and recorded on videotape. Thrombotic status of rats was expressed by the number of thrombosis required to complete occlusion of blood flow and in mice expressed as the cumulative thrombus size. The latter was calculated by continuous observation of the thrombus mass every 10 seconds in the first 10 minutes after irradiation.

2.4. *Shear-induced platelet-rich thrombus formation in non-anticoagulated blood*

a) Haemostatometry Details of haemostatometry have been described previously (Figure 1A) (*13*). Briefly, non-anticoagulated blood was withdrawn from the abdominal aorta of animals and tested with a Haemostatometer purpose-built in Kobe Gakuin University. Blood was forced to flow through a plastic tube by paraffin oil replacement technique. While blood was flowing in it, the tubing was punched with a fine needle to induce "bleeding" from the holes into the surrounding warm saline. The perfusion pressure was monitored to assess the thrombotic reaction. Punching the tube caused a sharp drop in the perfusion pressure. Eventually "bleeding" stopped due to formation of platelet-rich haemostatic plugs in the holes and with this, the perfusion pressure returned to the pre-punching level. The recorded pressure changes reflect both the haemostatic and coagulation processes. In

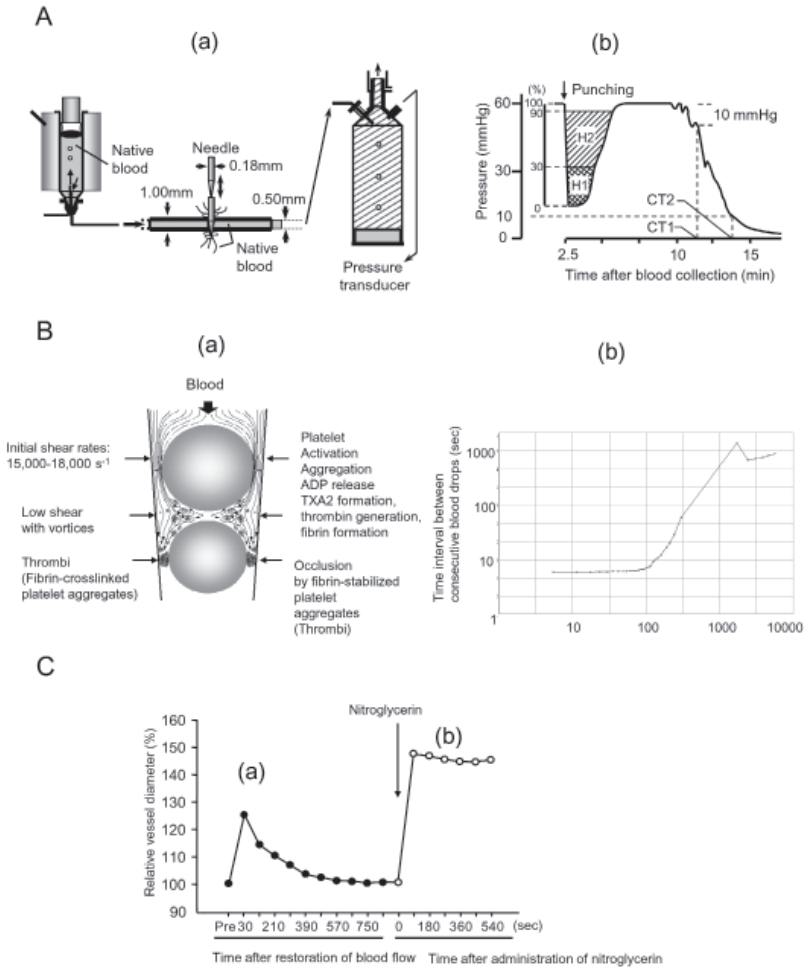

Figure 1. Shear-induced thrombosis/thrombolysis and endothelial function tests. (A) Principle of Haemostatometry (a); Haemostatogram (b). H1; H2: indices of platelet reactivity; CT1, CT2: indices of coagulation activity. **(B)** Principle of Global Thrombosis Test (GTT) (a); real-time recording of occlusion and lysis (b). OT: occlusion time (index of platelet reactivity); LT: lysis time (index of endogenous thrombolytic activity). **(C)** A typical pattern of flow-mediated endothelium dependent vasodilation (FMV) and endothelium independent vasodilation (NFV). FMV after restoration of blood flow (a); NFV after application of nitroglycerin (b).

the recorded pressure curve, areas of 30% (H1) and 90% (H2) pressure recovery reflect the primary and completed haemostasis. Increase or decrease of H1 and H2 reflected inhibition or enhancement of platelet reactivity, respectively.

b) Thrombotic Status Analyser Test (TSA) The principle of the TSA is similar to Haemostatometry. Punching a plastic tube to make a small hole was replaced by pre-existing small plastic tube with the diameter similar to the hole-size in Haemostatometry. Details have been described elsewhere (*7,8*).

c) Global Thrombosis Test (GTT) GTT (Thromboquest Ltd, London, UK) has been described in detail (*14*). Figure 1B shows the principle of the technique (a) and a typical recording (b). There are flat segments along the inner wall of a conical plastic tube and when a perfectly round stainless ball bearing (currently ceramic) is placed into such a conical tube, the flat segments prevent the ball bearing from occluding the lumen. When non-anticoagulated blood is added to such tube, it flows through the narrow gaps by the ball bearing and exits in droplets into an adjacent collecting tube. The latter is transilluminated by a light emitter and a sensor opposite the emitter generates a signal whenever a drop of blood interrupts the light path. In essence, the instrument detects the time interval (d; sec) between consecutive blood drops. Blood flows at 37°C by gravity through the narrow gaps formed between the upper ball bearing and the inner wall of the tube, where high shear stress activates and aggregates platelets. Platelet aggregates formed and then captured in the gaps by the lower ball bearing, arresting the blood flow. At the start, blood flow is rapid and hence (d) is small. Subsequently, the flow rate gradually decreases and hence (d) increases. When the actual (d) exceeds 15 seconds (occlusion-d), the instrument displays "Occlusion Time (OT)", which is the time elapsed from the detection of the first drop of blood until OT. Later, the blood flow is completely arrested. Eventually, due to thrombolysis, flow is restored as indicated by the detection of the first drop of blood after complete occlusion (Lysis Time- LT). Compared to controls, increased or decreased OT indicates inhibition

or enhancement of platelet reactivity, respectively. Increase or decrease of LT indicates inhibition or enhancement of spontaneous thrombolysis, respectively. The important characteristics of GTT are that GTT can measure platelet reactivity and thrombolytic activity simultaneously for a short time by simple technique.

2.5. *Flow-mediated Vasodilation test (FMV)*

FMV was used to assess endothelial function (*15-17*). We have adopted the endothelium-dependent and independent flow-mediated vasodilation technique to mice, as previously described in detail and a typical result is shown in Figure 1C (*18*). Baseline images of the diameter of the femoral artery of mice were taken before clamping and then at 30 sec intervals over 450 sec after restoration of blood flow. Nitroglycerin-mediated vasodilation was induced by placing 70 microliters of 2.2 mM nitroglycerin/saline solution on the artery. A typical pattern of vasodilation after restoration of flow was transferred to a computer and the artery diameter changes were calculated. Changes in vessel diameter after restoration of flow were expressed as percentage of the baseline values (before clamping) and the peak vasodilation was compared.

We used the above techniques to test extract of a variety of carrots (*19*), rice (*20*), strawberries (*21*), tomatoes (*22,23*) and grapes (*24*) for antithrombotic effect. From the several varieties tested, we could find some, which had significant experimental antithrombotic effect.

3. Comparison of He-Ne laser-induced thrombosis test with tests measuring global thrombotic and thrombolytic status *ex vivo.*

3.1. *Involvement of platelets and fibrin in the platelet-rich thrombi formed in vivo and in vitro.*

Platelets and fibrin are the main components of arterial thrombus. The involvement of these two components in the formation and lysis of a thrombus formed from non-anticoagulated (native) blood was measured by the *in vivo* test of He-Ne laser-induced thrombosis and the shear-induced *in vitro* thrombosis tests performed on native blood sample. In small arterial vessels of the microcirculation, laser-induced thrombi were composed of tightly packed platelets. Electron microscopy and specific antibody staining failed to detect fibrin in the microvessels. However, measurement of lysis or embolization of the formed thrombi suggested the presence of fibrin, as administration of plasminogen activators or inhibitors enhanced or inhibited thrombolysis, respectively (*25-29*).

High shear-induced haemostatic plug formed by Haemostatometry was composed predominantly of platelets, but minor amount of fibrin was also detected. This was confirmed by electron microscopy. The dominant presence of platelets in the formed haemostatic plug was shown directly by electron microscopy and indirectly by administration of antiplatelet agents such as aspirin, thromboxane A2 receptor antagonist, stable prostacyclin derivative and prostaglandin E1 prior the measured haemostasis (Table 1). When citrated or fully heparinized blood was tested, haemostasis did not occur, indicating the important role of thrombin and fibrin formation in the measured haemostasis (*30*). In a recent study using the Global Thrombosis Test, we also confirmed the cardinal role of thrombin in the formation of an occlusive thrombus (*31*).

3.2. *Effect of blood flow and shear stress on thrombus formation in microvessels in vivo and haemostatic plug formation in vitro*

As the mechanism of platelet-rich thrombus formation at various flow rates has been investigated, we measured the shear rate during thrombus formation *in vivo* (*32*) and investigated the mechanism of shear-induced thrombus formation using GTT (*33*).

Shear rates during thrombus formation in the microcirculation were 641 ± 40 s^{-1} in arterioles and 280 ± 20 s^{-1} in venules before the onset of thrombus formation. Shear rates increased during platelet-rich thrombus formation and reached a peak of approximately 2,500 s^{-1} in both arterioles and venules. It was demonstrated that under such conditions

Table 1. Effect of various antiplatelet agents on platelet reactivity and coagulation as measured by Haemostatometry

Items	Platelet plug formation H2 (mmHg x s)	Coagulation CT2 (min)
Control	4532 ± 383	9.53 ± 0.25
Aspirin		
0.3 mM	4742 ± 827	9.06 ± 0.48
1 mM	5439 ± 474**	9.75 ± 0.43
3 mM	6467 ± 963**	10.02 ± 0.56
Control	4148 ± 381	9.76 ± 0.33
TXA2Rant		
0.5 μM	4619 ± 439	10.19 ± 0.53
5 μM	5519 ± 420**	10.18 ± 0.44
Control	4491 ± 279	10.23 ± 0.31
sPGI2		
0.055 nM	4793 ± 308	10.16 ± 0.48
0.55 nM	5367 ± 536**	9.95 ± 0.29
Control	4277 ± 308	9.35 ± 0.28
sPGE1		
14.1 nM	4753 ± 574	9.52 ± 0.32
141 nM	6239 ± 382*	9.35 ± 0.28

TXA2Rant: thromboxane A2 receptor antagonist; sPGI2: stable prostacyclin derivative; sPGE1: stable prostaglandin E1. Final concentrations are shown. Data are expressed as mean ± SEM (n = 6-10 in each group) *$p < 0.05$; **$p < 0.01$ *vs*. control. (Revised; Yamamoto *et al*. Platelets. 1999; 10:178-187).

von Willebrand factor (vWF) played the major role in forming the initial platelet aggregates and fibrinogen (fibrin) was involved only in venules, but not in arterioles (*32*). These findings showed similar mechanisms of thrombus formation between the *in vivo* and *in vitro* tests used and those experiments which were performed on human blood (*33-35*).

Further, we demonstrated that thrombus formation in the GTT was similar to thrombus formation at high shear and flow conditions in terms of the activation of adhesive proteins and ligand receptors on platelets (Table 2) (*33*). The GTT allowed the assessment of the effect of tissue-type plasminogen activator, streptokinase and plasminogen activator inhibitor on the stability of formed thrombi, and therefore assess not only the efficacy of the spontaneous (endogenous) thrombolytic system but also response to activators and inhibitors of thrombolysis.

4. Correlation between He-Ne laser-induced platelet reactivity measurement *in vivo* and high shear-induced platelet reactivity *in vitro* test using non-anticoagulated blood

In a study measuring thrombotic status of diabetic rats, the *in vivo* He-Ne laser-induced thrombosis and the *in vitro* high shear-induced platelet reactivity test were compared. The thrombotic status of two kinds of spontaneously diabetic, insulin independent rats (Goto-Kakizaki [GK] rats and Otsuka Long-Evans Tokushima Fatty [OLETF] rats) was measured (Figure 2A, 2B) (*36,37*). GK rats were in a prothrombotic status as detected by the *in vivo* laser test and this corresponded with enhanced platelet reactivity measured by the *in vitro* Haemostatometry. Also the inhibited thrombotic status of OLETF rats as measured with the laser test corresponded with suppressed platelet reactivity, measured with Haemostatometry. These results indicate that thrombotic status is predominantly governed by platelet reactivity which is detected similarly by the *in vivo* laser-thrombosis and *in vitro* shear-induced platelet reactivity tests.

Table 2. GTT assessment of the effect of specific platelet inhibitors on human platelet reactivity

Aurin tricarboxylic acid (μmol/L)	0	20	200
OT (s)	211 ± 30	203 ± 33	462 ± 71***
6B4 (μg/L)	0	2	20
OT (s)	262 ± 14	421 ± 48*	470 ± 7*
12E4 (μg/L)	0	1	10
OT (s)	267 ± 24	403 ± 28	555 ± 32*
MA16N7C2 (μg/L)	0	0.5	5
OT (s)	294 ± 31	320 ± 32	529 ± 147**
Abciximab (μg/L)	0	2	20
OT (s)	283 ± 40	493 ± 72**	623 ± 38***
TAK-029 (nmol/L)	0	0.05	0.1
OT (s)	271 ± 24	555 ± 17***	487 ± 77***
Anti-vWF (μg/L)	0	0.5	1
OT (s)	287 ± 93	494 ± 46*	513 ± 65*
Anti-fibrinogen (μg/L)	0	10	100
OT (s)	253 ± 78	336 ± 525	261 ± 20
Argatroban (μmol/L)	0	5	10
OT (s)	341 ± 21	623 ± 40***	657 ± 46***

Aurin tricarboxylic acid: an inhibitor of the association of von Willebrand factor and platelet glycoprotein Ib (GPIb); 6B4 and 12E4: monoclonal antibodies against GPIb; MA16N7C2 and Abciximab: monoclonal antibodies against platelet glycoprotein IIb/IIIa (GPIIb/IIIa); TAK-029: an inhibitors of platelet glycoprotein IIb/IIIa; Anti-vWF: polyclonal antibody against von Willebrand Factor; Anti-fibrinogen: polyclonal antibody against fibrinogen; Argatroban: a thrombin inhibitor. Zero (0) shows vehicle (saline) controls. $^{*}p < 0.05$; $^{**}p < 0.01$; $^{***}p < 0.001$ *vs*. control; n = 4-6 human subjects in each group. (Revised; Yamamoto *et al*. Blood Coagulation & Fibrinolysis. 2003; 14:31-39).

5. Thrombotic status is determined by the balance between platelet reactivity and endothelial function

In contrast to diabetic rats, in SHRSP rats there was no correlation between the laser-thrombosis test and the shear-induced platelet reactivity test. While the laser-thrombosis test measured a prothrombotic state in SHRSP rats, the ex-vivo shear-induced platelet function test showed suppressed platelet reactivity (Figure 2C) (*38-40*). To try and identify the reason for

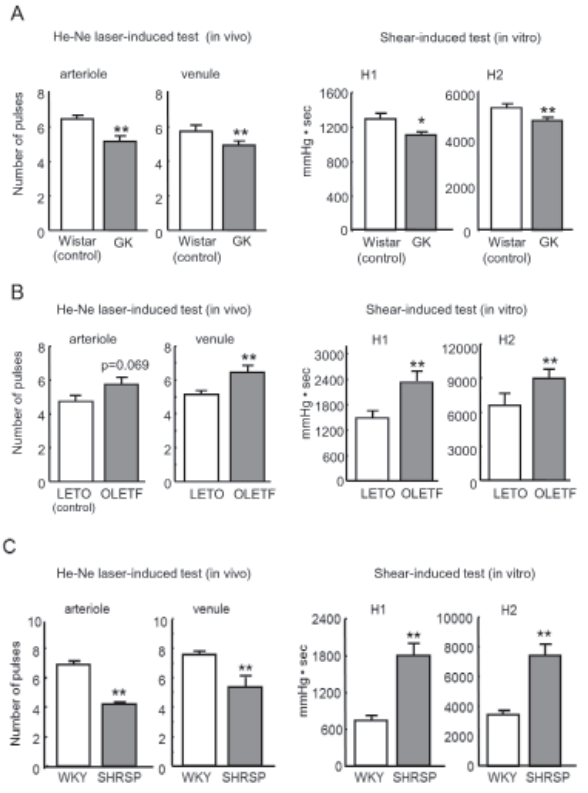

Figure 2. Thrombotic status and platelet reactivity of spontaneously diabetic GK rats (A), OLETF rats (B) and stroke-prone spontaneously hypertensive rats (SHRSP) (C). Results are expressed as means ± SEM. **A**: n = 6-14 in each group; **B**: n = 6-8 in each group; **C**: n = 6-8 in each group; $^{*}p < 0.05$; $^{**}p < 0.01$ *vs*. controls. (**A**: Revised; Taka *et al*. Platelets 2002; 13: 313-316; **B**: Taka *et al*. Diabetes Frontier 1999; 10: 582-583; **C**: Revised; Noguchi *et al*. Haemostasis 1997; 27:237-245, Yamashita et al. Thrombosis Research 2002; 105:507-511).

this inconsistency, endothelial function testing (FMV) was performed. FMV *in vivo* performed in SHRSP rats detected severely dysfunctional endothelium whilst the endothelium-independent vasodilation was normal (Figure 3A) (*39*). Similar inconsistencies were found between the *in vivo* and *in vitro* thrombosis tests in congenital apoE and LDLR deficient mice (Figure 3B) (*41,42*).

The laser-induced thrombosis test demonstrated a prothrombotic state in mice fed on high-triglyceride but not in mice fed on high-diglyceride diet. This was inconsistent with that detected with the shear-induced *in vitro* test, suggesting that the prothrombotic state may be due to endothelial dysfunction caused by the high-triglyceride diet.

These results provided evidence that the overall thrombotic status is determined by the balance between platelet reactivity, the determinant of the thrombotic status of blood, and the function of the vascular endothelium. For this reason, the sensitive *in vivo* FMV functional test is recommended as a test additional to platelet reactivity assessment, for the assessment of overall thrombotic status (Figure 4) (*43*).

6. Thrombotic status of blood is determined by the balance between prothrombotic and thrombolytic (fibrinolytic) activities

The overall thrombotic status of blood is determined by the balance between prothrombotic and thrombolytic factors. While platelet reactivity is measured by platelet function tests and thrombelastography measures the overall coagulation activities, conventional thrombosis tests cannot measure the (spontaneous) thrombolytic/fibrinolytic activity of blood. Using the GTT, we could detect both thrombotic and thrombolytic activities in sequence from one blood sample. Though, the influence of diet and nutrients on platelet function using conventional tests has been published (*4*), with this technique for many years we have been screening fruits and vegetables for antithrombotic effects. Importantly we demonstrated that such activity can be specific for a particular variety while other varieties do not show antithrombotic effects (*19-24*). Effects of specific varieties of red and white grapes on *in vitro* and *in vivo* thrombogenesis and thrombolysis are shown in Figure 5 (*24*). The use of GTT and *in vivo* laser thrombosis tests showed that a specific variety of red grapes inhibited platelet reactivity and enhanced thrombolysis, suggesting a potential antithrombotic effect. On the other hand, one variety of white grapes enhanced platelet reactivity and inhibited thrombolysis, suggesting a potential prothrombotic effect.

Platelet reactivity and thrombolytic activity of carrot varieties before and after heat treatment are shown in Figure 6. One variety SAKATA-0418 had no effect on platelet reactivity but enhanced thrombolysis before heat treatment. After heat treatment, as measured both with *in vitro* (GTT) and *in vivo* (laser thrombosis) techniques, this carrot variety enhanced platelet reactivity and lost the effect on thrombolysis. This finding suggests that heat treatment profoundly alters the pro- or antithrombotic activities of some fruit and vegetables.

Besides searching effective foods for preventing thrombosis, we have applied those methodologies to evaluation of antithrombotic effects of several traditional herbal drugs or Kampo medicines (*44*) and demonstrated

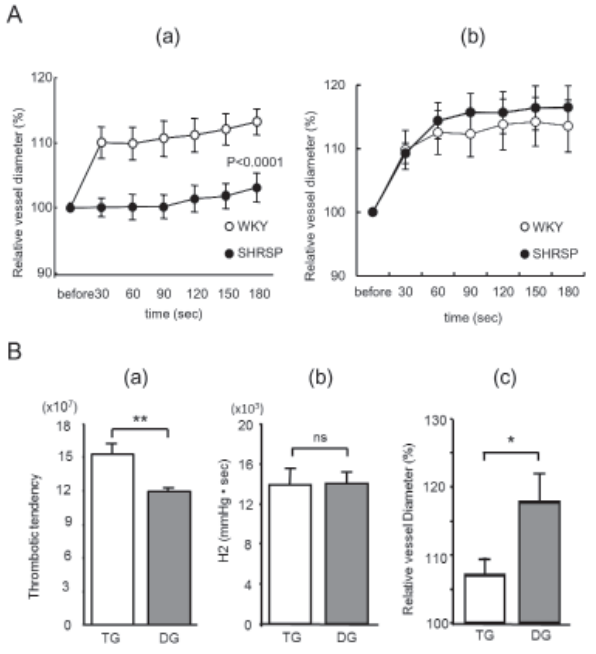

Figure 3. Endothelial dysfunction in SHRSP assessed by FMV (a) and NMV (b) (A). Effects of dietary oil, triglyceride (TG) and diglyceride (DG), on thrombotic status assessed by He-Ne laser test (a), Haemostatometry (b) and FMV (c), in apoE$^{-/-}$•LDLR$^{-/-}$ double knockout mice (B). Results are expressed as means ± SEM. n = 8 in each group (**A**) and n = 6-8 mice in each group (**B**); $^{*}p < 0.05$, $^{**}p < 0.01$. (**A**: Revised; Taka *et al*. Pathophysiology of Haemostasis and Thrombosis 2002; 32: 184-189, **B**: Ijiri *et al*. Thrombosis Research 2006; 117: 411-417).

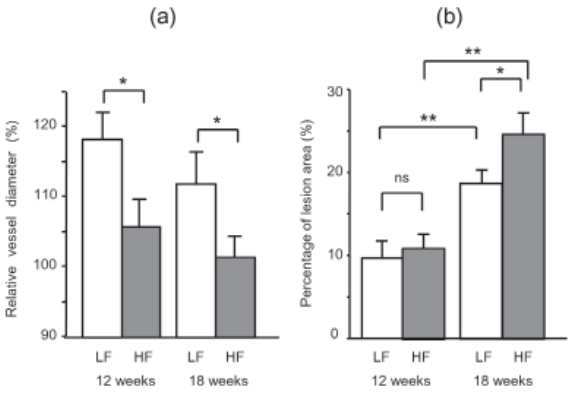

Figure 4. Effects of dietary fat (low fat diet (LF) or high fat diet (HF)) on endothelial function of apoE$^{-/-}$•LDLR$^{-/-}$DK mice, assessed by functional FMV (a) and morphological fat staining (b). Results are expressed as means ± SEM. **(A)** n = 14-20 in each group; **(B)** n = 3-5 in each group; $^{*}p < 0.05$; $^{**}p < 0.01$. (Revised; Aoki *et al*. Thrombosis Research 2006; 117: 529-535).

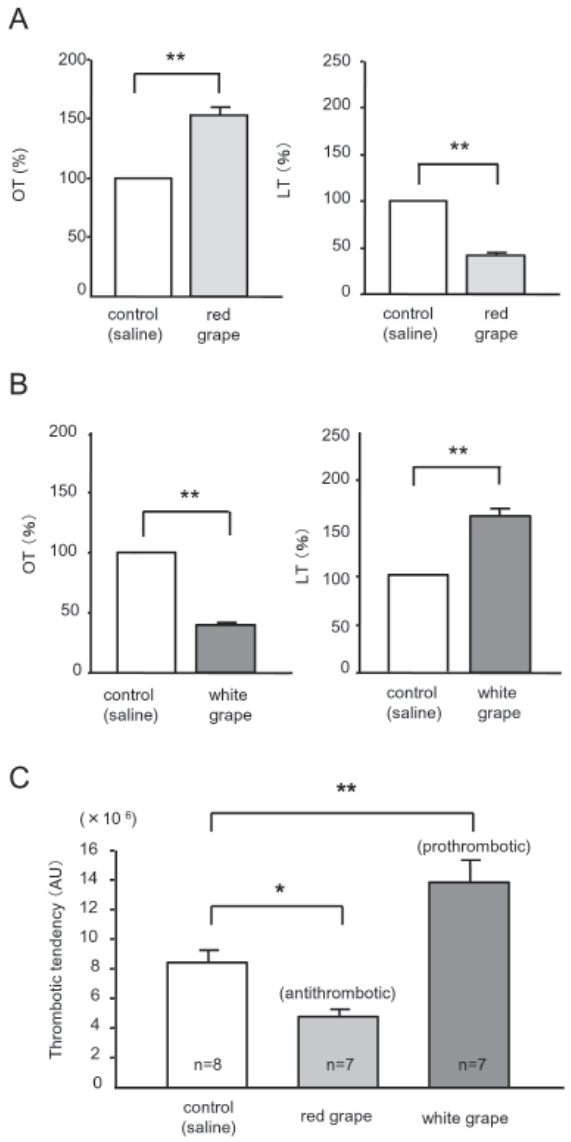

Figure 5. Effects of specified varieties of red and white grapes on platelet reactivity (OT) and thrombolytic activity (LT) as measured by GTT *in vitro* (A and B) and by He-Ne laser test *in vivo* (C). Results are expressed as means ± SEM; n = 7-8 in each group (**A-C**); $^{*}p < 0.05$; $^{**}p < 0.01$. (Revised; Iwasaki M. Master's thesis of Kobe Gakuin University 2006).

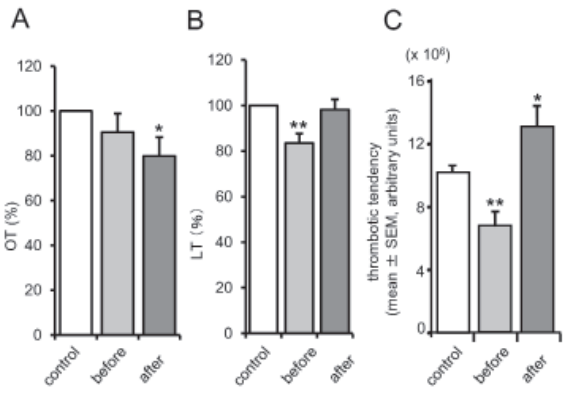

Figure 6. Balance between thrombotic (A) and thrombolytic (B) activities determines the actual thrombotic status (C). Assessment of juices of various carrot varieties without (before) and with heat treatment (after) using the GTT (*in vitro*) **(A, B)** and He-Ne laser thrombosis test (*in vivo*) **(C)**. Results are expressed as means ± SEM. n = 6-9 in each group **(A-C)**; $^{*}p < 0.05$; $^{**}p < 0.01$ *vs*. control group. OT: occlusion time; LT: lysis time. (Revised; Yamamoto *et al* Blood Coagulation & Fibrinolysis 19: 2008; 785-792).

that some of the medications for blood stagnation have significant antithrombotic effect as well. On the other hand, antithrombotic fractions from *Centella asiatica* have been also investigated (*45*). Thus, combination of shear-induced thrombosis test, Haemostatometry or GTT, and FMV should be useful in searching and developing antithrombotic drugs.

7. Measurement of thrombotic status of healthy volunteers and patients with the Haemostatometer and GTT

We assessed the thrombotic status of a small number of healthy volunteers and patients with thrombotic disorders using Haemostatometry and GTT. These tests proved to sensitively detect changes in the thrombotic status after physical exercise-load and gender differences, age and habitual smokers, and race differences between healthy Japanese and British volunteers (*46-54*).

8. Conclusions

The value of shear-induced *in vitro* Global Thrombosis Test and Haemostatometry in testing various components of nutrient and herbal drugs for antithrombotic effect was assessed. Results obtained with these *in vitro* tests were compared with the results obtained using the He-Ne laser-induced carotid artery and mesenteric microvessel thrombosis model *in vivo*. Our findings suggest that the use of Global Thrombosis Test together with the Flow-mediated Vasodilation *in vivo* test provides better assessment of the global thrombotic status than using the platelet function test alone.

References

1. Trichopoulou A, Costacou T, Bamia C, Trichopoulos D. Adherence to a Mediterranean diet and survival in a Greek population. N Engl J Med. 2003; 348:2599-2608.
2. de Lorgeril M, Renaud S, Mamelle N, Salen P, Martin JL, Monjaud I, Guidollet J, Touboul P, Delaye J. Mediterranean alpha-linolenic acid-rich diet in secondary prevention of coronary heart disease. Lancet. 1994; 343:1454-1459.
3. Key TJ, Appleby PN, Rosell MS. Health effects of vegetarian and vegan diets. Proc Nutr Soc. 2006; 65:35-41.
4. McEwen BJ. The influence of diet and nutrients on platelet function. Semin Thromb Hemost. 2014; 40:214-226.
5. Gorog DA, Fuster V. Platelet function tests in clinical cardiology: Unfulfilled expectations. J Am Coll Cardiol. 2013; 61:2115-2129.
6. Gorog DA, Jeong YH. Platelet function tests: Why they fail to guide personalized antithrombotic medication. J

Am Heart Assoc. 2015; 4:e002094.
7. Gorog DA, Kovacs IB. Thrombotic status analyser. Measurement of platelet-rich thrombus formation and lysis in native blood. Thromb Haemost. 1995; 73:514-520.
8. Nakajima S, Noguchi T, Taka T, Ueda T, Kaizu K, Fukamizu M, Fujita S, Tabuchi M, Yamamoto J. A global platelet test of thrombosis and thrombolysis detects a prothrombotic state in some patients with non-insulin dependent diabetes and in some patients with stroke. Platelets. 2000; 11:459-466.
9. Paniccia R, Priora R, Liotta AA, Abbate R. Platelet function tests: A comparative review. Vasc Health Risk Manag. 2015; 11:133-148.
10. Kovacs IB, Tigyi-Sebes A, Trombitas K, Gorog P. Evans blue: An ideal energy-absorbing material to produce intravascular microinjury by HE-NE gas laser. Microvasc Res. 1975; 10:107-124.
11. Yamamoto J, Iizumi H, Hirota R, Shimonaka K, Nagamatsu Y, Horie N, Morita S. Effect of physical training on thrombotic tendency in rats: Decrease in thrombotic tendency measured by the He-Ne laser-induced thrombus formation method. Haemostasis. 1989; 19:260-265.
12. Ijiri Y, Miura M, Hashimoto M, Fukunaga C, Watanabe S, Kubota A, Oiwa K, Okuda T, Yamamoto J. A new model to evaluate the diet-induced prothrombotic state, using He-Ne laser-induced thrombogenesis in the carotid artery of apolipoprotein E-deficient and low-density lipoprotein receptor-deficient mice. Blood Coagul Fibrinolysis. 2002; 13:497-504.
13. Ratnatunga CP, Edmondson SF, Rees GM, Kovacs IB. High-dose aspirin inhibits shear-induced platelet reaction involving thrombin generation. Circulation. 1992; 85:1077-1082.
14. Okafor ON, Gorog DA. Endogenous Fibrinolysis: An Important Mediator of Thrombus Formation and Cardiovascular Risk. J Am Coll Cardiol. 2015; 65:1683-1699.
15. Soga J, Nishioka K, Nakamura S, Umemura T, Jitsuiki D, Hidaka T, Teragawa H, Takemoto H, Goto C, Yoshizumi M, Chayama K, Higashi Y. Measurement of flow-mediated vasodilation of the brachial artery: A comparison of measurements in the seated and supine positions. Circ J. 2007; 71:736-740.
16. Iwamoto Y, Maruhashi T, Fujii Y, Idei N, Fujimura N, Mikami S, Kajikawa M, Matsumoto T, Kihara Y, Chayama K, Noma K, Nakashima A, Higashi Y. Intima-media thickness of brachial artery, vascular function, and cardiovascular risk factors. Arterioscler Thromb Vasc Biol. 2012; 32:2295-2303.
17. Maruhashi T, Soga J, Fujimura N, Idei N, Mikami S, Iwamoto Y, Kajikawa M, Matsumoto T, Hidaka T, Kihara Y, Chayama K, Noma K, Nakashima A, Goto C, Higashi Y. Nitroglycerine-induced vasodilation for assessment of vascular function: A comparison with flow-mediated vasodilation. Arterioscler Thromb Vasc Biol. 2013; 33:1401-1408.
18. Tamura Y, Naemura A, Inoue A, Ijiri Y, Seki J, Yada T, M, Shinohara M, Kawashima S, Giddings JC, Yamamoto J. Impaired endothelial function may be due to decreased aortic tetrahydrobiopterin, assessed by a new flow-mediated vasodilation *in vivo* in hypercholesterolemic/atherogenic mice. Blood Coagul Fibrinolysis. 2009; 20:699-705.
19. Yamamoto J, Naemura A, Ijiri Y, Ogawa K, Suzuki T, Shimada Y, Giddings JC. The antithrombotic effects of carrot filtrates in rats and mice. Blood Coagul Fibrinolysis. 2008; 19:785-792.
20. Naemura A, Ijiri Y, Kodama M, Honda Y, Yamamoto J. A rice variety (HYJA-Ri4) enhances arterial thrombus formation in an animal model of thrombosis. Pathophysiol Haemost Thromb. 2008; 36:241-244.
21. Naemura A, Mitani T, Ijiri Y, Tamura Y, Yamashita T, Okimura M, Yamamoto J. Anti-thrombotic effect of strawberries. Blood Coagul Fibrinolysis. 2005; 16:501-509.
22. Yamamoto J, Taka T, Yamada K, Ijiri Y, Murakami M, Hirata Y, Naemura A, Hashimoto M, Yamashita T, Oiwa K, Seki J, Suganuma H, Inakuma T, Yoshida T. Tomatoes have natural anti-thrombotic effects. Br J Nutr. 2003; 90:1031-1038.
23. Yamamoto J, Ohno H, Hyodo K, Onishi M, Giddings JC. The antithrombotic activity of mini-type tomatoes is dependent on the particular variety and the stage of harvest. Lycopene content does not contribute to antithrombotic activity. Health. 2013; 5:681-686.
24. Iwasaki M. Antithrombotic activity of grape varieties. Master's thesis of Kobe Gakuin University. 2006;
25. Yamamoto J, Kawano M, Hashimoto M, Sasaki Y, Yamashita T, Taka T, Watanabe S, Giddings JC. Adjuvant effect of antibodies against von Willebrand Factor, fibrinogen, and fibronectin on staphylokinase-induced thrombolysis as measured using mural thrombi formed in rat mesenteric venules. Thromb Res. 2000; 97:327-333.
26. Hashimoto M, Watanabe S, Oiwa K, Ohta Y, Kishi T, Okamoto T, Giddings JC, Yamamoto J. Enhanced thrombolysis induced by argatroban or activated protein C in the presence or absence of staphylokinase, measured in an *in vivo* animal model using mesenteric arterioles. Haemostasis. 2001; 31:80-89.
27. Hashimoto M, Yamashita T, Oiwa K, Watanabe S, Giddings JC, Yamamoto J. Enhancement of endogenous plasminogen activator-induced thrombolysis by argatroban and APC and its control by TAFI, measured in an arterial thrombolysis model *in vivo* using rat mesenteric arterioles. Thromb Haemost. 2002; 87:110-113.
28. Hashimoto M, Onobayashi Y, Oiwa K, Giddings JC, Yamamoto J. Enhanced endogenous thrombolysis induced by a specific factor Xa inhibitor, DX-9065a, evaluated in a rat arterial thrombolysis model *in vivo*. Thromb Res. 2002; 106:165-168.
29. Hashimoto M, Oiwa K, Matsuo O, Ueshima S, Okada K, Okada Y, Okamoto S, Giddings JC, Yamamoto J. Suppression of argatroban-induced endogenous thrombolysis by PKSI-527, and antibodies to TPA and UPA, evaluated in a rat arterial thrombolysis model. Thromb Haemost. 2003; 89:820-825.
30. Yamamoto J, Taka T, Nakajima S, Ueda M, Sugimoto E, Sasaki Y, Muraki T, Seki J, Watanabe S. A shear-induced *in vitro* platelet function test can assess clinically relevant anti-thrombotic effects. Platelets. 1999; 10:178-184.
31. Yamamoto J, Inoue N, Otsui K, Ishii H, Gorog DA. Global Thrombosis Test (GTT) can detect major determinants of haemostasis including platelet reactivity, endogenous fibrinolytic and thrombin generating potential. Thromb Res. 2014; 133:919-926.

32. Yamamoto J, Ishii I, Okita N, Sasaki Y, Yamashita T, Matsuoka A, Muraki T, Giddings JC, Watanabe S, Seki J. The differential involvement of von Willebrand factor, fibrinogen and fibronectin in acute experimental thrombosis in rat cerebral and mesenteric microvessels. Jpn J Physiol. 1997; 47:431-441.
33. Yamamoto J, Yamashita T, Ikarugi H, Taka T, Hashimoto M, Ishii H, Watanabe S, Kovacs IB. Gorog Thrombosis Test: A global in-vitro test of platelet function and thrombolysis. Blood Coagul Fibrinolysis. 2003; 14:31-39.
34. Weiss HJ, Hawiger J, Ruggeri ZM, Turitto VT, Thiagarajan P, Hoffmann T. Fibrinogen-independent platelet adhesion and thrombus formation on subendothelium mediated by glycoprotein IIb-IIIa complex at high shear rate. J Clin Invest. 1989; 83:288-297.
35. Weiss HJ, Turitto VT, Baumgartner HR. Effect of shear rate on platelet interaction with subendothelium in citrated and native blood. I. Shear rate--dependent decrease of adhesion in von Willebrand's disease and the Bernard-Soulier syndrome. J Lab Clin Med. 1978; 92:750-764.
36. Taka T, Yamashita T, Seki J, Yamamoto J. Different platelet reactivity of three spontaneously non-insulin dependent diabetic rat strains (GK, OLETF, WBN/Kob). Diabetes Frontier. 1999; 10:582-583. (in Japanese)
37. Taka T, Ono H, Sasaki Y, Seki J, Yamamoto J. Platelet reactivity in spontaneously diabetic rats is independent from blood glucose and insulin levels. Platelets. 2002; 13:313-316.
38. Noguchi T, Sasaki Y, Seki J, Giddings JC, Yamamoto J. Enhanced thrombogenicity and altered hemodynamics in the cerebral microvasculature of stroke-prone spontaneously hypertensive rats. Haemostasis. 1997; 27:237-245.
39. Taka T, Ohta Y, Seki J, Giddings JC, Yamamoto J. Impaired flow-mediated vasodilation *in vivo* and reduced shear-induced platelet reactivity *in vitro* in response to nitric oxide in prothrombotic, stroke-prone spontaneously hypertensive rats. Pathophysiol Haemost Thromb. 2002; 32:184-189.
40. Yamashita T, Taka T, Nojima R, Ohta Y, Seki J, Yamamoto J. There is no valid evidence presented as to an impaired endothelial NO system in the stroke-prone spontaneously hypertensive rats. Thromb Res. 2002; 105:507-511.
41. Ijiri Y, Naemura A, Yamashita T, Meguro S, Watanabe H, Tokimitsu I, Yamamoto J. Dietary diacylglycerol extenuates arterial thrombosis in apoE and LDLR deficient mice. Thromb Res. 2006; 117:411-417.
42. Ijiri Y, Naemura A, Yamashita T, Ikarugi H, Meguro S, Tokimitsu I, Yamamoto J. Mechanism of the antithrombotic effect of dietary diacylglycerol in atherogenic mice. Pathophysiol Haemost Thromb. 2006; 35:380-387.
43. Aoki R, Ikarugi H, Naemura A, Ijiri Y, Yamashita T, Yamamoto J. Endothelial dysfunction precedes atherosclerotic lesions and platelet activation in high fat diet-induced prothrombotic state. Thromb Res. 2006; 117:529-535.
44. Ijiri1 Y, Anzai H, Gao W, Takahashi K, Kajiwara N, Murakami M, Yamamoto J. Long-term administration of traditional kampo medicine shimotsuto, juzentaihoto and unseiin inhibits experimental thrombosis in mice. Health. 2010; 5:493-498.
45. Satake T, Kamiya K, An Y, Oishi T, Yamamoto J: The anti-thrombotic active constituents from *Centella asiatica*. Biological & pharmaceutical bulletin. 2007; 30:935-940.
46. Ikarugi H, Taka T, Nakajima S, Noguchi T, Watanabe S, Sasaki Y, Haga S, Ueda T, Seki J, Yamamoto J. Norepinephrine, but not epinephrine, enhances platelet reactivity and coagulation after exercise in humans. J Appl Physiol. 1999; 86:133-138.
47. Ikarugi H, Shibata M, Ishii K, Yamamoto J. Shear-induced platelet reactivity in middle-aged women after low-intensity exercise. Thromb Res. 2001; 104:347-351.
48. Ikarugi H, Shibata M, Shibata S, Ishii H, Taka T, Yamamoto J. High intensity exercise enhances platelet reactivity to shear stress and coagulation during and after exercise. Pathophysiol Haemost Thromb. 2003; 33:127-133.
49. Ikarugi H, Yamashita T, Aoki R, Ishii H, Kanki K, Yamamoto J. Impaired spontaneous thrombolytic activity in elderly and in habitual smokers, as measured by a new global thrombosis test. Blood Coagul Fibrinolysis. 2003; 14:781-784.
50. Yamashita T, Sato A, Ikarugi H, Inoue A, Kitamori K, Ishii H, Yamamoto J. Significantly reduced spontaneous thrombolytic activity in older men: A possible explanation for the gender differences in risk of acute coronary syndromes. Thromb Res. 2005; 116:127-131.
51. Suehiro A, Wakabayashi I, Yamashita T, Yamamoto J. Attenuation of spontaneous thrombolytic activity measured by the global thrombosis test in male habitual smokers. J Thromb Thrombolysis. 2014; 37:414-418.
52. Gorog DA, Yamamoto J, Saraf S, Ishii H, Ijiri Y, Ikarugi H, Wellsted DM, Mori M, Yamori Y. First direct comparison of platelet reactivity and thrombolytic status between Japanese and Western volunteers: Possible relationship to the "Japanese paradox". Int J Cardiol. 2011; 152:43-48.
53. Taomoto K, Ohnishi H, Kuga Y, Nakashima K, Ichioka T, Kodama Y, Kubota H, Tominaga T, Hirose T, Hayashi M, Kinugasa C, Yamashita T, Yamamoto J. Platelet function and spontaneous thrombolytic activity of patients with cerebral infarction assessed by the global thrombosis test. Pathophysiol Haemost Thromb. 2010; 37:43-48.
54. Suehiro A, Wakabayashi I, Uchida K, Yamashita T, Yamamoto J. Impaired spontaneous thrombolytic activity measured by global thrombosis test in males with metabolic syndrome. Thromb Res. 2012; 129:499-501.

(Received July 8, 2015; Revised July 26, 2015; Accepted August 25, 2015)

Review

DOI: 10.5582/ddt.2015.01050

An examination on the modern significance of "Yakushokudougen" in transferring to organic agriculture

Bai Hu*

Laboratory of Agricultural Economics and Farm Management, Department of Resources and Environmental Policy, Faculty of Agriculture, Ehime University, Matsuyama, Ehime, Japan.

Summary **This study attempts to identify whether and why the difference in corruption progress exists between organic and conventional farm products by conducting two corruption experiments of farm products and separation experiment of bacteria, as well as farmer survey. The results of corruption experiments for Wenzhou mandarin oranges (*Citrus unshiu*) and polished rice showed that conventional farm products demonstrated fast-growing corruption with strong unpleasant smell distinctively different from organic farm products. The separation experiment of bacteria indicated a high possibility of fungus appearance in organic farm products and coccus or bacillus appearance in conventional farm products, which are significantly consistent with the results of two corruption experiments and the fact that organic farmers are strongly conscious of the use of fermented organic fertilizers with effective microorganism in their cultivation. These results offer empirical evidences for supporting the development of organic agriculture and the consumption expansion of organic farm products, but further works are necessary.**

Keywords: Organic farm product, sustainable agriculture, corruption experiment of farm product, separation experiment of bacteria, ishokudougen

1. Introduction

Among organic farmers and researchers, it was well known that organic farm products are good at storage or "become hard to decay" compared with conventional farm products. Many of them also regarded this as an evidence to claim the necessity of transferring the existing agriculture to organic farming. For example, Tsuruda (2011) introduced this as a common view of an organic farmers group (1996, Mogura farmers group), based on their farming practices (*1*). However, Kimura, well known for his natural farming practice "miraculous apple", demonstrated that organic rice was easier to decay than natural farming rice, and organic cucumber had fast-growing corruption even more than conventional farm products (*2,3*). However, no evidences have been offered to a rational explanation why the corruption of farm products is different between organic and other farming systems. Some observers therefore argued that the corruption of farm products occurs just because they are organic matters, no relation with the difference of farming systems (*4*).

This study identified whether the difference exists between organic and conventional farming systems by conducting two corruption experiments of farm products. Then, empirical examination is given based on the results of separation experiment of bacteria and some surveys from organic farmers' practices. Finally, the policy applications of this study are discussed.

2. Methods and results of corruption experiment

2.1. *Methods*

Wenzhou mandarin oranges (*Citrus unshiu*) and polished rice were used. Organic oranges were purchased from a farmer of Nakajima town, and conventional oranges from B town where is famous for its citrus production, and Ehime University Senior High School (EUSHS, Ehime, Japan). The experiment of oranges was conducted in the Laboratory of Agricultural Economics and Farm Management, Faculty of Agriculture at

**Address correspondence to:*
Dr. Bai Hu, Department of Resources and Environmental Policy, Faculty of Agriculture, Ehime University, Tarumi 3-5-7, Matsuyama 790-8566, Ehime, Japan.
E-mail: richardh@agr.ehime-u.ac.jp

Ehime University. The procedure was as follows. *i*) The experimental jars were sterilized with boiled water. *ii*) Oranges were cut into half and put in the jars. *iii*) Sterilized water (20°C, 60 mL) was poured into the jars. Covers were put on the jar mouths for preventing the invasion of dust. *iv*) Jars were displayed under the sunlight to observe the corruption progress.

The experiment of rice was done with the same methods of orange experiment, for verifying the effects exhibited in orange experiment. The rice samples were purchased from farmers of Kihoku town (organic), Toon city (organic with duck-farming), and a supermarket of Ehime (conventional).

2.2. *Results*

The results of orange experiment are shown in Figure 1. The corruption progress was observed from the fourth day after the experiment started, and Figure 1 showed the state of the 39th day. The organic orange exhibited slow-growing corruption or good storable duration, with a sweet smell. By contrast, the conventional orange changed into burnt-blackish color with a stinking smell so much as to provoke nausea. The orange of EUSHS exhibited a state close to the organic orange. This may be caused from insufficient fertility management of the high school students, which consequently brought about the reduction of chemical fertilizer and agrichemical use.

However, one's likes or dislikes for a smell may depend on his/her tastes and experience to some extent, and therefore may not exist an absolute criterion for judging whether a smell is unpleasant or not. Funa-zushi, a famous traditional fish food of Shiga, could be a good example. A lot of persons are attracted by its unique fermentation smell and favorite to eat it, although it's strong smell or taste property. Its unique smell seems not unpleasant for them. However, we have never heard of a person who favorites the smell of animal wastes. Because of these facts, a smell test for students out of the corruption experiment was done just after the experiment. The results reported in Table 1 illustrate that all participants gave the same answers that organic orange did not have unpleasant smell, although the information of corruption experiment was not informed.

The results of rice experiment are shown in Figure 2. The organic rice exhibited a state almost without corruption indicating a good storable duration, followed by the organic duck-farming rice and conventional farm rice. White mold was observed on the surface of conventional rice, with unpleasant smell. Both organic rice and organic duck-farming rice appeared an amber color, but the latter looked slightly deeper with stronger smell. Ducks eat grass and feed, and finally excrete in paddy field every day in the growth period. The deeper color and stronger smell in the organic duck-farming rice may result in more accumulation of nitrogen than organic rice. As the difference of smells was extremely distinctive, a smell test as Table 1 was omitted.

Figure 1. Results of corruption experiment: oranges. The state of corruption progress is exhibited in order of conventional, organic, and EUSHS oranges from the left.

Table 1. Results of smell test (oranges)

Participants	Conventional	Organic	EUSHS
Student 1	1	3	2
Student 2	1	3	2
Student 3	1	3	2
Student 4	1	3	2
Student 5	1	3	2
Student 6	1	3	2
Student 7	2	3	1
Student 8	1	3	2
Student 9	1	3	2

Strongly unpleasant is indicated as 1, a little unpleasant as 2, without unpleasent smell as 3.

Figure 2. Results of corruption experiments: rice. The state of corruption progress is exhibited in order of organic, conventional and organic duck-farming rice from the left.

3. Separation experiment of bacteria for organic and conventional farm products

3.1. *A brief review about the relation between farming system and bacteria*

Hika (2012) pointed out that an unpleasant smell comes from a corruption resolution and a pleasant smell from a process of fermentation. A corruption resolution is caused by putrefactive bacteria, while fermentation derived by lactic acid bacteria and yeast (*5*). These views suggest a causal relation between corruption, fermentation and smell. But his views have no explanation with the evidence from an experimental process of farm products or empirical survey. Some organic farmers and observers argued that the difference in corruption progress and smell is mainly resulted from the residual of over-used

Table 2. Process of separation experiment of bacteria

Time	Process and content of experiment	Notes
Dec. 17, 2014	Put oranges and rice in 50 ml of tubes and add RO water. Then start the culture of bacterium with 30°C.	
	↓	
Dec. 22, 2014	Culture with sabouraud agar plate	
	↓	
Dec. 23, 2014	Colonies appear. Collect the plates to 4°C.	
	↓	
Dec. 24, 2014	Culture with Sabouraud liquid medium	
	↓	
Dec. 26, 2014	Full growth	
	↓	
Dec. 27, 2014	Inject the full growth into silkworms	
	↓	
Dec. 28, 2014	Progress observation	• A dead individual appeared after 27 hours. • 193 hours later, the silkworm injected a medium (sabouraud) lived. However, silkworms injected all samples died, except orange 7 (colony 2).
	↓	
Jan. 4 , 2015	Progress observation end	

The experiment was conducted by professor SEKIMIZU Kazuhisa, the Laboratory of Microbiology, Graduate School of Pharmaceutical Sciences at the University of Tokyo (Tokyo, Japan).

nitrogen fertilizers and agrichemicals, particularly the remaining of nitrate nitrogen occurred by the excessive use of non-fully ripened compost (*2,3*). On the other hand, there also has a report indicating that the density of nitrate nitrogen in organic farm products is not necessarily lower than conventional farm products (Photo Synthesis Ltd.). However, these arguments are almost based on farmer's practices or empirical explanation, not accompanied with conclusive evidences.

As mentioned above, if the corruption of farm products causes from the decomposition process of organic matter by bacteria, the difference in corruption progress and smell may come from the difference in composition of microorganism attached to or living symbiotically within farm products. This hypothesis implies that different kind of microorganism may be detected out from farm products with different farming systems. To identify this, the separation experiment of bacteria was conducted under our request, by the Laboratory of Microbiology, Graduate School of Pharmaceutical Sciences at the University of Tokyo (Tokyo, Japan).

3.2. *Materials and results*

As the corruption experiments, Wenzhou mandarin oranges and polished rice were used. For the orange experiment, 2 samples of low-input organic oranges close to the natural farming products (orange 1, 3), 3 samples of organic oranges (orange 2, 4, 5) were obtained from farmers, and 3 samples without the organic JAS label were purchased from farmers' market (orange 6, 7, 8, Ehime). In the rice experiment, organic rice (A) used in former corruption experiment shown in Figure 2, a rice sample produced for farmer's family use (B), and a normal commodity rice sample purchased from the Ehime consumers' cooperative (C), were used. The procedure and results of the experiments are reported in Table 2 and 3 respectively.

3.3. *Examination on the results of experiments*

Table 3 indicates the characters of samples and the detected bacterium. The survival times of silkworms infected with the detected bacterium are also included as a reference indicator. The main results can be summarized as follows.

(*i*) Among five organic orange samples, only fungi were detected in orange 1, 3 and 5. In orange 2 and 4, fungi were observed in the small size and cocci G (+) in the large size of colonies.

(*ii*) In the three orange samples except the organic oranges, cocci G (+) in orange 6, bacillus G (-) and coccus G (+) in 7 and fungi in 8 were detected respectively.

(*iii*) In the rice experiment, fungi in the small size, cocci G (-) in the large size of colonies were observed. The difference between the organic and conventional farm products observed in the orange experiment, was not detected in neither sample.

(*iv*) A silkworm died after 27 hours from injection (rice C). The dead times of silkworms in the rice experiment were in order of the conventional (rice C), farmer's family use (rice B), and the organic (rice A), suggesting that the bacterium separated from conventional farm products have stronger pathogenicity and lethality than organic products. However the same results were not observed in the orange experiment. There have the cases that dead silkworms appeared after approximately 50 h from injection in organic farm products (orange 2-1: small, 4-2, 5-1: small), but also the case that silkworm survived until the end

Table 3. Composition of bacterium separated from oranges and rice

Samples (*)	Results of gram staining	Reference indicator: Survival time of silkworms infected with the samples								
		12/27	12/28	12/29	12/30	12/31	1/1	1/2	1/3	1/4
	Date & time	15:30	18:30	18:20	11:50	17:50	23:51	17:40	15:45	16:20
	Elapsed time	0:00	27:00	50:50	68:20	98:20	128:21	146:10	168:15	192:50
Sabouraud liquid medium	–	50 µl×2	2/2	2/2	2/2	2/2	2/2	2/2	2/2	2/2
(Controll)	–	*i.h.*	2/2	2/2	2/2	2/2	2/2	2/2	2/2	2/2
Orange 1 1	Fungus		2/2	2/2	2/2	2/2	1/2	1/2	0/2	–
(Low input organic) 2	Fungus		2/2	2/2	2/2	2/2	2/2	2/2	0/2	–
Orange 2 1 (small)	Fungus		2/2	1/2	1/2	0/2	–	–	–	–
(Organic) 2 (large)	coccus G (+)		2/2	2/2	2/2	2/2	1/2	1/2	0/2	–
Orange 3 1	Fungus		2/2	2/2	2/2	2/2	1/2	0/2	–	–
(Low input organic) 2	Fungus		2/2	2/2	2/2	1/2	0/2	–	–	–
Orange 4 1	Fungus		2/2	2/2	1/2	0/2	–	–	–	–
(Organic) 2	coccus G (+)		2/2	1/2	0/2	–	–	–	–	–
Orange 5 1 (small)	Fungus		2/2	1/2	0/2	–	–	–	–	–
(Organic) 2 (large)	Fungus		2/2	2/2	1/2	0/2	–	–	–	–
Orange 6 1	coccus G (+)		2/2	2/2	2/2	2/2	1/2	1/2	0/2	–
(No organic label) 2	coccus G (+)		2/2	2/2	2/2	2/2	0/2	–	–	–
Orange 7 1 (large)	bacillus G (-)		2/2	2/2	2/2	2/2	2/2	1/2	0/2	
(No organic label) 2 (small)	coccus G (+)		2/2	2/2	2/2	2/2	2/2	2/2	1/2	1/2
Orange 8 1	Fungus		2/2	2/2	2/2	1/2	1/2	0/2	–	–
(No organic label) 2	Fungus		2/2	2/2	1/2	0/2	–	–	–	–
Rice A 1 (small)	Fungus		2/2	2/2	2/2	2/2	0/2	–	–	–
(Organic) 2 (large)	coccus G (-)		2/2	2/2	2/2	1/2	0/2	–	–	–
Rice B 1 (small)	Fungus		2/2	2/2	2/2	2/2	0/2	–	–	–
(Family use) 2 (large)	coccus G (-)		2/2	1/2	1/2	1/2	1/2	1/2	0/2	–
Rice C 1 (small)	Fungus		1/2	0/2	–	–	–	–	–	–
(Conventional) 2 (large)	coccus G (-)		2/2	2/2	2/2	2/2	2/2	0/2	–	–

* Choose 2 colonies from the plates of orange 1-8 and rice A-C respectively and inject the culture fluid. The difference in the size of the colonies is indicated by "large" or "small". Others are chosen by different cononies with the same size. The experiment was conducted by professor SEKIMIZU Kazuhisa, the Laboratory of Microbiology, Graduate School of Pharmaceutical Sciences at the University of Tokyo.

of experiment period in conventional farm products (orange 7-2: small). The difference between the farming systems was not found.

Although some issues such as why the bacterial species vary with the size of colonies and what kind of species of bacterium is it remain to confirming furtherly, a distinctive feature can be found in the above-mentioned. Fungi were detected out in all samples of organic farm products, indicating a high probability of fungus appearance, while other samples showed a high probability of coccus or bacillus appearance, or a low probability of fungus appearance including the cases of non-fungus appearance. These results may suggest a symbiotic relation between organic farm products and fungus. As well known, fungi are mainly comprised of yeast and saprobe, in which yeast is necessary for producing different fermented foods such as alcoholic drinks, miso, *etc*., while saprobe is known as a source for making physiologically active substance such as vitamins and enzyme. On the other hand, coccus and bacillus are known as pathogenic bacterium which causes different kind of infectious diseases. In context with this, the results of Table 3 may suggest a high consistency with the results of two corruption experiments in Figures 1 and 2, as well as Hika's views (*5*).

The evidences from farming practices may offer possible interpretation to the result that fungi were detected out in all organic farm products as shown in Table 3. Table 4 indicates the organic materials use in the production of sample farm products from farmer surveys. All organic farmers are strongly conscious of the use of microorganism and apply fermented organic fertilizers made by utilizing effective microorganism in their cultivation. The farmers of orange 1 and 3 which only fungi were detected out have 40 years of experience in low-input organic farming. The farmer of orange 5 utilized organic fertilizers with microorganism and minerals in his fertility management, and carried out the leaf surface spraying of mineral liquid fertilizers, amino acid materials and different kind of vinegars for promoting the work of enzyme, from three weeks to one week ago of harvesting. These evidences may suggest a causal dependence between the results of Table 3 and farmers' farming practices, although further research is necessary for identifying whether the bacterium or fungi detected are adhesive or symbiotic microorganism.

A problem is why different results were observed from organic farm products (orange 1-5 and rice A) in the separation experiment of bacteria. The reasons may be explained from the different farming practices of organic farmers.

The first reason may be from the difference in the kinds and quality of organic fertilizers used in farm

Table 4. Organic materials use in the production of sample farm products

Samples	Farming systems	Obtained routes of samples	Organic materials used	Years of organic farming
Orange 1	Low input organic	Farmer	Fermented manures (Bokashi) with the uses of fish wastes, *etc*.	40
Orange 2	Organic	Farmer	Bokashi with soil microorganism, fermented natural green liquid, wood vinegars, *etc*.	26
Orange 3	Low input organic	Farmer	Potting soil with native bacterium, fermented natural green liquid, fermented fowl droppings	40
Orange 4	Organic	Farmer	Fermented fowl dropping, Bokashi manures with fish wastes, fully ripened hog droppings compost	11
Orange 5	Organic	Farmer	Bokashi manures, fully fermented manures with the main constituent of fish powder, manures containing the ground oyster shell, natural magnesium sulfate, mineral energies, vinegars, *etc*.	15
Orange 6	No organic label	Farmers market	Unknown	Unknown
Orange 7	No organic label	Farmers market	Unknown	Unknown
Orange 8	No organic label	Farmers market	Unknown	Unknown
Rice A	Organic	Farmer	Native microorganism, home-made Bokashi fertilizers utilizing "Ehime AI-1"	10
Rice B	Farmer's family use	Farmer	Unknown	Unknown
Rice C	Conventional	Consumers' cooperative	Unknown	Unknown

The data of oranic farmers are from farmer surveys."Ehime AI-1" is a kind of microbial materials developed by the Ehime Industrial Technology Center, a liquid fermenting yeast, lactic acid bacterium, and bacillus natto by using molasses.

production. *e.g.*, the use of raw organic manure or non-fully ripened compost will lead to the corruption and therefore putrefactive bacterium. By contrast, the application of organic fertilizers with effective microorganism may result in the adhesion or symbiosis of microorganism in farm products. In this case, fungus may be detected from the farm products even if they are not produced by organic farming, like orange 8 in Table 3.

The second reason may be related to the period of transferring conventional farming systems to organic farming. The crops in the farmland with a short period of organic farming practice may be influenced by the residual of chemical fertilizers and agrichemicals used in the conventional farming period, which therefore lead to putrefactive bacteria detection.

The third reason may associate with the storage time and whether there is the invasion of putrefactive bacterium in the meantime. A long time from harvest to getting the sample may cause the invasion of putrefactive bacterium, and then lead to putrefactive bacteria detection regardless of the difference in farming systems or farmers' practices.

The fourth reason may come from the difference in production environment of the farm products. The six samples of organic farm products are obtained from different farmers. The difference in production conditions among the farmers may exert influence on the composition of microorganism attached to or living symbiotically within crops and therefore the results of experiments.

In any case, further evidences are needed.

4. Policy applications of the findings: the modern significance of "Yakushokudougen" in transferring to organic agriculture

The common point of two corruption experiments is that conventional farm products illustrated fast-growing corruption with strong unpleasant smell distinctively different from organic farm products. Furthermore, the separation experiments of bacterium indicated a high possibility of fungus appearance in organic farm products and coccus or bacillus appearance in conventional farm products, which are significantly consistent with the results of two corruption experiments and farmers' farming practices in Table 4. These findings suggest some policy applications, although further evidences are needed.

One of the policy applications is that these results suggest the necessity of reconsidering the significance of "Yakushokudougen". In Japanese agriculture, the ratio of organic farming is only 0.2-0.4%. This fact indicates that almost all farm products are produced by conventional farming. Our findings suggest that our dietary life, for a long time, has relied on the farm products that are easy to decay and with a high probability of appearance of pathogenic bacterium causing infectious diseases. It is therefore an important issue to consider how we should accept this.

There is a thought of "Yakushokudougen" in

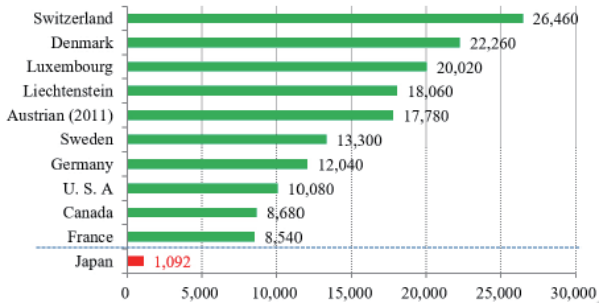

Figure 3. The 10 countries with the highest per capita consumption of organic food products and Japan: 2012. The figures are calculated by 1 euro = 140 JPY according to FiBL and IFOAM.

traditional Chinese medicine (Kampo medicine), which means that using medicinal herbs or food products in the daily meals is effective for preventing health from diseases or health improvement. It is also explained that a healthy and balanced diet by choosing the food products suitable for one's health can improve health and therefore reduce the medicine use. The meaning of "Yakushokudougen" is extended as "Ishokudougen" in Japanese, implying that a sound daily eating habit will lead to disease prevention and health improvement. This thought suggests that the health or life of people, and therefore the medical expenses to pay for them may be influenced by the food products that we choose or eat. Therefore, many Japanese organic farmers and researchers regard organic farm products as safe and trust-worthy food products, convinced of the thought of "Ishokudougen" (*2,3,6*). Hika argued that the farm products produced with the use of effective microorganism could improve the intestinal environment because of the work of useful enzyme, and then enhance the antioxidant or immune system of people (*5*). The results of this study may offer some evidences for these views.

According to the Ministry of Health, Labor and Welfare, the national medical expenses of Japan have increased year by year and reached 39,300 billion yen in 2013. This amount is equivalent to 10.9% of national income, 49.8% of domestic output of food industry, and 4.6 times of gross agricultural product. If the huge medical expenses are related with the results of this study, namely, conventional farm products become easy to decay and with a high possibility of appearance of pathogenic bacterium causing infectious diseases, the effort of transferring existing agriculture to organic agriculture may contribute not only to the environmental conservation and the establishment of a healthy dietary life, but also to the reduction of national medical expenses or fiscal improvement.

The results of this study also propose an issue about what the relationship between food and farming systems should be like. If the fertility management of farmers and the choice of farming systems (organic or conventional) bring substantial effects in the property of farm products as shown in the results of our experiments and exert influence on the health of people such as the antioxidant or immune system of one's body, as Hika argued, the problems of what kind of "food" is desirable for us and therefore what kind of "agriculture" should be chosen may arise as important policy issues. Furthermore, if the health of people is involved in the results of this study as mentioned, a farming system aimed to supply safer and more reliable farm products should be viewed as a rational choice. This therefore suggests a policy alternative to further develop organic farming or sustainable agriculture that supplies farm products with environmentally safe and trusted food.

According to the Ministry of Agriculture, Forestry and Fisheries, 28% of farm-job applicants want to adopt organic farming, and 65% show their interest in organic farming. Moreover, 44% of consumers have the experience of buying organic farm products, and 55% express a willing of buying organic food products. These surveys suggest a high level of awareness for organic farming and food products. But on the other hand, both organic farmers and farming area are only 0.2-0.4% of Japanese agriculture. One of the reasons is that the understanding of consumers is not enough for the further development of organic farming (*8,9*). As shown in Figure 3, per capita consumption of organic food products in Japan was 1,092 Japanese yen, while Switzerland with the highest level in the top 10 countries was 26,460 yen, and France in the last place of the 10 countries was 8,540 yen (*7*). The Engel's coefficients of Japan and the European countries are approximately in the first half of 20%, without significant difference. However, per capita consumption of organic food products exhibits a wide difference from 8 to 24 times. The reason that Japanese organic farming did not greatly extend may be right here.

To improve the current situation, both the effort of agricultural side and the true understanding of consumers are necessary. This study offers empirical evidences for supporting the development of organic agriculture and the consumption expansion of organic farm products, but further works are needed.

Acknowledgements

This study was supported in part by the Grant-in-Aid for Scientific Research (C) (2010-2012: 22580251 and 2013-2015: 25450325). The author thanks professor SEKIMIZU Kazuhisa (the Laboratory of Microbiology, Graduate School of Pharmaceutical Sciences at The University of Tokyo) for conducting the separation experiment of bacteria.

References

1. Shiro T. Fruit cultivation and organic agriculture. An invited lecture in the ninth open seminar of organic farming in Yamanashi, by the Council for Organic

Farming Technology. January 23, 2011. (in Japanese)
2. Akinori K. A Way to Natural Farming. Soshinsha Inc., 2007. (in Japanese)
3. Akinori K. What Apple Taught Us. Nikkei Publishing Inc., 2009. (in Japanese)
4. Izumi Y. Difference between organic JAS farming and natural farming. 2015. (*http://www.j-organic.org/different.html*) (in Japanese)
5. Teruo H. What is fermentation, what is corruption? – The roles of microorganism in distinguishing fermentation and corruption. Kenko Seikatsu Sengen. 2012:3-12. (in Japanese)
6. Masaaki K. Basic and Practice of Organic Farming. Nobunkyo Inc., 2005. (in Japanese)
7. FiBL and IFOAM, the World of Organic Agriculture: Statistics and Emerging Trends 2014.
8. Hu B. Economic Analysis of Sustainable Agriculture. Norin Tokei Kyokai Inc., 2007. (in Japanese)
9. Hu B. Agriculture and Environmental Issues under Rising Input Prices and Depression. Tsukuba Shobo Inc., 2012. (in Japanese)

(Received July 27, 2015; Revised August 4, 2015; Accepted August 25, 2015)

Original Article

DOI: 10.5582/ddt.2015.01044

Association between maternal diabetes mellitus and the risk of congenital malformations: A meta-analysis of cohort studies

Enfa Zhao[1,*], Yafei Zhang[2,*], Xianling Zeng[3], Baomin Liu[1,]**

[1] *Department of Ultrasound, Second Affiliated Hospital, Xi'an Jiaotong University School of Medicine, Xi'an, Shanxi, China;*
[2] *Department of General Surgery, Second Affiliated Hospital, Xi'an Jiaotong University School of Medicine, Xi'an, Shanxi, China;*
[3] *Department of Obstetrics and Gynecology, the First Affiliated Hospital, Xi'an Jiao Tong University, Xi'an, Shanxi, China.*

Summary **Increasing studies suggest that gestational diabetes mellitus (GDM) and pre-gestational diabetes mellitus (PGDM) may be associated with an increased risk of major congenital malformations (MCM) in the offspring. To determine whether GDM or PGDM is associated with an increased risk of congenital malformations, we performed a meta-analysis of cohort studies. We systematically searched the PubMed, Web of Science and Cochrane Library (from January, 1990 to October, 2014) and reviewed the reference lists of included papers to search for additional studies. Meta-analysis tools were used to summarize results. Summary relative risks (RRs) with 95% confidence intervals (CIs) were calculated with random-effects models or fixed-effects models. Study quality was assessed using the Newcastle-Ottawa scale. A total of 21 cohort studies were included in the meta-analysis. Analysis of all studies showed that both PGDM and GDM were associated with an increased risk of MCM (RR = 2.44, 95% CI = 1.92-3.10, I^2 = 78.3%, p = 0.342; RR = 1.11, 95% CI = 1.11-1.27, I^2 = 9.9%, p < 0.001, respectively). There is a slightly higher risk of major congenital malformations in women with GDM than in the reference group. However, this risk is much lower than in women with PGDM. Further large-scale prospective cohort studies are needed to test the effect of PGDM and GDM on specific congenital malformations risk.**

Keywords: Gestational diabetes, pre-gestational diabetes, congenital malformations, meta-analysis

1. Introduction

Women with diabetes in pregnancy can be divided into two groups: women with diabetes diagnosed before pregnancy (pre-gestational diabetes) and women with glucose intolerance diagnosed during pregnancy (gestational diabetes mellitus). Women with diabetes before pregnancy, that is, pre-gestational diabetes mellitus (PGDM), have an increased risk of pregnancy complications (*1-5*), including serious perinatal outcomes such as stillbirth, perinatal mortality, and major congenital malformations. It is reported that in the offspring of women with PGDM, the incidence of cardiovascular abnormalities ranges from 2 to 34 per 1,000 births, central nervous system abnormalities from 1 to 5 per 1,000 births, musculoskeletal abnormalities from 2 to 20 per 1,000 births, genitourinary abnormalities from 2 to 32 per 1,000 births (*6-8*). However, whether the risk of MCH is also increased in gestational diabetes mellitus (GDM) remains inconsistent. Some authors (*8-12*) have reported that GDM is associated with an increased risk of CM in the offspring, while others (*13,14*) have reported a risk comparable with that in the reference group. Still other papers (*7,15-17*) reported that women with gestational diabetes are not at risk for infant malformations. Therefore, this study was designed to perform a meta-analysis of cohort studies to evaluate the association between maternal diabetes mellitus and the risk of congenital malformations in the offspring.

2. Materials and Methods

2.1. *Search strategy*

We systematically conducted a literature search of

*These authors contributed equally to this works.
***Address correspondence to:*
Dr. Baomin Liu, Department of Ultrasound, Second Affiliated Hospital, School of Medicine, Xi'an Jiaotong University, No. 157, Xiwu Road, Xi'an, Shanxi 710004, China.
E-mail: zhaoenfasy@stu.xjtu.edu.cn

PubMed, Web of Science and Cochrane Library from January 1990 to October 2014, for human studies of maternal diabetes mellitus and the risk of congenital malformations in any language. Our overall search strategy included medical subject heading terms and/or text words: diabetes mellitus (PGDM, pregestational diabetes, pregnancy in diabetes, pregnancy in diabetics, GDM, gestational diabetes mellitus, pregnancy-induced diabetes), complications or outcomes (anomalies, congenital anomalies, malformations, congenital malformations, defects, birth defects, congenital defects). In addition, we reviewed the reference lists of including articles and recent reviews. Two independent investigators screened titles/abstracts according to the following inclusion and exclusion criteria.

2.2. *Inclusion and exclusion criteria*

A study was included in this meta-analysis if it met the following criteria: *i*) the study design was based on cohort studies; *ii*) the study evaluated the association between maternal diabetes mellitus and congenital malformations risk; *iii*) one of the outcomes under study contains congenital malformation; and *iv*) study must contains reference group. Studies were excluded if they only provided a percentage of the incidence of congenital malformation. If the publications were duplicated or shared in more than one study, the most recent publications were included.

2.3. *Data extraction*

Two authors independently extracted the following data from each publication: publication data (author, year of publication and country of population studied), methods of diabetes assessment (self-reported, registration and measuring blood glucose). Number of exposed and unexposed. Disagreements were resolved by discussion, consensus and arbitration by a third author. We evaluated the methodological quality based on the Newcastle–Ottawa Scale (NOS). The NOS contains eight items, categorised into three dimensions including selection, comparability and outcome. We defined NOS scores of 1–3, 4–6, and 7–9 for low, intermediate, and high-quality studies, respectively. And maximum score = 9. Ethical consent for the work was not required.

2.4. *Statistical analysis*

We conducted a meta-analysis of maternal diabetes mellitus and the risk of congenital malformations. Relative risk (RR) was used to estimate the effect sizes. To describe the percentage of total variation across studies attributable to heterogeneity, we used the I^2 statistic (18). A fixed-effect model was used to evaluate the RR and 95% CI if no significant heterogeneity ($p > 0.05$ and $I^2 < 50\%$) existed. Otherwise, a random-effect model was selected. For I^2, a value > 50% was considered to have severe heterogeneity. In an attempt to evaluate the possible publication bias, Begg's test (rank correlation method) (*19*) were used, and a p value of < 0.05 was considered representative of significant statistical publication bias. All statistical analyses were performed with STATA version 11.0 software (StataCorp, College Station, TX).

3. Results

3.1. *Characteristics of the subjects in selected studies*

Detailed search procedures are summarized in Figure 1. The search strategy identified 4,854 references. Two studies (*20,21*) were added through reference lists of including articles searches. After excluding duplicate articles, we reviewed titles and abstracts of all identified studies to exclude those that were clearly irrelevant. Next, the full texts of the remaining articles were examined according to the inclusion and exclusion criteria. We identified 74 relevant publications for detailed evaluation and inclusion in the meta-analysis. After examining these articles in more detail, a further 53 studies were excluded. At the end of this process, 21 studies were included in the meta-analysis (*5,7,8,10-15,20-31*).

Table 1 provides information about the characteristics of the studies included (21, from five continents). The numbers of included women amount to 2,788,521 for the reference group, 34,225 for GDM and 11,210 for PGDM.

3.2. *Study quality*

We assessed study quality using the Newcastle-Ottawa scale. Since the assessment of quality related strongly to the reporting of results, a well conducted study could score poorly if the methods and results were not reported in sufficient detail. Therefore, we reported the assessment in scores. The mean NOS score for the studies was 5.43, which indicated that the study had an intermediate quality (Table 2).

3.3. *Publication bias*

To assess bias across studies, funnel plot asymmetry was checked with Begg's test to identify small study effects for the association between GDM and the risk of congenital malformations ($p = 0.979$, 95% CI = –0.84-0.82), indicating a low probability of publication bias (Figure 2). Begg's test was also used to identify small study effects for the association between PGDM and the risk of congenital malformations ($p = 0.947$, 95% CI = –2.39-2.25), indicating a low probability of publication bias (Figure 3).

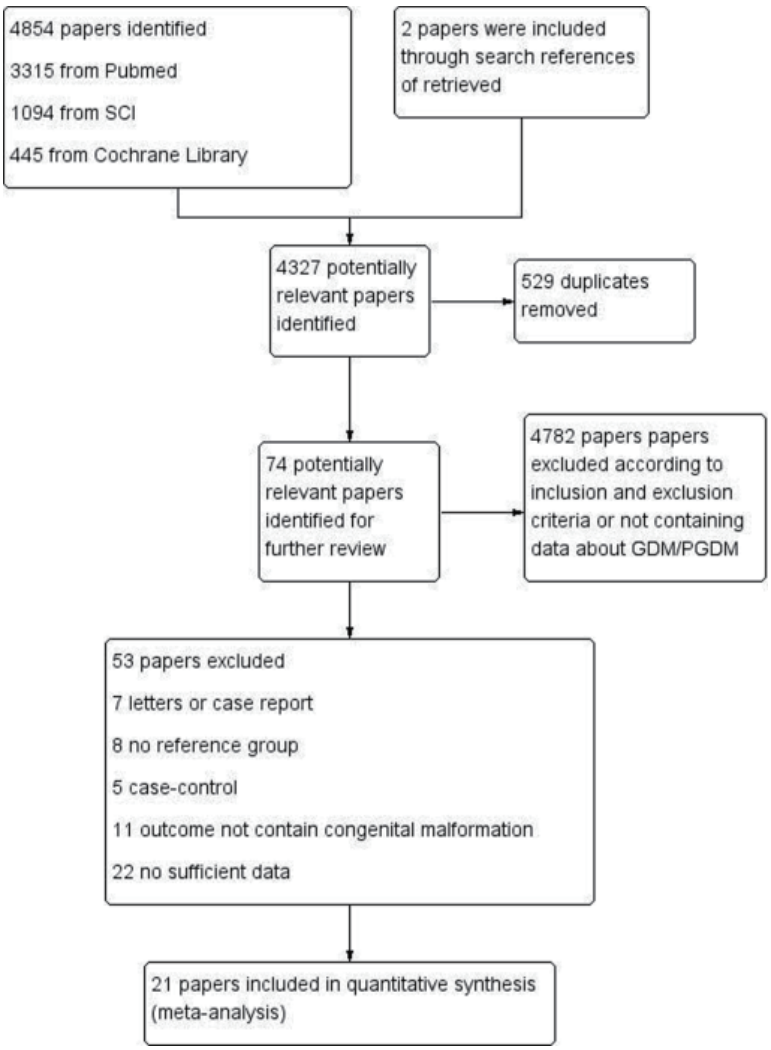

Figure 1. Flow chart on the articles selection process.

Table 1. Characteristics of studies included in the meta-analysis

Author/year	Country	GDM criteria	GDM		PGDM		Reference	
			Events (*n*)	Total (*n*)	Events (*n*)	Total (*n*)	Events (*n*)	Total (*n*)
Hod/1991	Israel	ADA	26	878	8	132	7	380
Janssen/1996	USA	NP	242	8,868	111	1,511	214	8,926
Hod/1996	Israel	ADA	4	250			9	470
Kimmerle/1997	Germany	NP			50	2,402	7,185	595,393
Djelmis/1997	Croatia	WHO (IGT/GDM)	0	94			0	46
Ramachandran1998	India	NDDG	5	211			8	851
Moore/2000	USA	NP	7	506	4	68	299	22,377
Suhonen/2000	Finland	NP			30	709	10	735
Sheffield/2002	USA	NDDG	35	2,277	25	410	2,075	142,509
Abdelgadir/2003	Sudan	WHO (DM)	0	19	3	69	0	50
Savona-Ventura/2003	Malta	OGTT*	4	242	3	47	318	8,547
Bo/2004	Italy	C and C	3	135			10	496
Chico/2005	Spain	C and C/NDDG	7	404			83	5,844
Ricart/2005	Spain	ADA/NDDG	17	819			133	8,451
Sharpe/2005	Australia	OGTT**	405	6,735	96	946	14,257	282,260
Shefali/2006	India	ADA/WHO	2	146	3	79	0	30
Abolfazl/2008	Iran	NP	4	70			3	350
Peticca/2009	Canadian	NDDG	26	2,046	18	891	727	50,914
Fadl/2010	Sweden	OGTT***	242	10,525			22,496	1,249,772
Bell/2012	UK	NP				1,677	7,613	399,472
Vinceti/2014	Italy	NP				2,269	202	10,648

C and C, Carpenter and Coustan; IGT, impaired glucose tolerance; NDDG, National Diabetes Data Group; GDM, gestational diabetes mellitus; PGDM, pregestational diabetes mellitus; ADA, American Diabetes Association; OGTT*, 2 h post-OGTT ≥ 8.6 mmol/L; OGTT**, 2 h post-OGTT ≥ 8.0 mmol/L; OGTT***, 2 h post-OGTT ≥ 9.0 mmol/L; NP, Not Provided.

Table 2. Assessment of study quality

Cohort studies		Quality Assessment Items					
		Representativeness of the cohort	Ascertainment of exposure: secure record or structured interview	Study controls for age, year, smoking, body mass index (BMI), diabetes mellitus (DM) status	Assessment of outcome: independent blind assessment or record linkage	Was follow-up long enough for outcomes to occur	Adequacy of follow-up of cohorts
1	Hod 1991	+	+	+	-	+	-
2	Janssen 1996	+	- (self-report)	+	-	+	-
3	Hod 1996	+	+	+	-	+	-
4	Kimmerle 1997	+	- (self-report)	+	-	-	-
5	Djelmis 1997	+	+	+	-	-	-
6	Ramachandran 1998	+	+	+	-	+	-
7	Moore 2000	+	- (self-report)	+	-	+	-
8	Suhonen 2000	+	- (self-report)	+	-	+	-
9	Sheffield 2002	+	- (self-report)	+	-	+	-
10	Abdelgadir 2003	+	+	++	-	+	-
11	Savona-Ventura 2003	+	- (self-report)	-	-	+	- 58.5%
12	Bo 2004	+	+	+	+	-	-
13	Chico 2005	+	+	+	-	-	-
14	Ricart 2005	+	+	+	-	-	-
15	Sharpe 2005	+	+	+	+	+	-
16	Shefali 2006	+	+	+	+	-	-
17	Abolfazl 2008	+	- (self-report)	+	-	-	-
18	Peticca 2009	+	+	-	+	-	-
19	Fadl 2010	+	+	+	-	-	-
20	Bell 2012	+	- (self-report)	+	+	+	-
21	Vinceti 2014	+	- (self-report)	++	+	+	-

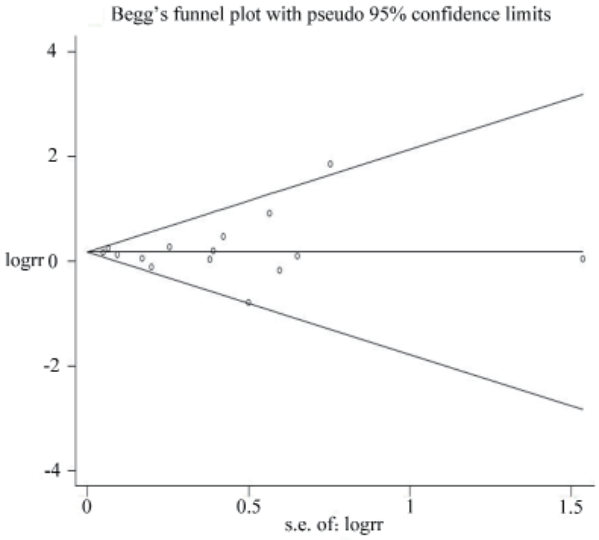

Figure 2. Funnel plot of studies evaluating the association between GDM and congenital malformations. Begg's regression asymmetry test ($p = 0.979$).

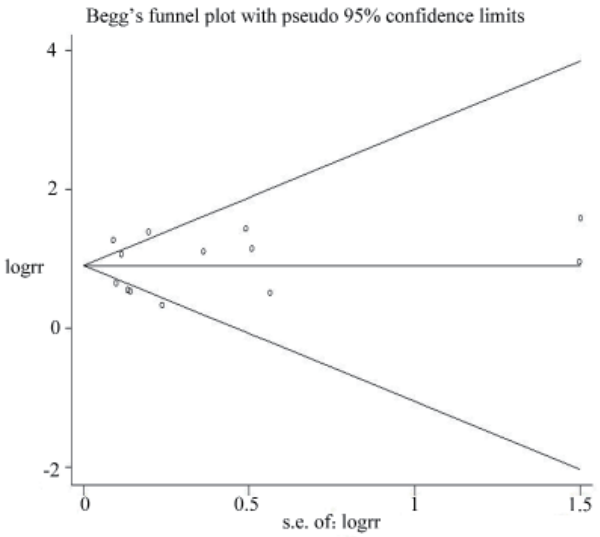

Figure 3. Funnel plot of studies evaluating the association between PGDM and major congenital malformations. Begg's regression asymmetry test ($p = 0.947$).

3.4. *GDM and major congenital malformations*

The pooled RR of GDM from the 17 cohort studies is shown in Figure 4. The meta-analysis of the 17 studies showed a positive association between gestational diabetes mellitus and major congenital malformations (summary RR = 1.18, 95% CI = 1.11-1.26) without noticeable heterogeneity among these studies ($p = 0.342$, $I^2 = 9.9\%$).

3.5. *PGDM and major congenital malformations*

The pooled RR of PGDM from the 13 cohort studies is shown in Figure 5. Compared with GDM, the meta-analysis of the 13 studies showed a stronger positive association between pre-gestational diabetes mellitus and major congenital malformations (summary RR = 2.44, 95% CI = 1.92-3.10) with noticeable heterogeneity

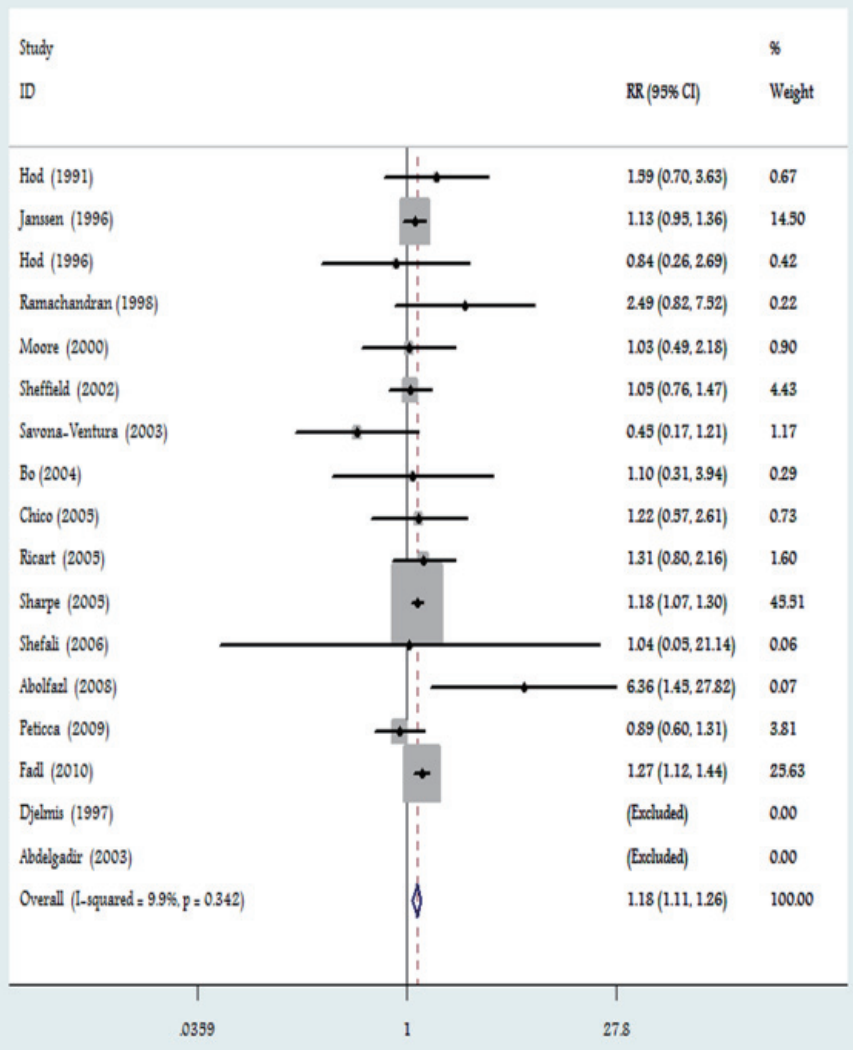

Figure 4. Relative risks (RRs) for the association between GDM and major congenital malformations in 17 studies. The diamond denotes the pooled RR. Shaded rectangles indicate the RR in each study, with sizes inversely proportional to the SE of the RR. Horizontal lines indicate the 95% confidence interval (CI).

among these studies ($p < 0.001$, $I^2 = 78.3\%$). In sensitivity analysis with omission of one study at a time and analysis of the rest, the association between PGDM and major congenital malformations remains unchanged, which suggesting that the heterogeneity may come from factors outside a single study. From the analysis, we found a significant positive association between PGDM and major congenital malformations.

4. Discussion

In this study, we evaluated the effect of maternal diabetes mellitus on congenital malformations of offspring using the results of previous cohort studies. The conclusion of this 25-year meta-analysis is that offspring of GDM women have a mild but distinctly higher risk of major congenital malformations (RR = 1.18, 95% CI = 1.11-1.26) than the reference group. This risk is much lower than that observed in women with established diabetes (RR = 2.44, 95% CI = 1.92-3.10). However, the role of etiologic factors, such as age, obesity or hyperglycemia still cannot be ascertained. Several opinions on potential links between maternal diabetes mellitus and the risk of congenital malformations have been proposed.

The pathogenesis of major congenital malformations of all types is complicated and has possibly a multifactorial origin (*32,33*). The link between hyperglycemia and congenital anomalies has been established, but the precise mechanism it occurs has not been completely elaborated. It is supposed that hyperglycemia could cause damage to the developing yolk sac, an increased production and liberation of free oxygen radicals, deficiency of myoinositol and arachidonic acid and a disruption in signal transduction (*34*); increasing evidences suggest that embriopathies may be connected to a disruption in intracellular signaling by inositol-derived effectors and prostaglandin precursors such as arachidonic acid (35). As a result of the presence of these fuels, some type of genotoxic effect might occur which could cause morphologic damages in the fetus (*33,36*). Nowadays, there is compelling evidence linking epigenetic factors to GDM. Some

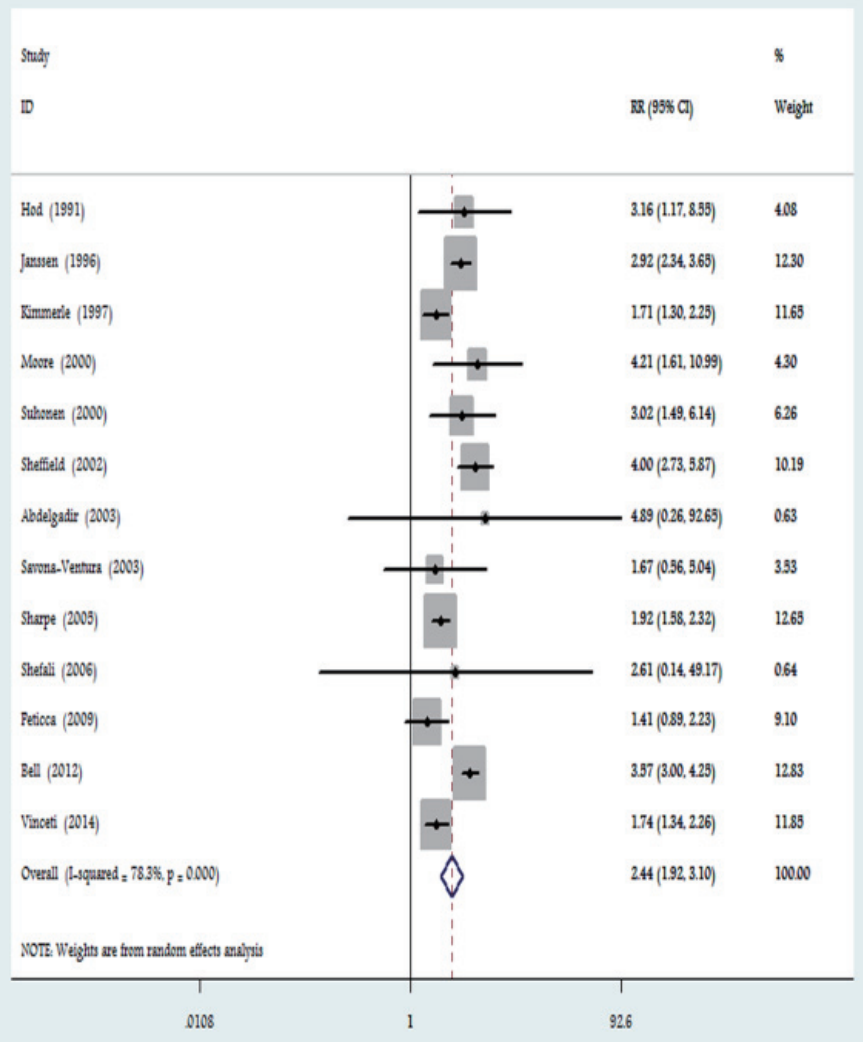

Figure 5. Relative risks (RRs) for the association between PGDM and major congenital malformations in 13 studies. The diamond denotes the pooled RR. Shaded rectangles indicate the RR in each study, with sizes inversely proportional to the SE of the RR. Horizontal lines indicate the 95% confidence interval (CI).

epigenetic alterations mainly related to beta cell function and intrauterine growth retardation have been described recently. These alterations could result in reduction of expression of PDX-1, a transcription factor that regulates beta cell development (*37*). And it is important to note that epigenetic effects are defined as heritable changes to DNA structure that do not involve changes to the DNA sequence. Previous studies have showed that folic acid, that is a methyl donor, which prevents genomic damage in human lymphocytes in vitro and maybe also the cytotoxicity, genotoxicity, and perhaps have cytostatic effects on the human genome. However, randomized trials recently have confirmed that periconceptional supplementation with folic acid can reduce the frequency of midline embryonic defects, as well as heart defects, orofacial clefts and miscarriages (38).

Negrato *et al*. hold that pre-gestational diabetes can predispose the fetus to many alterations in organogenesis and growth restriction (*39*), and all fetal adverse pregnancy outcomes are closely related to poor glycemic control during the organogenesis period. Hyperglycemia during the periconceptional period is probably the major teratogenic existing factor, the increased risk of congenital abnormalities found in diabetic mothers seems to be associated to poor metabolic control during the period of organogenesis that occurs in the first trimester of pregnancy probably due to the negative impact of a hyperglycemic milieu in the growing fetus (*33*). But obesity, hypertension and other factors associated with the metabolic syndrome might also be relevant (40).

Our meta-analysis has several strengths. First, the number of cases included was large, suggesting the solid evidence in evaluating the epidemiologic association between maternal diabetes mellitus and congenital malformations risk. Second, the included studies were conducted in different countries, making the results more acceptable. Third, based on the NOS, all of the studies included in this meta-analysis were of high or intermediate quality, making the results more reliable. However, our meta-analysis also has several limitations. First, we cannot to perform a

meta-regression analysis to evaluate the influence of variables such as age and BMI on the risk of MCM because of these variables were not always available. Second, the diagnostic criteria of GDM in some of the studies were based on self-report, which may lead to some misclassification. However, earlier studies have shown that self-reported responses for many common chronic diseases such as DM are reliable compared with medical record (*41*). In our analysis, we did not find significant different RRs between studies using medical records, or blood level as a means of DM diagnostic criteria and using self-report data to determine GDM status. Another limitation is methodological issue related to study design. Although nearly all the cases were confirmed after delivery, reporting may be not completed. Some misclassification of outcome is likely to occur. Finally, maternal diabetes mellitus and congenital malformations share several risk factors that may confound the relationship. However, confounding cannot be fully excluded because our analyses were based on observational studies.

In summary, our analysis further confirms that maternal diabetes mellitus is associated with an increased risk of congenital malformations. With a worldwide increasing prevalence of GDM, the incidence of congenital malformations may increase. Our findings furthermore underline the importance of preventing the emerging worldwide epidemic of GDM. These results suggest that more aggressive management is needed for pregnant women with PGDM and GDM.

References

1 Persson M, Norman M, Hanson U. Obstetric and perinatal outcomes in type 1 diabetic pregnancies: A large, population-based study. Diabetes care. 2009; 32:2005-2009.

2. Lapolla A, Dalfra MG, Di Cianni G, Bonomo M, Parretti E, Mello G; Scientific Committee of the GISOGD Group. A multicenter Italian study on pregnancy outcome in women with diabetes. Nutr Metab Cardiovasc Dis. 2008; 18:291-297.

3. Shand AW, Bell JC, McElduff A, Morris J, Roberts CL. Outcomes of pregnancies in women with pre-gestational diabetes mellitus and gestational diabetes mellitus; a population-based study in New South Wales, Australia, 1998-2002. Diabet Med. 2008;25:708-715.

4. Evers IM, de Valk HW, Visser GH. Risk of complications of pregnancy in women with type 1 diabetes: Nationwide prospective study in the Netherlands. BMJ. 2004; 328:915.

5. Vinceti M, Malagoli C, Rothman KJ, Rodolfi R, Astolfi G, Calzolari E, Puccini A, Bertolotti M, Lunt M, Paterlini L, Martini M, Nicolini F. Risk of birth defects associated with maternal pregestational diabetes. Eur J Epidemiol. 2014; 29:411-418.

6. Aberg A, Westbom L. Association between maternal pre-existing or gestational diabetes and health problems in children. Acta Paediatr. 2001; 90:746-750.

7. Sheffield JS, Butler-Koster EL, Casey BM, McIntire DD, Leveno KJ. Maternal diabetes mellitus and infant malformations. Obstet Gynecol. 2002; 100:925-930.

8. Sharpe PB, Chan A, Haan EA, Hiller JE. Maternal diabetes and congenital anomalies in South Australia 1986-2000: A population-based cohort study. Birth Defects Res A Clin Mol Teratol. 2005; 73:605-611.

9. Gasim T. Gestational diabetes mellitus: Maternal and perinatal outcomes in 220 saudi women. Oman Med J. 2012; 27:140-144.

10. Fadl HE, Ostlund IKM, Magnuson AFK, Hanson USB. Maternal and neonatal outcomes and time trends of gestational diabetes mellitus in Sweden from 1991 to 2003. Diabet Med. 2010; 27:436-441.

11. Abolfazl M, Hamidreza TS, Narges M, Maryam Y. Gestational diabetes and its association with unpleasant outcomes of pregnancy. Pakistan Journal of Medical Sciences. 2008; 24:566-570.

12. Kimmerle R, Von Kries R, Berger M. Pregnancy outcomes in mothers with pregestational diabetes (PGD): A population-based study in northrhine (Germany). Diabetologia. 1996; 39:A207-A207.

13. Hod M, Rabinerson D, Kaplan B, Peled Y, Bar J, Shindel B, Merlob P, Ovadia J, Neri A. Perinatal complications following gestational diabetes mellitus how 'sweet' is ill? Acta Obstet Gynecol Scand. 1996; 75:809-815.

14. Peticca P, Keely EJ, Walker MC, Yang Q, Bottomley J. Pregnancy outcomes in diabetes subtypes: How do they compare? A province-based study of Ontario, 2005-2006. J Obstet Gynaecol Can. 2009; 31:487-496.

15. Ramachandran A, Snehalatha C, Clementina M, Sasikala R, Vijay V. Foetal outcome in gestational diabetes in south Indians. Diabetes Res Clin Pract. 1998; 41:185-189.

16. Garner P. Type I diabetes mellitus and pregnancy. Lancet. 1995; 346:157-161.

17. Kjos SL, Buchanan TA. Gestational diabetes mellitus. N Engl J Med. 1999; 341:1749-1756.

18. Higgins JP, Thompson SG. Quantifying heterogeneity in a meta-analysis. Stat Med. 2002; 21:1539-1558.

19. Begg CB, Mazumdar M. Operating characteristics of a rank correlation test for publication bias. Biometrics. 1994; 50:1088-1101.

20. Shefali AK, Kavitha M, Deepa R, Mohan V. Pregnancy outcomes in pre-gestational and gestational diabetic women in comparison to non-diabetic women − A prospective study in Asian Indian mothers (CURES-35). J Assoc Physicians India. 2006; 54:613-618.

21. Suhonen L, Hiilesmaa V, Teramo K. Glycaemic control during early pregnancy and fetal malformations in women with Type I diabetes mellitus. Diabetologia. 2000; 43:79-82.

22. Hod M, Merlob P, Friedman S, Schoenfeld A, Ovadia J. Gestational diabetes mellitus. A survey of perinatal complications in the 1980s. Diabetes. 1991; 40:74-78.

23. Janssen PA, Rothman I, Schwartz SM. Congenital malformations in newborns of women with established and gestational diabetes in Washington State, 1984-91. Paediatr Perinat Epidemiol. 1996; 10:52-63.

24. Djelmis J, Blajić J, Buković D, Pfeifer D, Ivanisević M, Kendić S, Votava-Raić A. Glycosylated hemoglobin and fetal growth in normal, gestational and insulin dependent diabetes mellitus pregnancies. Coll Antropol. 1997; 21:621-629.

25. Moore LL, Singer MR, Bradlee ML, Rothman KJ, Milunsky A. A prospective study of the risk of congenital

defects associated with maternal obesity and diabetes mellitus. Epidemiology. 2000; 11:689-694.
26. Abdelgadir M, Elbagir M, Eltom A, Eltom M, Berne C. Factors affecting perinatal morbidity and mortality in pregnancies complicated by diabetes mellitus in Sudan. Diabetes Res Clin Pract. 2003; 60:41-47.
27. Savona-Ventura C, Ellul A, Chircop M. The outcome of diabetic pregnancies in Malta. Int J Gynaecol Obstet. 2003; 82:217-218.
28. Bo S, Menato G, Gallo ML, Bardelli C, Lezo A, Signorile A, Gambino R, Cassader M, Massobrio M, Pagano G. Mild gestational hyperglycemia, the metabolic syndrome and adverse neonatal outcomes. Acta Obstet Gynecol Scand. 2004; 83:335-340.
29. Chico A, Lopez-Rodo V, Rodriguez-Vaca D, Novials A. Features and outcome of pregnancies complicated by impaired glucose tolerance and gestational diabetes diagnosed using different criteria in a Spanish population. Diabetes Res Clin Pract. 2005; 68:141-146.
30. Ricart W, Lopez J, Mozas J, et al. Potential impact of American Diabetes Association (2000) criteria for diagnosis of gestational diabetes mellitus in Spain. Diabetologia. 2005; 48:1135-1141.
31. Bell R, Glinianaia SV, Tennant PW, Bilous RW, Rankin J. Peri-conception hyperglycaemia and nephropathy are associated with risk of congenital anomaly in women with pre-existing diabetes: A population-based cohort study. Diabetologia. 2012; 55:936-947.
32. Hawthorne G, Robson S, Ryall EA, Sen D, Roberts SH, Ward Platt MP. Prospective population based survey of outcome of pregnancy in diabetic women: Results of the Northern Diabetic Pregnancy Audit, 1994. BMJ. 1997; 315:279-281.
33. Reece EA, Homko CJ. Why do diabetic women deliver malformed infants? Clin Obstet Gynecol. 2000; 43:32-45.
34. Eriksson UJ, Borg LA. Diabetes and embryonic malformations. Role of substrate-induced free-oxygen radical production for dysmorphogenesis in cultured rat embryos. Diabetes. 1993; 42:411-419.
35. Hod M. Advances in the understanding of diabetic embryopathy: Signal transduction. Early pregnancy. 1996; 2:121-128.
36. Reece EA, Homko CJ, Wu YK. Multifactorial basis of the syndrome of diabetic embryopathy. Teratology. 1996; 54:171-182.
37. Pollin TI. Epigenetics and diabetes risk: Not just for imprinting anymore? Diabetes. 2011; 60:1859-1860.
38. Bailey LB, Berry RJ. Folic acid supplementation and the occurrence of congenital heart defects, orofacial clefts, multiple births, and miscarriage. Am J Clin Nutr. 2005; 81:1213S-1217S.
39. Negrato CA, Mattar R, Gomes MB. Adverse pregnancy outcomes in women with diabetes. Diabetol Metab Syndr. 2012; 4:41.
40. Jovanovic L, Pettitt DJ. Gestational diabetes mellitus. JAMA. 2001; 286:2516-2518.
41. Okura Y, Urban LH, Mahoney DW, Jacobsen SJ, Rodeheffer RJ. Agreement between self-report questionnaires and medical record data was substantial for diabetes, hypertension, myocardial infarction and stroke but not for heart failure. J Clin Epidemiol. 2004; 57:1096-1103.

(Received July 11, 2015; Revised August 22, 2015; Accepted August 25, 2015)

Original Article

DOI: 10.5582/ddt.2015.01014

Niemann-Pick disease type C2 protein induces autophagy and inhibits growth in FM3A breast cancer cells

Tatsuo Adachi, Yasuhiko Matsumoto, Yoshinori Inagaki, Kazuhisa Sekimizu*

Laboratory of Microbiology, Graduate School of Pharmaceutical Sciences, The University of Tokyo, Tokyo, Japan.

Summary **Some peptides that are highly conserved between insects and mammals have anti-tumor action. Screening for inhibitors of cell growth from animal fluids may provide useful clues to anti-tumor drugs. Inducers of autophagy also have anti-tumor activity. The current authors recently studied a protein found in silkworm hemolymph, Niemann-Pick disease type C2 (NPC2). This protein, which is highly conserved among eukaryotes, was found to have anti-proliferative action on a silkworm cell line. The current study found that the silkworm NPC2 protein also inhibits the growth of FM3A murine breast cancer cells. In FM3A cells, silkworm NPC2 increased phosphorylation of AMP-activated protein kinase and decreased phosphorylation of Akt and mammalian target of rapamycin, which are regulators of autophagy. This study also found that NPC2 increased the amount of microtubule-associated protein light chain 3 (LC3)-II, an autophagosome marker, in FM3A cells. Silkworm NPC2 also induced an increase in the number of LC3-dots, a marker of pre-autophagic endosomes, in FM3A cells. When silkworm NPC2 was used to inhibit FM3A cell growth, that inhibition was attenuated by chloroquine, which inhibits autophagic activity by preventing lysosomal acidification. Murine NPC2 also inhibited growth and induced autophagy in FM3A cells. These findings suggest that NPC2 is involved in the induction and/or maintenance of autophagy and may help to elucidate the mechanisms underlying other neurodegenerative disorders such as Niemann-Pick disease.**

Keywords: Niemann-Pick disease type C2, autophagy, breast cancer cell, silkworm

1. Introduction

The identification of natural products that suppress cancer cell growth provides clues to potential anti-cancer drugs. Animal fluids, including insect hemolymph, are often used as a resource with which to identify inhibitors of the growth of mammalian cancer cells (*1-5*). Some peptides are highly conserved between insects and mammals and are believed to function as tumor suppressors in humans (*6,7*). Therefore, screening for novel inhibitors of growth in animal fluids may provide clues to potential anti-cancer drugs as well as insight into endogenous anti-tumor systems.

Released online in J-STAGE as advance publication April 6, 2015.

**Address correspondence to:*
Dr. Kazuhisa Sekimizu, Laboratory of Microbiology, Graduate School of Pharmaceutical Sciences, The University of Tokyo, 7-3-1 Hongo, Bunkyo-ku, Tokyo 113-0033, Japan.
E-mail: sekimizu@mol.f.y-tokyo.ac.jp

Recent studies have revealed that autophagy is an important mechanism for suppressing tumors in animal bodies. The *BECN1* autophagy gene is monoallelically deleted in 40% to 75% of cases of human sporadic breast, ovarian, and prostate cancers (*8*). Atg genes encode canonical autophagy components and are associated with the suppression of cancer in mouse models. Mice with systemic mosaic deletion of *Atg5* and liver-specific *Atg7-/-* develop benign liver adenomas (*9*). AMP-activated protein kinase (AMPK) is an upstream kinase that positively regulates autophagy, whereas mammalian target of rapamycin (mTOR) is a negative regulator (*10*). AMPK activators and mTOR inhibitors, which are potent inducers of autophagy, have anti-tumor activity *in vitro* (*11-13*). The induction of autophagy might therefore be an effective method for controlling malignant cell growth.

The current authors recently reported that silkworm hemolymph inhibits proliferation of BmN4 cells, a silkworm-derived cell line, and that the silkworm NPC2 protein is the factor responsible (*14*). NPC2 is

highly conserved among eukaryotes, and mutations of the human *NPC2* gene are observed in 5% of patients with Niemann-Pick disease type C (*15,16*). The current authors previously reported that NPC2 activates AMPK in BmN4 cells (*14*). NPC-model mice, which carry a mutation in *Npc1*, present with a progressive loss of cerebellar Purkinje cells, hepatomegaly, and splenomegaly (*17*). Intriguingly, mice with impaired autophagy also have these features (*18-20*). These findings and the fact that AMPK is a positive regulator of autophagy led the current authors to hypothesize that NPC2 contributes to induction of the autophagy of malignant cells. This study has sought to verify whether both silkworm NPC2 and murine NPC2 induce autophagy and inhibit cell growth in the FM3A murine breast cancer cell line.

2. Materials and Methods

2.1. *Cell culture*

The FM3A murine breast cancer cell line was generously donated by Dr. Fumio Hanaoka (Gakushuin University, Japan). The FM3A cells were cultured and maintained in Dulbecco's modified Eagle medium (DMEM; Gibco, Grand Island, NY, USA) containing 10% fetal bovine serum (FBS; Hyclone, Logan, UT, USA), penicillin (100 IU), and streptomycin (100 µg/mL) at 33°C and 5% CO_2. For all cell growth assays, Western blotting, and immunofluorescent analyses, the culture medium for FM3A cells was replaced with DMEM without FBS and incubated at 33°C for 24 h in 5% CO_2. Samples containing medium were supplemented with 5% FBS instead of 10% FBS.

2.2. *Antibodies*

Anti-silkworm NPC2 antiserum was prepared as described previously (*14*). Primary rabbit antibodies to total AMPK (#2532), phospho AMPK (#2531), total Akt (#4691), phospho Akt (#9271), total mTOR (#2983), total S6K (#2708), microtubule-associated protein light chain 3 (LC3)-B (#2775), and β-actin (#4967) were obtained from Cell Signaling Technology Japan. Antibodies to phospho mTOR (#09-213) and phospho S6K (#07-018) were purchased from Millipore. Anti-rabbit IgG, HRP-Linked Whole Ab (from donkeys, #NA934) was purchased from GE Healthcare (Piscataway, NJ, USA). Anti-rabbit IgG, fluorescein isothiocyanate (FITC)-conjugated (from goats) (#sc-2012) was obtained from Santa Cruz Biotechnology (Dallas, TX, USA).

2.3. *Preparation of silkworm hemolymph and recombinant proteins*

Abdominal legs of silkworm larvae (day 5 or 6 of 5th instar) were cut with scissors, and blood from the wound was collected in ice-cold tubes. Silkworm blood was incubated at 60°C for 30 min and then centrifuged. The supernatant was frozen in liquid nitrogen and stored at -80°C before use. This fraction is hereafter referred to as silkworm hemolymph. Recombinant silkworm NPC2 and murine NPC2 were prepared as described previously (*14*).

2.4. *Measurement of cell growth*

FM3A cells were suspended by pipetting and counted using a cytometer at the indicated time. To test the inhibition of growth by silkworm hemolymph, various media were prepared as follows: control (45% DMEM, 5% FBS, 50% saline, 50 IU penicillin, 50 µg/mL streptomycin); 20% silkworm hemolymph (45% DMEM, 5% FBS, 30% saline, 20% silkworm hemolymph, 50 IU penicillin, 50 µg/mL streptomycin), and 40% silkworm hemolymph (45% DMEM, 5% FBS, 10% saline, 40% silkworm hemolymph, 50 IU penicillin, 50 µg/mL streptomycin). For recombinant proteins, the sample volume was increased to 10% of the medium volume, and a vehicle (25 mM HEPES [pH 7.2], 10% glycerol, 100 mM NaCl) was used as the control..

2.5. *Western blotting and immunofluorescence analysis*

For Western blotting, the cells were harvested and lysed after treatment. The samples were subjected to sodium dodecyl sulfate-polyacrylamide gel electrophoresis and then transferred to a polyvinylidene-difluoride membrane (Millipore, Billerica, MA, USA). The membrane was immersed in 5% skim milk or 5% PhosphoBLOCKER™ (Cell Biolabs, Inc., San Diego, CA, USA) for 1 h at room temperature. After rinsing, the primary and secondary antibodies were allowed to react with Can Get Signal® reagent (TOYOBO) and detected using chemical luminescence. For immunofluorescence analysis, cells were harvested and washed with phosphate-buffered saline (PBS). Cells were suspended in ice-cold methanol and incubated at -20°C for 15 min. After washing twice in PBS, the cells were suspended in blocking solution (PBS containing 3% normal goat serum, 0.1% Triton X-100) and incubated at room temperature for 1 h. Cells were precipitated by centrifugation and suspended in blocking solution containing anti-LC3B (1:200) antibody. After incubation at room temperature for 1 h, the cells were washed three times with PBS and suspended in anti-rabbit FITC-conjugated IgG (1:200). Cells were further incubated in the dark for 1 h. Cells were then washed three times with PBS. Finally, the cells were gently mixed with ProLong® Gold Antifade with 4',6-diamidino-2-phenylindole (Invitrogen, Carlsbad, CA, USA) and mounted on glass slides. Images were obtained on a Leica DM 4000B fluorescence microscope (Leica Microsystems, Wetzlar, Germany).

2.6. *Statistical analysis*

For statistical analysis, experiments were performed at least twice and the data are presented as the mean ± SEM. To evaluate the growth rate, the slope of each growth curve was compared with the log-linear model. Significant differences were calculated using the Student's *t*-test. A *p*-value of less than 0.05 was considered statistically significant.

3. Results

3.1. *Silkworm hemolymph inhibits growth of FM3A cells*

The current authors recently reported that silkworm hemolymph inhibits growth of BmN4 cells, a silkworm-derived cell line (*14*). To test whether silkworm hemolymph also inhibits the growth of mammalian cells, silkworm hemolymph was added to culture medium containing FM3A cells. The 40% silkworm hemolymph medium inhibited FM3A cell growth (Figure 1A). Boiling the hemolymph at 100°C for 5 min eliminated this inhibition of growth (Figure 1B). Since NPC2 protein in silkworm hemolymph inhibits BmN4 cell growth (*14*), the current study also evaluated whether NPC2 is capable of inhibiting FM3A cell growth. Cultures of FM3A cells with 20 µg/mL recombinant NPC2 had lower cell counts than cultures of FM3A without NPC2 (Figure 2A). The amount of NPC2 in silkworm hemolymph was determined using immunoblot analysis with anti-NPC2 antiserum. The amount of NPC2 in the hemolymph was estimated to be 240 µg/mL (*i.e.*, 20% (v/v) hemolymph contains 50 µg/mL NPC2; Figure 2B). This result suggests that NPC2 is present in a sufficient quantity in silkworm hemolymph to suppress FM3A cell growth.

3.2. *Silkworm NPC2 induces autophagy in FM3A cells*

The current authors previously found that silkworm NPC2 induces phosphorylation of AMPK, one of the major protein kinases responsible for signal transduction, in BmN4 cells (*14*). Therefore, the current authors hypothesized that NPC2 would also stimulate the phosphorylation of AMPK in FM3A cells. As expected, treatment with silkworm NPC2 increased AMPK phosphorylation in FM3A cells (Figure 2C). AMPK phosphorylation induces autophagy in mammalian cells (*10*). Therefore, the current authors hypothesized that silkworm NPC2 would induce autophagy in FM3A, resulting in apparent inhibition of cell growth. Immunoblot analysis was used to examine levels of LC3-II, an autophagosome marker, in FM3A cells treated with silkworm NPC2. Silkworm NPC2 increased the amount of LC3-II in FM3A cells (Figure 2C). mTOR, a well-known negative regulator of autophagy, was also examined. Akt and S6K, the upstream and downstream kinases of mTOR, respectively, were examined. Silkworm NPC2 decreased the phosphorylation of Akt, mTOR, and S6K in FM3A cells in a concentration-dependent manner (Figure 2C). Whether treatment with silkworm hemolymph modulated the Akt/mTOR/S6K signaling pathway in FM3A cells was then examined. Silkworm hemolymph induced both an increase in AMPK phosphorylation and a decrease in Akt, mTOR, and S6K phosphorylation in FM3A cells (Figure 2D). Silkworm hemolymph increased the amount of LC3-II in FM3A cells (Figure 2D). These findings suggest that NPC2 in silkworm hemolymph activates the AMPK and the Akt/mTOR/S6K signaling pathways, inducing autophagy in the FM3A murine cell line.

Autophagosome formation is required for autophagy. Autophagosomes fuse with lysosomes to form

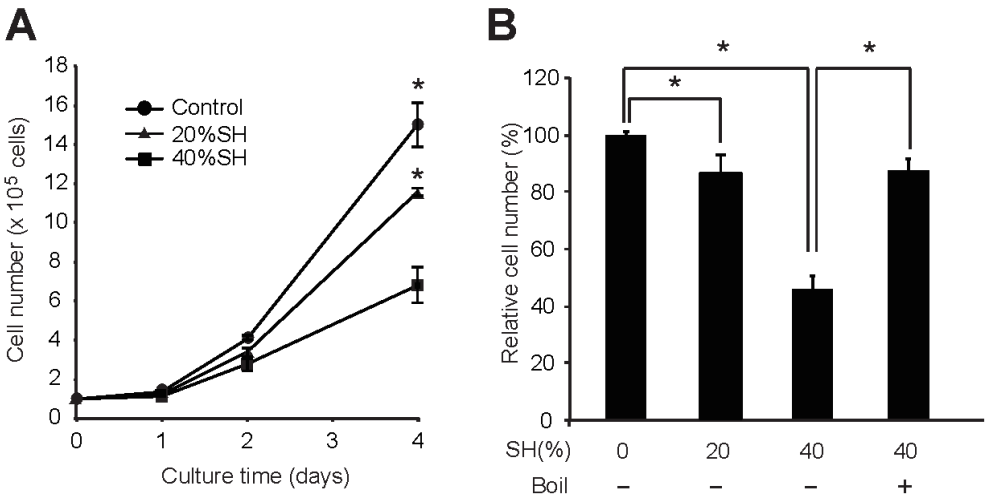

Figure 1. Inhibitory effects of silkworm hemolymph (SH) on FM3A murine breast cancer cell growth. (A) FM3A cells were incubated in culture medium containing 0% (circle), 20% (triangle), or 40% (square) silkworm hemolymph. Cell numbers were counted with a cytometer. Data are presented as the mean ± SEM of three experiments. Statistical significance between the slope of the control group and that of the sample groups was determined with the Student's *t*-test (*: $p < 0.05$). **(B)** Silkworm hemolymph was boiled at 100°C for 5 min before it was added to the culture medium. FM3A cells were cultured for 48 h and then counted. Data are presented as the mean ± SEM ($n = 3$). Statistical significance was determined with the Student's *t*-test (*: $p < 0.05$).

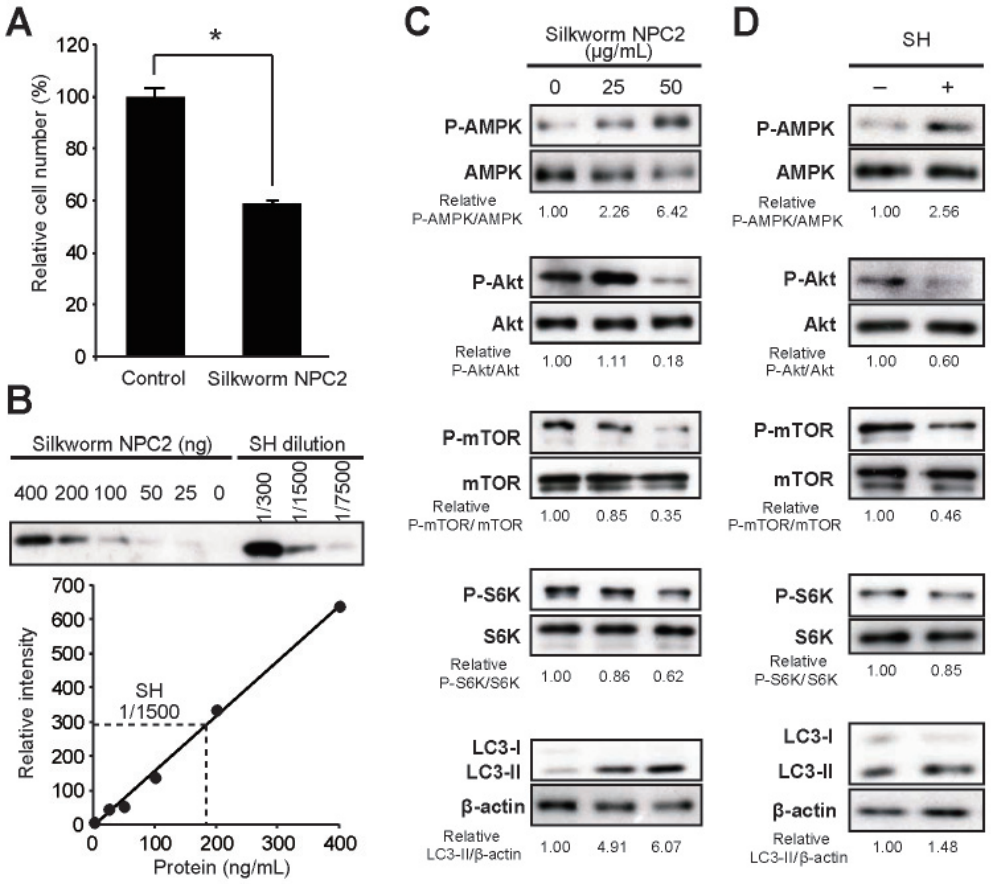

Figure 2. Silkworm NPC2 led to inhibition of growth, AMPK activation, and LC3-II accumulation in FM3A cells. (A) FM3A cells were cultured for 48 h in the presence or absence of 20 μg/mL silkworm NPC2. Cell numbers were counted with a cytometer. Data are presented as the mean ± SEM ($n = 3$). Statistical significance was determined with the Student's *t*-test (*: $p < 0.05$). **(B)** The amount of NPC2 protein in silkworm hemolymph was estimated using Western blotting. Indicated amounts of recombinant NPC2 protein and 10 μL of diluted silkworm hemolymph were subjected to Western blotting analysis with anti-silkworm NPC2 antiserum. Band intensities were quantified with an Image J-based densitometer. The amount of NPC2 protein in silkworm hemolymph was calculated using the linear regression curve of recombinant protein. **(C)** Images of Western blot analysis of FM3A cells treated with the indicated amount of silkworm NPC2 at 48 h are shown. **(D)** Images of Western blotting of FM3A cells treated with or without 20% silkworm hemolymph at 48 h are shown.

autolysosomes. Acidification of autophagosomes via fusion with lysosomes is required for the degradation of unnecessary organelles and bacteria captured by phagocytosis (*21*). Chloroquine prevents lysosomal acidification, resulting in the inhibition of autophagy (*22*). The current study examined the effect of chloroquine on inhibition of FM3A cell growth by silkworm NPC2. Chloroquine partially suppressed the inhibition of growth by silkworm NPC2 (10 μg/mL) in FM3A cells (Figure 3). Chloroquine's inhibition of autolysosome formation resulted in the accumulation of autophagosomes in several mammalian cell lines (*22*). The current study measured the autophagic flux affected by chloroquine and NPC2 using an accepted method (*23*). Chloroquine increased the accumulation of LC3-II in FM3A cells under experimental conditions (Supplementary Figure 1), suggesting NPC2 induced autophagic flux. These findings suggest that silkworm NPC2 induces autophagy, resulting in the inhibition of FM3A cell growth.

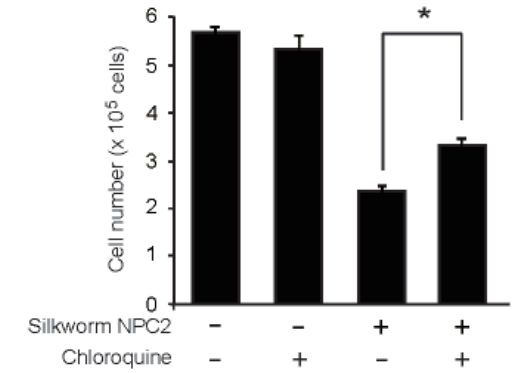

Figure 3. Suppressive effect of chloroquine on inhibition of FM3A cell growth by silkworm NPC2. FM3A cells were cultured with or without 10 μg/mL silkworm NPC2 and/or 10 μM chloroquine. After culturing for 48 h, cells were counted with a cytometer. Data are presented as the mean ± SEM ($n = 3$). Statistical significance was determined with the Student's *t*-test (*: $p < 0.05$).

3.3. *Murine NPC2 induced both cessation of cell growth and autophagy in FM3A cells*

The biological activity of NPC2 in fibroblasts is interchangable among species (*14,15*). Thus, both silkworm NPC2 and murine NPC2 were predicted to

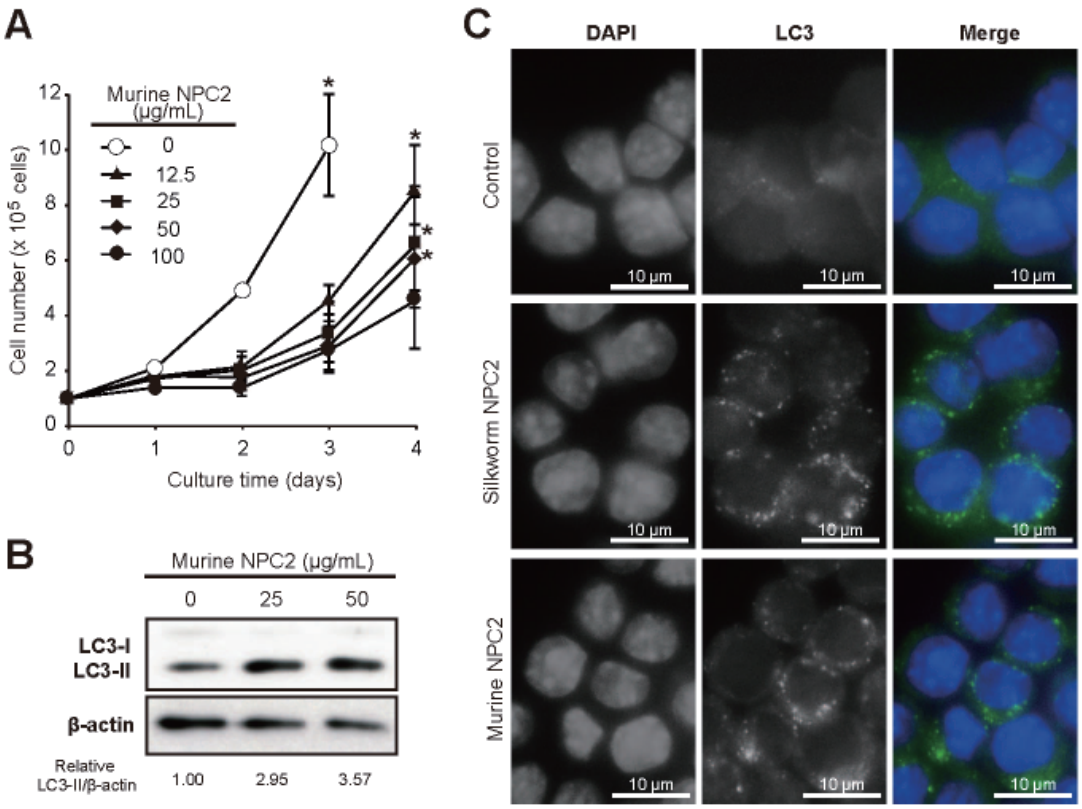

Figure 4. Inhibition of growth and induction of autophagy by murine NPC2 in FM3A cells. (A) FM3A cells were cultured with the indicated amount of murine NPC2 and cells were then counted. Data are presented as the mean ± SEM of two experiments. Statistical significance between the slope of the control group and that of the sample group was determined with the Student's *t*-test (*: $p < 0.05$). **(B)** The accumulation of LC3-II was detected after culturing for 48 h. **(C)** LC3 foci were detected with immunofluorescence analysis. FM3A cells were cultured with 20 μg/mL silkworm NPC2 or 20 μg/mL murine NPC2. Cells were fixed and permeabilized after 48 h. Anti-LC3B antibody was used as the primary antibody and anti-rabbit FITC-conjugated IgG antibody was used as the secondary antibody..

inhibit growth and induce autophagy in FM3A murine cancer cells. Murine NPC2 suppressed growth in FM3A in a dose-dependent manner (Figure 4A). Furthermore, LC3-II accumulated in FM3A cells treated with murine NPC2 (Figure 4B). Immunofluorescence analysis verified that treatment with murine or silkworm NPC2 increased autophagosome formation in FM3A cells (Figure 4C). These results suggest that both murine NPC2 and silkworm NPC2 lead to the induction of autophagy and inhibition of the growth of FM3A cells.

4. Discussion

The current findings revealed that NPC2 protein induced autophagy and inhibited cell growth in FM3A murine breast cancer cells. Both the AMPK and Akt/mTOR pathways were affected by NPC2 treatment, resulting in the induction of autophagy. To the extent known, this is the first study to report that NPC2 is a humoral factor that induces autophagy. However, non-specific inhibition caused by chloroquine cannot be ruled out as a possibility. Further analysis with more specific inhibition, such as genetic manipulation, will help to further clarify the association between the induction of autophagy and inhibition of growth by NPC2.

NPC2 is a highly conserved soluble protein in body fluids of various animal species. NPC2 is found in high concentrations in epididymal fluids (*24*). Some studies suggest that NPC2 functions as an endocrine factor (*14,25*). The current study found that both murine and silkworm NPC2 inhibited growth of FM3A cells. Thus, NPC2 appears to ubiquitously act as an anti-tumor endocrine molecule in both insects and mammals.

NPC1 is a membrane protein that is considered to function similarly to NPC2 during various physiological events because the phenotypes of NPC1-, NPC2-, and NPC1/NPC2-double knockout mice have an almost identical disease onset and progression, pathology, and neuronal storage (*26*). NPC1-deficient mice have phenotypes similar to those of mutant mice, which have phenotypes that include a defect in autophagy in terms of progressive loss of cerebellar Purkinje cells, axonal swelling, and hepatosplenomegaly. Both NPC2 and autophagy components affect hematopoiesis in hematopoietic stem cells (*20,25*) and adipogenesis in fibroblasts (*14,27,28*). The NPC1 and NPC2 proteins are thought to act together in the autophagic pathway. Recent studies suggest that NPC1 deficiency results in impaired completion of autophagy (*29,30*). The current results suggest that NPC2 is involved in the induction and/or

maintenance of autophagy. This notion may enhance the understanding of NPC and other neurodegenerative diseases.

Acknowledgements

The authors wish to thank Dr. Fumio Hanaoka for providing the FM3A cells. This work was supported by a Grant-in-Aid for the Japan Society for the Promotion of Science Fellows [24•10784] from the Japan Society for the Promotion of Science

References

1. Lichtenstein A, Ganz T, Selsted ME, Lehrer RI. *In vitro* tumor cell cytolysis mediated by peptide defensins of human and rabbit granulocytes. Blood. 1986; 68:1407-1410.
2. Koyama K, Wakabayashi K, Masutani M, Koiwai K, Watanabe M, Yamazaki S, Kono T, Miki K, Sugimura T. Presence in Pieris rapae of cytotoxic activity against human carcinoma cells. Jpn J Cancer Res. 1996; 87:1259-1262.
3. Chen HM, Wang W, Smith D, Chan SC. Effects of the anti-bacterial peptide cecropin B and its analogs, cecropins B-1 and B-2, on liposomes, bacteria, and cancer cells. Biochim Biophys Acta. 1997; 1336:171-179.
4. Xu N, Wang YS, Pan WB, Xiao B, Wen YJ, Chen XC, Chen LJ, Deng HX, You J, Kan B, Fu AF, Li D, Zhao X, Wei YQ. Human alpha-defensin-1 inhibits growth of human lung adenocarcinoma xenograft in nude mice. Mol Cancer Ther. 2008; 7:1588-1597.
5. Iwasaki T, Ishibashi J, Tanaka H, Sato M, Asaoka A, Taylor D, Yamakawa M. Selective cancer cell cytotoxicity of enantiomeric 9-mer peptides derived from beetle defensins depends on negatively charged phosphatidylserine on the cell surface. Peptides. 2009; 30:660-668.
6. Sun CQ, Arnold R, Fernandez-Golarz C, Parrish AB, Almekinder T, He J, Ho SM, Svoboda P, Pohl J, Marshall FF, Petros JA. Human beta-defensin-1, a potential chromosome 8p tumor suppressor: control of transcription and induction of apoptosis in renal cell carcinoma. Cancer Res. 2006; 66:8542-8549.
7. Han Q, Wang R, Sun C, Jin X, Liu D, Zhao X, Wang L, Ji N, Li J, Zhou Y, Ye L, Liang X, Jiang L, Liao G, Dan H, Zeng X, Chen Q. Human beta-defensin-1 suppresses tumor migration and invasion and is an independent predictor for survival of oral squamous cell carcinoma patients. PLoS ONE. 2014; 9:e91867.
8. Qu X, Yu J, Bhagat G, Furuya N, Hibshoosh H, Troxel A, Rosen J, Eskelinen EL, Mizushima N, Ohsumi Y, Cattoretti G, Levine B. Promotion of tumorigenesis by heterozygous disruption of the beclin 1 autophagy gene. J Clin Invest. 2003; 112:1809-1820.
9. Takamura A, Komatsu M, Hara T, Sakamoto A, Kishi C, Waguri S, Eishi Y, Hino O, Tanaka K, Mizushima N. Autophagy-deficient mice develop multiple liver tumors. Genes Dev. 2011; 25:795-800.
10. Kim J, Kundu M, Viollet B, Guan KL. AMPK and mTOR regulate autophagy through direct phosphorylation of Ulk1. Nat Cell Biol. 2011; 13:132-141.
11. Feng Y, Ke C, Tang Q, Dong H, Zheng X, Lin W, Ke J, Huang J, Yeung SCJ, Zhang H. Metformin promotes autophagy and apoptosis in esophageal squamous cell carcinoma by downregulating Stat3 signaling. Cell Death Dis. 2014; 5:e1088.
12. Feldman M E, Apsel B, Uotila A, Loewith R, Knight ZA, Ruggero D, Shokat KM. Active-site inhibitors of mTOR target rapamycin-resistant outputs of mTORC1 and mTORC2. PLoS Biol. 2009; 7:e38
13. Chresta CM, Davies BR, Hickson I, *et al*. AZD8055 is a potent, selective, and orally bioavailable ATP-competitive mammalian target of rapamycin kinase inhibitor with *in vitro* and *in vivo* antitumor activity. Cancer Res. 2010; 70:288-298.
14. Adachi T, Ishii K, Matsumoto Y, Hayashi Y, Hamamoto H, Sekimizu K. Niemann-Pick disease type C2 protein induces triglyceride accumulation in silkworm and mammalian cell lines. Biochem J. 2014; 459:137-147.
15. Berger AC, Vanderford TH, Gernert KM, Nichols JW, Faundez V, Corbett AH. *Saccharomyces cerevisiae* Npc2p is a functionally conserved homologue of the human Niemann-Pick disease type C 2 protein, hNPC2. Eukaryotic Cell. 2005; 4:1851-1862.
16. Millat G, Chikh K, Naureckiene S, Sleat DE, Fensom AH, Higaki K, Elleder M, Lobel P, Vanier MT. Niemann-Pick disease type C: spectrum of HE1 mutations and genotype/phenotype correlations in the NPC2 group. Am J Hum Genet. 2001; 69:1013-1021.
17. Maue RA, Burgess RW, Wang B, *et al*. A novel mouse model of Niemann-Pick type C disease carrying a D1005G-Npc1 mutation comparable to commonly observed human mutations. Hum Mol Genet. 2012; 21:730-750.
18. Nishiyama J, Miura E, Mizushima N, Watanabe M, Yuzaki M. Aberrant membranes and double-membrane structures accumulate in the axons of Atg5-null Purkinje cells before neuronal death. Autophagy. 2007; 3:591-596.
19. Komatsu M, Waguri S, Ueno T, Iwata J, Murata S, Tanida I, Ezaki J, Mizushima N, Ohsumi Y, Uchiyama Y, Kominami E, Tanaka K, Chiba T. Impairment of starvation-induced and constitutive autophagy in *Atg7*-deficient mice. J Cell Biol. 2005; 169:425-434.
20. Mortensen M, Ferguson DJP, Edelmann M, Kessler B, Morten KJ, Komatsu M, Simon AK. Loss of autophagy in erythroid cells leads to defective removal of mitochondria and severe anemia *in vivo*. Proc Natl Acad Sci U S A. 2010; 107:832-837.
21. Kabeya Y, Mizushima N, Ueno T, Yamamoto A, Kirisako T, Noda T, Kominami E, Ohsumi Y, Yoshimori T. LC3, a mammalian homologue of yeast Apg8p, is localized in autophagosome membranes after processing. EMBO J. 2000; 19:5720-5728.
22. Mizushima N, Yoshimori T, Levine B. Methods in mammalian autophagy research. Cell. 2010; 140:313-326.
23. Klionsky DJ, Abdalla FC, Abeliovich H, *et al*. Guidelines for the use and interpretation of assays for monitoring autophagy. Autophagy. 2012; 8:445-544.
24. Kirchhoff C, Osterhoff C, Young L. Molecular cloning and characterization of HE1, a major secretory protein of the human epididymis. Biol Reprod. 1996; 54:847-856.
25. Heo K, Jariwala U, Woo J, Zhan Y, Burke KA, Zhu L, Anderson WF, Zhao Y. Involvement of Niemann-Pick type C2 protein in hematopoiesis regulation. Stem Cells. 2006; 24:1549-1555.
26. Sleat DE, Wiseman JA, El-Banna M, Price SM, Verot L, Shen MM, Tint GS, Vanier MT, Walkley SU, Lobel P. Genetic evidence for nonredundant functional cooperativity between NPC1 and NPC2 in lipid transport.

Proc Natl Acad Sci U S A. 2004; 101:5886-5891.
27. Csepeggi C, Jiang M, Frolov A. Somatic cell plasticity and Niemann-pick type C2 protein: adipocyte differentiation and function. J Biol Chem. 2010; 285:30347-30354.
28. Ro SH, Jung CH, Hahn WS, Xu X, Kim YM, Yun YS, Park JM, Kim KH, Seo M, Ha TY, Arriaga EA, Bernlohr DA, Kim DH. Distinct functions of Ulk1 and Ulk2 in the regulation of lipid metabolism in adipocytes. Autophagy. 2013; 9:2103-2114.
29. Elrick MJ, Yu T, Chung C, Lieberman AP. Impaired proteolysis underlies autophagic dysfunction in Niemann-Pick type C disease. Hum Mol Genet. 2012; 21:4876-4887.
30. Sarkar S, Carroll B, Buganim Y, Maetzel D, Ng AHM, Cassady JP, Cohen MA, Chakraborty S, Wang H, Spooner E, Ploegh H, Gsponer J, Korolchuk VI, Jaenisch R. Impaired autophagy in the lipid-storage disorder Niemann-Pick type C1 disease. Cell Rep. 2013; 5:1302-1315.

(Received March 15, 2015; Revised March 30, 2015; Accepted March 31, 2015)

Supplementary Figure

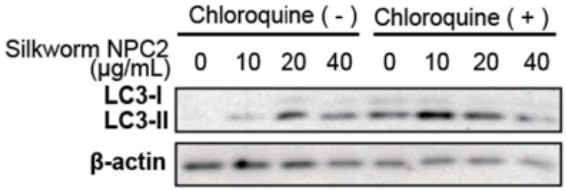

Supplementary Figure 1. Effect of chloroquine on LC3-II accumulation in FM3A cells. FM3A cells were cultured with or without the indicated amount of silkworm NPC2 and/or 10 μM chloroquine. After culturing for 48 h, the cells were subjected to Western blotting. LC3-II accumulation was detected using anti-LC3B antibody

Original Article

DOI: 10.5582/ddt.2015.01041

Combination of immunoprecipitation (IP)-ATP_Glo kinase assay and melanogenesis for the assessment of potent and safe PAK1-blockers in cell culture

Binh Cao Quan Nguyen[1,2,*], Pham Thi Be Tu[1,2,*], Shinkichi Tawata[1], Hiroshi Maruta[1,]**

[1] *PAK Research Center, Okinawa, Japan;*
[2] *Department of Biochemistry and Applied Bioscience, The United Graduate School of Agricultural Sciences, Kagoshima University, Kagoshima, Japan.*

Summary **Cucurbitacin I (CBI) is a triterpene from a bitter melon called Goya grown in Okinawa, Japan, and directly inhibits both the Tyr-kinase JAK2 and the G protein RAC, leading to the inactivation of PAK1 (RAC/CDC42-activated kinase 1). Bio 30, a propolis produced in New Zealand, contains CAPE (caffeic acid phenethyl ester) as the major anti-cancer ingredient which directly down-regulates RAC, leading to the inactivation of PAK1. Since PAK1 is essential for the growth of RAS cancer cells such as A549 cell line which carry an oncogenic K-RAS mutant, and the melanogenesis in skin cells, here using these PAK1-blockers as model compounds, we introduce a new approach to the quick assessment of PAK1-blockers in cell culture. First, combining the immuno-precipitation (IP) of PAK1 from cell lysate and the *in vitro* ATP_Glo kinase assay kit (called "Macaroni-Western" assay), we confirmed that both CBI and Bio 30 inactivate PAK1 in A549 lung cancer cells in 24 h, and inhibit their PAK1-dependent growth in 72 h. Furthermore, we verified that CBI inhibits the PAK1/PAK4-dependent melanogenesis in melanoma cells by far more than 50%, while Bio 30 inhibits the melanogenesis only by 50%, with only a merginal effect on their growth *per se*. Since the "Macaroni-Western" kinase assay and melanogenesis are both rather simple and quick, the combination of these two cell culture assays would be highly useful for selecting both "potent" (highly cell-permeable) and "safe" (non-toxic) natural or synthetic PAK1-blockers.**

Keywords: PAK1, melanogenesis, immunoprecipitation, ATP_Glo kinase assay, cucurbitacin, propolis

1. Introduction

PAK1 (RAC/CDC42-activated kinase 1) is essential for the growth of various solid tumors and a numerous other diseases such as AD (Alzheimer's disease), PD (Parkinson's disease), epilepsy, schizophrenia, depression, autism, diabetes (type 2), hypertension, obesity, inflammatory diseases, and infectious diseases (*1*). Also it has recently shown to be essential for the melanogenesis in skin cells (*2*). Thus, PAK1-blockers would have a potentially huge market value as therapeutics and cosmetics. However, so far only a few PAK1-blockers are available on the market. Thus, a quick, inexpensive and simple screening system is needed for identification and development of potent (highly cell permeable) and safe (non-toxic) PAK1-blockers.

In the past decade(s), the initial screening for PAK1-blockers has been performed mainly in test tubes to select compounds that inhibit directly PAK1. Unfortunately, however, most of these PAK1-inhibitors turned out to have a poor cell-permeability. For instance, the IC_{50} for PAK1 in test tube of FRAX486 and FRAX597 are around 10 nM, but their IC_{50} for the PAK1-dependent growth of NF2-deficient tumor cells in cell culture are above 1 μM (1000 nM). Since the

*These authors contributed equally to this work.
**Address correspondence to:
Dr. Hiroshi Maruta, PAK Research Center, 1-Senbaru, Nishihara-cho, Okinawa 903-0213, Japan.
E-mail: maruta20420@yahoo.co.jp

NF2 gene product (merlin) is a PAK1 inhibitor (*1*), it is most likely that less than 100th of these molecules could pass through cell membranes (*3,4*). In order to screen for highly cell-permeable PAK1-blockers more effectively, we have to conduct the assessment of test compounds in cell culture or *in vivo*, instead of in test tubes, in the earliest possible stage, in order to save both time and money. The current peculiar culture among pharmaceuticals that puts the first priority on the kinase-specificity of each compound in test tube over its cell-permeability needs to be reconsidered, simply because no drug would be useful for clinical application, if it hardly passes through the cell membranes.

Here we present a new approach to the more effective assessment of PAK1-blockers in cell culture, based on the fact that PAK1 and PAK4 independently contribute to melanogenesis (each by around 50%) (*2*). In addition, instead of the rather unreliable pPAK1-blot analysis, combining the IP (immuno-precipitation) of PAK1 from cells treated with a given compound, and *in vitro* ATP_Glo kinase assay kit (*5*), we introduced the "Macaroni-Western" PAK1 assay system to determine whether a given compound inactivates PAK1 in cell culture or not. Here we used two potent herbal PAK1-blockers called cucurbitacin I (CBI) and Bio 30, a CAPE (caffeic acid phenethyl ester)-based propolis as model test samples. In the past, it was shown that cucurbitacin D (CBD) which is structurally related to CBI, inhibits the melanogenesis in melanoma cells almost completely (*6*), while CAPE from a propolis inhibits the melanogenesis only by 50% (*7*). In the light of our recent findings, it is speculated that CBD blocks both PAK1 and PAK4, while CAPE blocks only PAK1.

In the past, basically two ways were used to assay the kinase activity of PAK1 in cell culture. The first (old) assay method is a "radioactive" approach in which PAK1 is immunoprecipitated (IP) with a polyclonal antibody (IgG) against PAK1 from cell lysates by means of protein A/G beads, and the resulting PAK1-IgG-bead complex is then incubated with the "radioactive" (gamma-^{32}P) ATP and the substrate MBP (myelin basic protein) *in vitro* (test tube), and the phosphorylated (radioactive) MBP band is separated by SDS-PAGE, and the radioactivity of this band is quantitated by the auto-radiography (*8*). This method is getting less and less popular in this century, simply because the handling of radioisotopes is rather restricted in research laboratories world-wide.

The alternative (more recent) approach is the immuno-blot (also called "western-blot") approach in which a cell-lysate is separated by SDS-PAGE, and proteins including PAK1 are transferred onto nitrocellulose paper, and phosphorylated PAK1 (called "pPAK1" at Thr423, Ser199, or Ser144, case by case) band is blotted with an antibody against each pPAK1, and in the end the amount of this antibody is quantified by fluorescence technique associated with probes (biotin or horse radish labeling). Unfortunately, however, the "western-blot" analysis based on pPAK1 is not reliable, simply because the activation of PAK1 in cells does not always depend on the auto-phosphorylation of PAK1 at these Ser/Thr residues. The full activation of PAK1 depends on its Tyr-phosphorylation by three distinct Tyr-kinases (ETK, JAK2 and FYN) at least (*9-11*), and dephosphorylation of PAK1 at Thr^{109} as well (*12*). For instance, melanogenic hormones such as α-melanocyte-stimulating hormone (α-MSH) and 3-isobutyl-1-methyl xanthine (IBMX) activate PAK1 in melanoma cells, with no change in pPAK1 (Thr423) level (*2*). Thus, strictly speaking, this popularized and over-simplified pPAK1-based "western-blot" analysis is rather unreliable or misleading, least to speak.

Around a decade ago, an Italian group introduced a third kinase assay system which we call here "Macaroni-Western" kinase assay (*5*). This is a clever modification of the old radioactive approach by simply replacing "radioactive" ATP with a newly developed "ATP_Glo kinase assay kit" (Promega). Accordingly, PAK1 immunoprecipitated from cell lysates (after cells are treated with a given test compound) is incubated with this kit with ATP and MBP, and the remaining ATP could be quantified by the ATP-dependent "luciferin-luciferase" reaction which produces the fluorescence/luminescence. Thus, the universal "Macaroni-Western" system allows us to monitor any change in the kinase activity of PAK1 in cells directly, independent of its auto-phosphorylation sites, without SDS-PAGE.

2. Materials and Methods

2.1. *Reagents and cell lines*

Cucurbitacin I (CBI) was purified from bitter melon called "Goya" by our own laboratory as previously described (*13*). Bio 30, a CAPE (caffeic acid phenethyl ester)-based propolis (tincture) from New Zealand was obtained from Manuka Health in Auckland. The content of major ingredients in Bio 30 was described in detail previously (*14*).

Human A549 lung cancer cell line and murine B16F10 melanoma cell line were obtained from Japanese Collection of Research Bioresources Cell Bank (Osaka, Japan) and American Type Culture Collection (ATCC; Rockville, MD, USA), respectively. 3-(4,5-dimethylthiazol-2-yl)-2,5-diphenyl-tetrazolium bromide (MTT), myelin basic protein (MBP) and protein A-agarose beads were purchased from Sigma Aldrich Chemical Co. (St. Louis, MO, USA). Rabbit polyclonal anti-PAK1 IgG was obtained from Cell Signalling Technology (Danver, MA, USA). Kinase Glo reagent and ATP (ATP_Glo kinase kit) were purchased from Promega (Madison, Wisconsin, USA). Dulbecco's modified Eagle medium (DMEM), 3-isobutyl-1-methyl xanthine (IBMX), fetal bovine serum (FBS),

and triton-X were purchased from Wako Pure Chemical Industries, Ltd. (Osaka, Japan). All reagents were of the highest grade available.

2.2. *Cell culture*

Human A549 lung cancer cell line was cultured as described previously (*13*). Murine B16F10 melanoma cell line was cultured as described previously (*2,15*).

2.3. *MTT assay for cell viability or growth of B16F10 and A549 cell lines*

Cell viability (or growth rate) was determined using an MTT assay, as previously described (*16*). Briefly, B16F10 or A549 cells (2×10^4 cells/well) were seeded on a 24-well plate. After 48 h of preculture, cells were treated with either CBI or Bio 30 at various concentrations for either 48 h (B16F10) or 24 h and 72 h (A549) at 37°C. Then cells were washed with phosphate buffer and incubated with MTT solution (0.5 mg/mL) for 3 hrs at 37°C. After the medium was replaced by 200 µL of ethanol, the absorbance of each well was measured at 570 nm using a microplate spectrophotometer (Bio-Rad Laboratories, Inc., Hercules, CA, USA)

2.4. *Measurement of melanin content*

Melanin content was determined as previously described (*17*). In brief, B16F10 cells were plated at a density of 2×10^4 cells/well in a 24-well plate. After 48 h of preculture, cells were treated with either CBI (100-800 nM) or Bio 30 (1-16 µg/mL). After 1 h, 100 µM isobutyl-1-methylxanthine (IBMX), a melanogenic hormone which activates PAK1 (*2*), was added and incubated for additional 48 hrs at 37°C. After washed with phosphate buffer, cells were dissolved in 500 µL NaOH (1 N) containing 10% dimethyl sulfoxide (DMSO). Samples were incubated at 80°C for 1 h, to solubilize the melanin. The optical density of the mixed homogenate was measured at 490 nm.

2.5. *"Macaroni-Western" (IP-ATP_Glo) kinase assay for PAK1 in A549 cells*

2.5.1. *Protocol for drug-treatment of cells followed by IPing PAK1 from cell lysates*

The intracellular content of PAK1 is quite low compared with other kinases. Thus, in an attempt to optimize the selective immuno-precipitation (IP) of PAK1 alone, in particular for minimizing the non-specific binding of other kinases to beads, and maximizing the IgG-protein A beads interaction, the following protocol for monitoring the effect of test drugs on PAK1 activity in cell culture includes our substantial improvement of a decade old method (which we coined "Macaroni-Western") published by an Italian group who initially developed for monitoring in test tube the direct effect of drugs on a variety of native abundant kinases such as CDKs (cyclin-dependent kinases) from cultured cells (*5*). The initial concentration of ATP for "test tube" kinase assay also has been optimized for monitoring both activation and inactivation of PAK1 in cells by a variety of test drugs.

Step 1: pre-culture A549 lung cancer cell line (2×10^5 cells/mL) on 6-well plate for 24 h.

Step 2: replace by the fresh medium containing test compounds at various concentrations, and incubate for 24 h.

Step 3: wash with 500 µL of ice-cold PBS (-) twice.

Step 4: add 500 µL of 50 mM Tris-HCl pH 7.5 and 150 mM NaCl and 1% Triton-X (lysis buffer).

Step 5: incubate on ice for 30 min.

Step 6: cell lysates were transferred into 1.5 mL tube.

Step 7: spin at 1,000 rpm for 5 min at 4°C.

Step 8: transfer the supernatant to 1.5 mL new tubes.

Step 9: add 50 µL of dilution buffer alone or anti-PAK1 IgG (1:50 dilution)* to each tube.

Step 10: incubate for 1 h on ice.

Step 11: add 10 µL of protein A-agarose beads.

Step 12: incubate for 1 h in cold room with continuous shaking by a rotary mixer (Nissin, Suginami-ku, Tokyo, Japan).

Step 13: spin at 1,000 rpm for 5 min, 4°C.

Step 14: remove the supernatant.

Step 15: resuspend the pellet with 500 µL of 50 mM Tris-HCl pH 7.5 and 150 mM NaCl (washing buffer).

Step 16: spin at 1000 rpm for 5 min, 4°C.

Step 17: repeat steps 15 and 16.

Step 18: resuspend the PAK1 pellet in 35 µL of 50 mM Tris-HCl pH 7.5 and 150 mM NaCl, 20 mM $MgCl_2$, 0.1 mg/mL BSA (kinase buffer).

**Note*: Anti-PAK1 IgG is diluted in buffer (50 mM Tris pH 7.5, 150 mM NaCl, 100 µg/mL BSA) in ratio 1:50 (dilution buffer)

2.5.2. *ATP_ Glo kinase assay*

PAK1 assay was carried out in a 100 µL total volume. 35 µL of kinase buffer alone or immuno-precipitated PAK1 and 5 µL of the substrate MBP (1 mg/mL in distilled water) were incubated at 37°C for 10 min. Then, 10 µL of 2 µM ATP in distilled water was added to each well. The reaction was incubated for 1 hr at 37°C with continuous shaking. After the kinase reaction, the equal volume (50 µL) of kinase Glo reagent (Promega) was added to each well, and the plate was further incubated for 30 min to stabilize luminescent signal. The suspension was centrifuged, and the supernatant was transferred to 96-well plate for reading. Luminescence was recorded by MTP-880Lab microplate reader (Corona, Hitachinaka-ku, Ibaraki, Japan) with an integration time of 0.5 s per well.

2.6. *Effect of CBI and Bio 30 on the growth of A549 cancer cells*

A549 cells were seeded on 6-well plate at the density of 2×10^5 cells/well in D-MEM supplemented with 10% FBS, and after preculture for 24 h, cells were treated with either CBI or Bio 30 at indicated concentrations for further 72 h. Then cells were stained with trypan blue as described previously (*18*). Both dead cells and the total cells were counted using hemocytometer. The percentage of viable treated cells in relative to the control (non-treated) cells was calculated.

2.7. *Statistical analysis*

Data are expressed as mean values with their standard errors. Statistical comparisons were performed by oneway ANOVA followed by Duncan's multiple-range test. Statistical analysis was conducted using SAS (release 9.2; SAS Institute, Cary, NC, USA) and $p < 0.05$ was considered significant.

3. Results and Discussion

3.1. *"Macaroni-Western" kinase assay for the inactivation of PAK1 by CBI and Bio 30 in cell culture for 24 h*

In this study, we have chosen CBI and Bio 30 as potential model PAK1-blockers for the following reasons: CBI inhibits directly two activators (JAK2 and RAC) of PAK1 (*19, 20*), while Bio 30 contains CAPE which down-regulates RAC by inhibiting directly AKR (Aldo-Keto-Reductase) 1B10 (*21*), and suppresses completely the PAK1-dependent growth of NF2-deficient tumor (schwannoma) *in vivo* (*14*).

Since the PAK1 (protein) level in melanoma cell line B16F10 is extremely low (*15*), as the PAK1 source for the "Macaroni-Western" kinase assay, we used A549 lung cancer cell line in which the oncogenic K-RAS mutant highly activates PAK1, and whose growth almost solely depends on PAK1. After preculture of A549 cells for 24 h, they were treated with either CBI or Bio 30 at two indicated concentrations for 24 h, and the non-treated cells as well as treated cells were lyzed, and cell lysates were incubated with anti-PAK1 IgG and protein A-beads for immuno-precipitation (IP) of PAK1. After the PAK1-IgG-protein A-bead complex was incubated with ATP and MBP for 1 h, ATP_Glo kinase assay kit was added to measure the remaining ATP level by the released luminescence (for detail, see Figure 1). The higher the luminescence, the lower the kinase activity. As shown in Figure 2, both CBI and Bio 30 clearly inactivate PAK1 in this cancer cell line with the apparent IC_{50} around 600 nM and 60 µg/mL, respectively. The apparent down-regulation of PAK1 by these

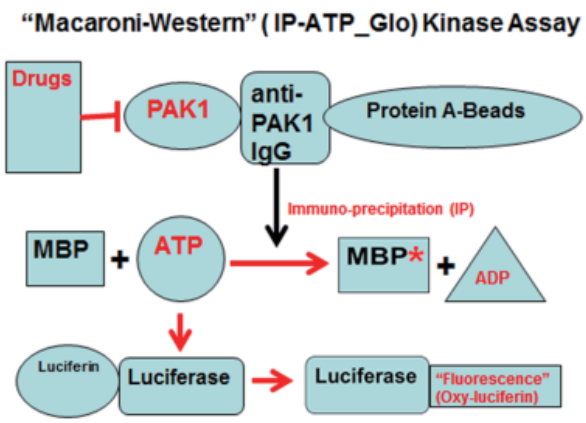

Figure 1. "Macaroni-Western" (IP-ATP_Glo) kinase assay. PAK1 is treated (activated or inactivated) with a given test sample in cell culture, and PAK1 is immuno-precipitated (IP) from cell lysate, and its kinase activity is measured by ATP_Glo kinase kit in test tube using ATP-dependent luciferin/luciferase reaction.

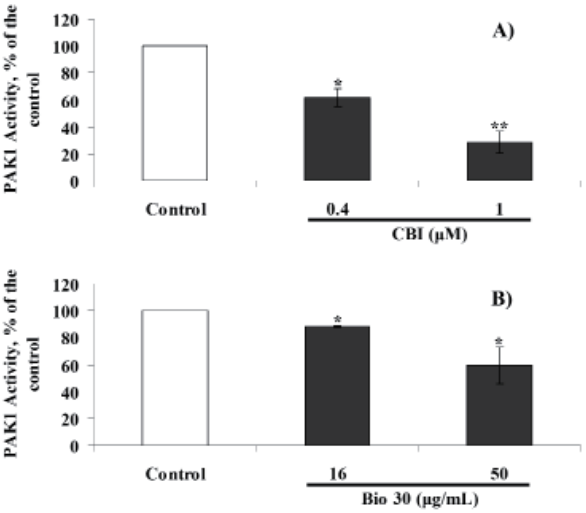

Figure 2. Both CBI (A) and Bio 30 (B) inactivate PAK1 in A549 cancer cells for 24 h. Inactivation of PAK1 in cells with CBI and Bio 30 was monitored by the "Macaroni-Western" kinase assay in test tube. For detail of the assay procedure, see under Materials and Methods. Data have significant difference by ANOVA analysis at $p \leq 0.05$. Statistically significant differences relative to control are indicated by asterisks. * $0.01 \leq p \leq 0.05$, ** $p < 0.01$.

compounds is not due to the growth inhibition of this cell line by these compounds, because for the first 24 h (just one generation of cell cycle) no growth inhibition was observed with either CBI or Bio 30 (see Figure 3).

3.2. *Growth inhibition of A549 cancer cells by CBI and Bio 30 for 72 hrs*

However, after treatment of A549 cancer cells with either CBI or Bio 30 for 72 h (3-4 generations of cell cycle), both CBI and Bio 30 strongly inhibit the growth of this "RAS" cancer cell line with the IC_{50} around

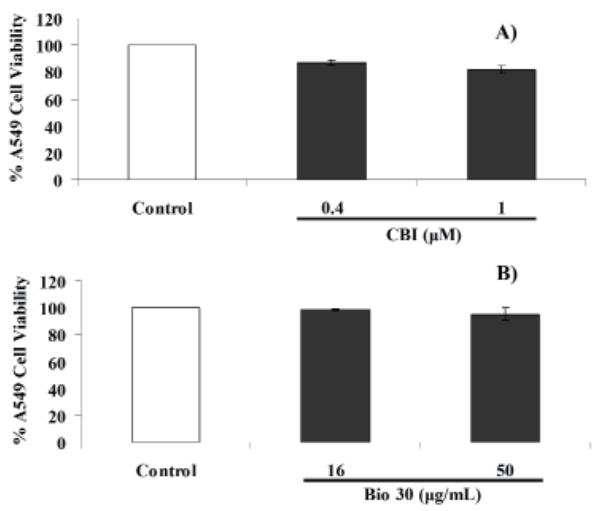

Figure 3. Neither CBI (A) nor Bio 30 (B) affects the viability/growth of A549 cells for the first 24 h. Data have significant difference by ANOVA analysis at $p \leq 0.05$.

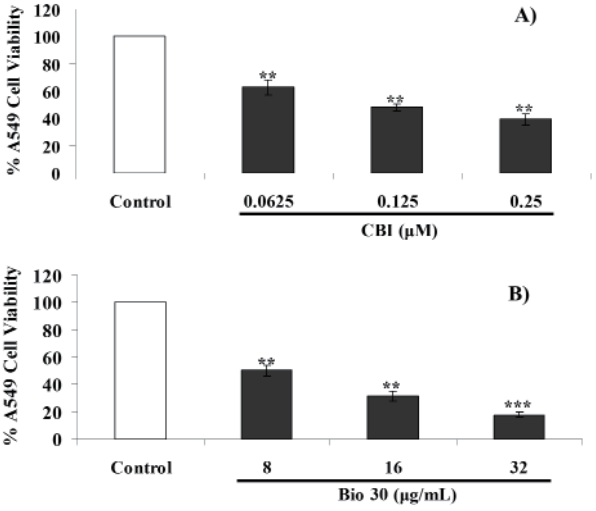

Figure 4. Both CBI (A) and Bio 30 (B) inhibit the growth of A549 cells for 72 h. The IC_{50} of CBI and Bio 30 are around 140 nM and 8 μg/mL (ppm), respectively. Data have significant difference by ANOVA analysis at $p \leq 0.05$. Statistically significant differences relative to control are indicated by asterisks. ** $p < 0.01$, *** $p < 0.001$.

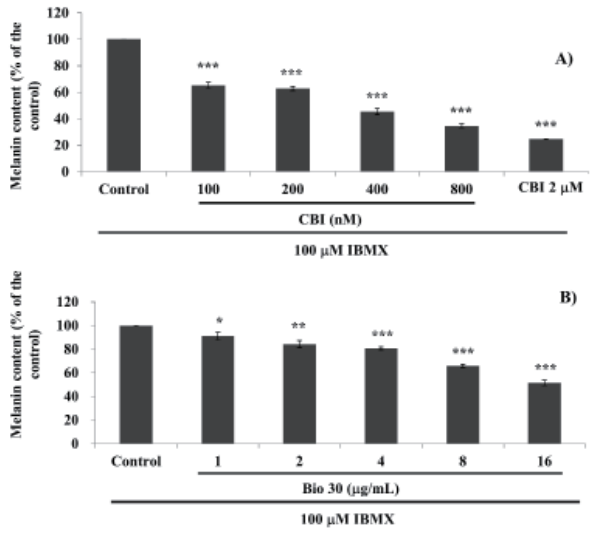

Figure 5. Both CBI (A) and Bio 30 (B) inhibit the melanogenesis in melanoma cells for 72 h. The IC_{50} of CBI and Bio 30 are around 400 nM and 16 μg/mL (ppm), respectively. Data have significant difference by ANOVA analysis at $p \leq 0.05$. Statistically significant differences relative to control are indicated by asterisks. * $0.01 \leq p \leq 0.05$, ** $p < 0.01$, *** $p < 0.001$.

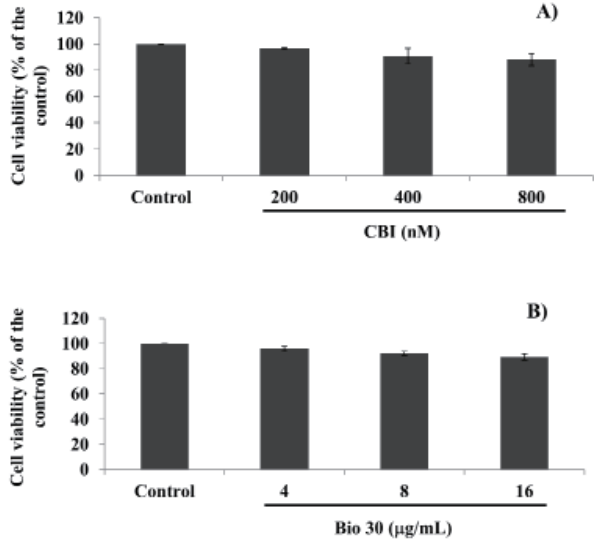

Figure 6. Either CBI (A) or Bio 30 (B) shows little effect on the viability/growth of melanoma cells during 48 h. Data have significant difference by ANOVA analysis at $p \leq 0.05$.

140 nM and 8 μg/mL, respectively (see Figure 4), confirming that PAK1 is absolutely essential for the growth of this RAS cancer cell line.

The major and most likely reason why the IC_{50} for the growth is several times lower than the apparent IC_{50} for the kinase activity is the following: both IP procedure and test tube assay for PAK1 activity isolated from cells takes more than 3 hrs in total, and in the absence of PAK1-blockers (CBI and Bio 30), the suppression of PAK1 activity could be gradually released over time. In other words, during this "time-consuming" test tube kinase assay, we cannot freeze the exact (activated or inactivated) status of PAK1 in the end of cell-treatment. That is the major demerit associated with this kinase assay, although any significant change in the kinase activity during cell culture can be monitored regardless of the phosphorylation sites of PAK1. Thus, the apparent IC_{50} for the kinase assay obtained in test tube is only a reflection of PAK1 inhibition during cell culture, and not the true IC_{50} during cell culture. Nevertheless, the apparent IC_{50} tells clearly that CBI is far more potent

than Bio 30 in suppressing PAK1 during the cell culture, as does in the cancer cell growth.

3.3. *Anti-melanogenic effect of CBI and Bio 30*

We and others recently established that both PAK1 and PAK4 are essential for the melanogenesis of skin cells such as melanoma cell line B16F10, and each contributes independently by around 50% to their melanogenesis (*2,15*). In other words, if a given compound blocks only PAK1 or PAK4, it could inhibit the melanogenesis only by 50% at the highest concentrations, whereas if a given compound blocks both kinases, it could inhibit the melanogenesis almost completely, as does the pan-PAK inhibitor PF3758309 at 300 nM (*15*). As shown in Figure 5, CBI inhibits the melanogenesis by more than 70% at 800 nM, whereas Bio 30 inhibits the melanogenesis only by 50% at 16 μg/mL. Under these concentrations, either CBI or Bio 30 showed only a marginal effect on the growth of the melanoma cells (see Figure 6). In addition, we have confirmed that melanogenic stimulators such as IBMX and α-MSH indeed activate significantly the kinase activity of PAK1 in this melanoma cell line as judged by the "Macaroni-Western kinase assay" (*2*). It might be worth noting that the IC_{25} of Bio 30 for the PAK1/PAK4-dependent melanogenesis is around 8 μg/mL, which is the same of the IC_{50} for the PAK1-dependent growth of A549 cells, suggesting that when Bio 30 inactivates PAK1 by 50%, both the PAK1-dependent cancer cell growth and melanogenesis are reduced to around a half.

These findings indicate the following two things: (*i*) it is most likely that CBI blocks both PAK1 and PAK4 as CBD does, while Bio 30 probably blocks only PAK1 as CAPE does. (*ii*) the growth of A549 cancer cells depends on PAK1, while the growth of melanoma cell line B16F10 is independent of PAK1. In other words, either CBI or Bio 30 is not simply a poison, but both are highly selective (non-poisonous) and cell-permeable PAK1-blockers. In fact neither edible Okinawa Goya rich in CBI nor the propolis Bio 30 has ever caused any side effect during human consumption as foods.

So far no herbal compound has been found to inhibit only PAK4. The majority of herbal anti-melanogenic compounds such as CAPE, curcumin, and shikonin, blocks only PAK1, and a few herbal compounds such as glaucarubinone are known to block both PAK1 and PAK4 (*19*). In other words, if a given herbal compound inhibits the melanogenesis by only 50%, it is most likely that it is a PAK1-blocker rather than PAK4-blocker, and would be useful for improving our health and extending our lifespan. Of course, we could easily verify its anti-PAK1 activity through the quick "Macaroni-Western" kinase assay in the end.

Finally, using this opportunity, we would like to point out the followings: there are so many PAK1-blocking herbal products such as propolis available on the market world-wide which could be very useful for improving our health and even therapy of cancer and many other PAK1-dependent diseases/disorders such as Alzheimer's disease (*1*). However, unlike FDA-approved drugs, none of them is associated with any reliable international quality control standard such as IC_{50} or ED (effective dose). For instance, the quality of propolis depends on the sources of plants where bees harvest from, and the actual content of PAK1-blocking ingredients such CAPE, apigenin, ARC (artepillin C) and propolin G in each propolis. However, since 1960s till present, the only available quality standard used for propolis is either "the total flavonoid content" for CAPE-based propolis or the ARC content in Brazillian green propolis. If these "herbal" health-promoting products are regulated by a single reliable pharmacological quality standard, we could compare the quality or effectiveness from one sample to another quite objectively.

Hence, we would propose here for the first time to use a universal standard called "Anti-PAK index" which is the 100 × reciprocal of the IC_{50} in ppm (μg/mL). For instance, "Anti-PAK index" of Bio 30 is 12.5 since its IC_{50} for A549 cancer cells is around 8 ppm, whereas the "Anti-PAK index" of the "pure" compound CBI is around 1400, as the IC_{50} for A549 is around 140 nM (0.07 ppm). The higher the Anti-PAK index, the more potent a given sample. In other words, 1 mg of CBI is equivalent to 112 mg of Bio 30 for therapy of cancers and many other PAK1-dependent diseases/disorders. This rough estimation is not far from the actual *in vivo* data where the daily dose of cucurbitacin B (1 mg/kg), closely related to CBI, and that of Bio 30 (50 mg/kg) are their effective dose to suppress the PAK1-dependent growth of pancreatic cancers or NF tumors in mice (*14,20*), suggesting that their *in vivo* bioavailability is quite similar.

The only difference between these two is that Bio 30 has been available on the market world-wide for clinical uses for almost a decade, but CBI is not as yet. The only way for us to take CBI is to eat the edible bitter melon (Goya) grown in Okinawa (which contains around 1 g of CBI per kg) or drink Goya tea. Since roughly 90% of Goya is water, the "Anti-PAK index" of Goya extract/tea could be around 14, pretty close to that of Bio 30. Thus, we shall measure the IC_{50} of Goya extract/tea on the market for calculating their "Anti-PAK index" more precisely.

References

1. Maruta H. Herbal therapeutics that block the oncogenic kinase PAK1: A practical approach towards PAK1-dependent diseases and longevity. Phytother Res. 2014; 28:656-672.
2. Be Tu PT, Nguyen BCQ, Tawata S, Yun, CY, Kim EG,

Maruta H. PAK1 is essential for the melanogenesis in skin. J Dermatol Sci. 2015; manuscript submitted.
3. Hayashi-Takagi A, Araki Y, Nakamura M, Vollrath B, Duron SG, Yan Z, Kasai H, Huganir RL, Campbell DA, Sawa A. PAKs inhibitors ameliorate schizophrenia-associated dendritic spine deterioration *in vitro* and *in vivo* during late adolescence. Proc Natl Acad Sci U S A. 2014; 111:6461-6466.
4. Licciulli S, Maksimoska J, Zhou C, Troutman S, Kota S, Liu Q, Duron S, Campbell D, Chernoff J, Field J, Marmorstein R, Kissil JL. FRAX597, a small molecule inhibitor of the p21-activated kinases, inhibits tumorigenesis of neurofibromatosis type 2 (NF2)-associated schwannomas. J Biol Chem. 2013; 288:29105-29114.
5. Tagliati F, Bottoni A, Bosetti A, Zatelli MC, degli Uberti EC. Utilization of luminescent technology to develop a kinase assay: Cdk4 as a model system. J Pharm Biomed Anal. 2005; 39:811-814.
6. Oh H, Mun YJ, Im SJ, Lee SY, Song HJ, Lee HS, Woo WH. Cucurbitacins from Trichosanthes kirilowii as the inhibitory components on tyrosinase activity and melanin synthesis of B16/F10 melanoma cells. Planta Med. 2002; 68:832-833.
7. Lee JY, Choi HJ, Chung TW, Kim CH, Jeong HS, Ha KT. Caffeic acid phenethyl ester inhibits alpha-melanocyte stimulating hormone-induced melanin synthesis through suppressing transactivation activity of microphthalmia-associated transcription factor. J Nat Prod. 2013; 76:1399-1405.
8. He H, Hirokawa Y, Manser E, Lim L, Levitzki A, Maruta H. Signal therapy for RAS-induced cancers in combination of AG 879 and PP1, specific inhibitors for ErbB2 and Src family kinases, that block PAK activation. Cancer J. 2001; 7:191-202.
9. Rider L, Shatrova A, Feener EP, Webb L, Diakonova M. JAK2 tyrosine kinase phosphorylates PAK1 and regulates PAK1 activity and functions. J Biol Chem. 2007; 282:30985-30996.
10. He H, Hirokawa Y, Gazit A, Yamashita Y, Mano H, Kawakami Y, Kawakami, Hsieh CY, Kung HJ, Lessene G, Baell J, Levitzki A, Maruta H. The Tyr-kinase inhibitor AG879, that blocks the ETK-PAK1 interaction, suppresses the RAS-induced PAK1 activation and malignant transformation. Cancer Biol Ther. 2004; 3:96-101.
11. Hirokawa Y, Levitzki A, Lessene G, Baell J, Xiao Y, Zhu H, Maruta H. Signal therapy of human pancreatic cancer and *NF1*-deficient breast cancer xenograft in mice by a combination of PP1 and GL-2003, anti-PAK1 drugs (Tyr-kinase inhibitors). Cancer Lett. 2007; 245:242-251.
12. Deguchi A, Miyoshi H, Kojima Y, Okawa K, Aoki M, Taketo MM. LKB1 suppresses p21-activated kinase-1 (PAK1) by phosphorylation of Thr^{109} in the p21-binding domain. J Biol Chem. 2010; 285:18283-18290.
13. Nguyen BCQ, Taira N, Tawata S. Several herbal compounds in Okinawa plants directly inhibit the oncogenic/aging kinase PAK1. Drug Discov Ther. 2014; 8:238-244.
14. Demestre M, Messerli SM, Celli N, Shahhossini M, Kluwe L, Mautner V, Maruta H. CAPE (caffeic acid phenethyl ester)-based propolis extract (Bio 30) suppresses the growth of human neurofibromatosis (NF) tumor xenografts in mice. Phytother Res. 2009; 23:226-230.
15. Yun CY, You ST, Kim JH, Chung JH, Han SB, Shin EY, Kim EG. p21-activated kinase 4 critically regulates melanogenesis *via* activation of the CREB/MITF and β-catenin/MITF pathways. J Invest Dermatol. 2015; 135:1385-1394.
16. Campos PM, da Silva Horinouchi CD, da Silveira Prudente A, Cechinel-Filho V, de Almeida Cabrini D, Otuki MF. Effect of a *Garcinia gardneriana* (Planchon and Triana) Zappi hydroalcoholic extract on melanogenesis in B16F10 melanoma cells. J Ethnopharmacol. 2013; 148:199-204.
17. Yoon NY, Eom TK, Kim MM, Kim SK. Inhibitory effect of phlorotannins isolated from *Ecklonia cava* on mushroom tyrosinase activity and melanin formation in mouse B16F10 melanoma cells. J Agric Food Chem. 2009; 57:4124-4129.
18. Wu J, Wu Y, Yang BB. Anticancer activity of Hemsleya amabilis extract. Life Sci. 2002; 71:2161-2170.
19. Blaskovich MA, Sun J, Cantor A, Turkson J, Jove R, Sebti SM. Discovery of JSI-124 (Cucurbitacin I), a selective janus kinase/signal transducer and activator of transcription 3 signaling pathway inhibitor with potent antitumor activity against human and murine cancer cells in mice. Cancer Res. 2003; 63:1270-1279.
20. Lopez-Haber C, Kazanietz MG. Cucurbitacin I inhibits Rac1 activation in breast cancer cells by a reactive oxygen species-mediated mechanism and independently of janus tyrosine kinase 2 and p-rex1. Mol Pharmacol. 2013; 83:1141-1154.
21. Soda M, Hu D, Endo S, Takemura M, Li J, Wada R, Ifuku S, Zhao HT, El-Kabbani O, Ohta S, Yamamura K, Toyooka N, Hara A, Matsunaga T. Design, synthesis and evaluation of caffeic acid phenethyl ester-based inhibitors targeting a selectivity pocket in the active site of human aldo-keto reductase 1B10. Eur J Med Chem. 2012; 48:321-329.
22. Yeo D, Huynh N, Beutler JA, Christophi C, Shulkes A, Baldwin GS, Nikfarjam M, He H. Glaucarubinone and gemcitabine synergistically reduce pancreatic cancer growth *via* down-regulation of P21-activated kinases. Cancer Lett. 2014; 346:264-272.
23. Iwanski GB, Lee DH, En-Gal S, Doan NB, Castor B, Vogt M, Toh M, Bokemeyer C, Said JW, Thoennissen NH, Koeffler HP. Cucurbitacin B, a novel *in vivo* potentiator of gemcitabine with low toxicity in the treatment of pancreatic cancer. Br J Pharmacol. 2010; 160:998-1007.

(Received June 21, 2015; Revised July 23, 2015; Accepted August 24, 2015)

Original Article

DOI: 10.5582/ddt.2015.01046

Evaluation of stroke volume variation and pulse pressure variation as predictors of fluid responsiveness in patients undergoing protective one-lung ventilation

Qiang Fu[1,*], Mingda Duan[2,*], Feng Zhao[1], Weidong Mi[1,]**

[1] *Department of Anesthesiology, General Hospital of People's Liberation Army, Beijing, China;*
[2] *Department of Anesthesiology, Hainan Branch of General Hospital of People's Liberation Army, Sanya, Hainan, China.*

Summary **In order to investigate whether the hemodynamic indices, including stroke volume variation (SVV) and pulse pressure variation (PPV) could predict fluid responsiveness in patients undergoing protective one-lung ventilation. 60 patients scheduled for a combined thoracoscopic and laparoscopic esophagectomy were enrolled and randomized into two groups. The patients in the protective group (Group P) were ventilated with a tidal volume of 6 mL/kg, an inspired oxygen fraction (FiO_2) of 80%, and a positive end expiratory pressure (PEEP) of 5 cm H_2O. Patients in the conventional group (Group C) were ventilated with a tidal volume of 8 mL/kg and a FiO_2 of 100%. Dynamic variables were collected before and after fluid loading (7 mL/kg hydroxyethyl starch 6%, 0.4 mL/kg/min). Patients whose stroke volume index (SVI) increased by more than 15% were defined as responders. Data collected from 45 patients were finally analyzed. Twelve of 24 patients in Group P and 10 of 21 patients in Group C were responders. SVV and PPV significantly changed after the fluid loading. The receive operating characteristic (ROC) analysis showed that the thresholds for SVV and PPV to discriminate responders were 8.5% for each, with a sensitivity of 66.7% (SVV) and 75% (PPV) and a specificity of 50% (SVV) and 83.3% (PPV) in Group P. However, the thresholds for SVV and PPV were 8.5% and 7.5% with a sensitivity of 80% (SVV) and 90% (PPV) and a specificity of 70% (SVV) and 80% (PPV) in Group C. We found SVV and PPV could predict fluid responsiveness in protective one-lung ventilation, but the accuracy and ability of SVV and PPV were weak compared with the role they played in a conventional ventilation strategy.**

Keywords: Stroke volume variation, pulse pressure variation, one lung ventilation, protective ventilation, fluid responsiveness

1. Introduction

One-lung ventilation (OLV) is necessary for thoracic surgery since the surgery requires adequate visualization of the operative field. OLV can cause a series of pathophysiological changes, such as an imbalance in the ventilation-perfusion ratio, increased intrapulmonary shunt, and increased risk of pulmonary edema. In recent years, along with the advances in the equipment and theory of mechanical ventilation, lung protective ventilation strategies have gained popularity in clinical practice. The core mechanism underlying this strategy is to use low tidal volume ventilation with positive end expiratory pressure (PEEP) in an attempt to reduce shear stresses generated by repeated alveolar inflation through mechanical ventilation, reduce the risk of lung injury, and thereby improve prognosis (*1-3*).

However, proper fluid infusion in perioperative settings is also critical for maintaining the balance between oxygen supply and demand. Volume monitoring and evaluation of the patient's response to fluid loading are particularly essential in maintaining sufficient blood volume to ensure organ perfusion in

*These authors contributed equally to this works.

***Address correspondence to:*
Dr. Weidong Mi, Department of Anesthesiology, General Hospital of People's Liberation Army, Fuxing road, Haidian district, Beijing 100853, China.
E-mail: 301mz@163.com

cases where the risk of pulmonary edema is increased. Conventional hemodynamic parameters cannot fulfill these requirements, and other monitoring strategies such as the use of a floating pulmonary artery catheter and transesophageal echocardiography are not advocated due to concerns about risk, cost, and technology (*4,5*). Therefore, stroke volume variation (SVV) and pulse pressure variation (PPV) have attracted increasing attention, and a growing number of studies have been conducted on these parameters due to their minimally invasive nature and accuracy (*6-9*). Previous studies have demonstrated that the hemodynamic parameters represented by SVV can predict fluid responsiveness in patients undergoing thoracic surgery but the accuracy was affected by many factors including the depth of tidal volume, the use of PEEP and so on (*10-13*), which limits its application in patients undergoing OLV. For this reason, the aim of this study was to investigate the ability of SVV, PPV and other hemodynamic parameters to predict fluid responsiveness in patients undergoing protective OLV.

2. Methods

2.1. *Ethics and patients*

This study was approved by the Institutional Ethics Committee of People's Liberation Army General Hospital, Beijing, China and written informed consent were obtained from all patients before surgery. Sixty ASA I-II patients (age, 18-70 years; BMI, 18-30 kg/m^2) undergoing elective radical esophagectomy of esophageal carcinoma using combined laparoscopic and thoracoscopic approaches were enrolled in this study from December 2013 to July 2014 at People's Liberation Army General Hospital. Patients were otherwise healthy without severe cardiopulmonary diseases, coagulation disorders, hepatic or renal dysfunction prior to surgery.

2.2. *Anaesthesia managment*

Atropine (0.5mg) was administered intramuscularly 30 min before surgery. Surgery was performed with the patient in a supine position. An oxygen mask and peripheral venous lines were kept ready, if needed, for further intervention. An electrocardiogram, non-invasive blood pressure measurement and oxygen saturation were recorded. General anesthesia was induced with midazolam (0.03 mg/kg), sufentanil (0.3 μg/kg), propofol (1.5 mg/kg), and rocuronium (0.9 mg/kg). Endotracheal intubation was performed using double-lumen endotracheal tube(Broncho-cath, Tyco Healthcare, Argyle, Mansfield, MA, USA) 3 min after anesthetic induction. After accurate positioning, patients received mechanical ventilation on volume-controlled mode with fractional inspired oxygen concentration (FiO_2) of 100%, a tidal volume of 8 mg/kg, respiratory rate of 12 breaths/min, respiratory ratio of 1:2, and end-tidal CO_2 partial pressure ($P_{ET}CO_2$) of 30-35 mmHg. Arterial catheterization was performed *via* a puncture of the left radial artery and was connected to the FloTrac-Vigileo system (Edwards Lifescience, LLC, Irvine, CA, USA). Hemodynamic parameters were recorded after zeroing and entering patient data. Anesthesia was maintained with sevoflurane at an inspired concentration of 1-1.5% and propofol and remifentanil were delivered with an infusion pump. The depth of anesthesia was controlled to maintain a bispectral index (BIS) (Aspect Medical Systems Inc., Natick, MA, USA) value between 40-60. Rocuronium and sufentanil were administered if needed.

2.3. *Study protocol*

After the procedure of laparoscopic part, patients were placed in a lateral position and the position of the monitoring system was adjusted accordingly. Five minutes after zeroing the system, SVV, PPV, mean arterial pressure (MAP), heart rate (HR), cardiac output (CO), cardiac index (CI), stroke volume index (SVI), maximum airway pressure (P_{MAX}) and $P_{ET}CO_2$ were recorded. After starting OLV, patients were randomized into two ventilation strategic groups: Group P (protected group, tidal volume: 6 mL/kg, PEEP: 5 cmH_2O, and FiO_2: 80%) and Group C (conventional group, tidal volume: 8 mL/kg, FiO_2: 100% without PEEP). For the randomization method, the random numbers with odd mantissa were included in the protective group and those with even mantissa were included in the conventional group. For both groups, each patient's respiratory ratio was adjusted to maintain $P_{ET}CO_2 \leq 45$ mmHg and plateau pressure ≤ 35 cmH_2O. The first set of data (before fluid loading) was recorded 0.5 h after OLV followed by intravenous infusion of hydroxyethyl starch (130/0.4) 7 mL/mg at a speed of 0.4 mL/kg/min. The second set of data (after fluid loading) was recorded 5 min after stabilization of the data. The test designer was responsible only for data collecting rather than grouping and anesthesia management.

In order to maximize the accuracy and reliability of the data derived from the transducer of the system, the exclusion criterion during the study were as followed: (*a*) surgical procedures altered; (*b*) incidents that affects the stability of the respiratory/circulatory system; (*c*) non-sustainable OLV; (*d*) repeatedly vasoactive drugs used.

2.4. *Statistical analysis*

A responder was defined as a subject with a demonstrated increase of > 15% in SVI; otherwise, the patient was defined as a non-responder. Statistical analysis was performed using SPSS 17.0 software (SPSS Inc., Chicago, IL, USA). Quantitative data were presented as mean ± standard deviation ($\overline{\chi} \pm s$). Normality and

homogeneity of variance were verified. Patient general information and data before and after volume expansion were compared using univariate analysis of variance (ANOVA). For responders, a correlation between pre-fluid loading SVV, PPV and ΔSVI were analyzed, and the predictive capacity of SVV and PPV was tested by receiver operating characteristic analysis (ROC) to determine the specificity, sensitivity and threshold of these parameters.

3. Results

3.1. *Patients demographics*

At last, Data collected from forty-five patients were analyzed. The Group P (n = 24) comprised 12 patients who had a response (responders) and 12 patients with no response (non-responders), and Group C (n = 21) had 10 responders and 11 non-responders. No significant differences were observed in age, gender, BMI, prior medical history and cardiac ejection fraction either between groups or within groups (Figure1 and Table1).

3.2. *Comparasion of hemodynamic variables*

The CO, CI, and SVI of responders in both groups significantly increased after fluid loading. Significant changes were observed in SVV and PPV after fluid loading while no significant changes were observed in

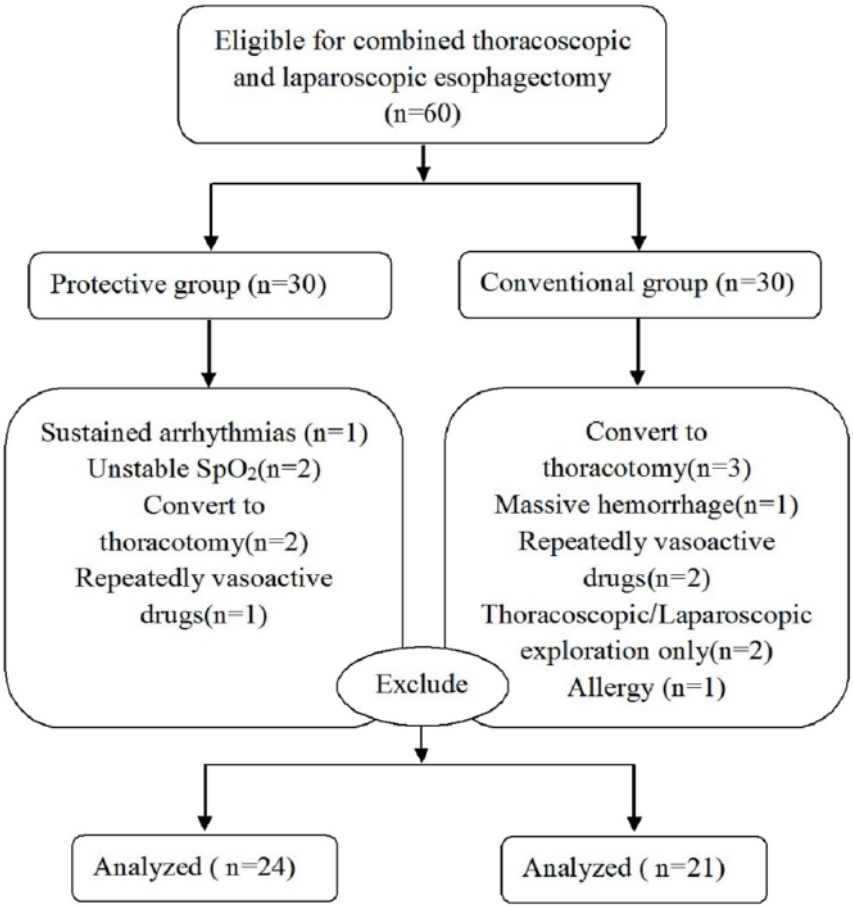

Figure 1. Flow chat of patients selection and distribution.

Table 1. Comparison of patients' general conditions between groups ($\overline{\chi} \pm s$)

Groups	Group P (n = 24)			Group C (n = 21)			p1	p2	p3
	overall	R (n = 12)	NR (n = 12)	overall	R (n = 10)	NR (n = 11)			
Gender (F/M)	2/22	1/11	1/11	0/21	0/10	0/11	/	/	/
age	60.63 ± 6.16	61.00 ± 6.67	60.25 ± 5.87	61.57 ± 4.91	60.50 ± 4.74	62.55 ± 1.53	0.58	0.79	0.64
BMI	23.03 ± 1.79	23.33 ± 1.73	22.74 ± 1.87	23.31 ± 1.64	23.37 ± 1.71	23.25 ± 1.65	0.59	0.18	0.89
Ejection fraction	63.38 ± 3.50	63.42 ± 3.29	63.33 ± 3.85	63.43 ± 2.73	63.90 ± 2.69	63.00 ± 2.83	0.96	0.92	0.68
History of hypertension	7/24	4/12	3/12	5/21	2/10	3/11	/	/	/
History of diabetes	3/24	2/12	1/12	2/21	1/10	1/11	/	/	/

R: Responders; NR: Non-Responders; p1 value: Group C *vs*. Group P; p2 value: intra-Group P comparison; p3 value: intra-Group C comparison.

Table 2. Comparison of hemodynamic parameters and relevant variables before and after fluid loading during protective OLV ($\overline{\chi} \pm s$)

Items	Responders (n = 12)			Non-Responders (n = 12)		
	Before	After	p value	Before	After	p value
MAP (mmHg)	77.75 ± 5.82	80.08 ± 6.44	0.36	77.42 ± 6.31	78.83 ± 7.19	0.61
HR (beat/min)	74.92 ± 5.79	72.42 ± 6.54	0.33	68.25 ± 8.06	67.83 ± 5.69	0.89
SVV (%)	9.67 ± 2.01	7.41 ± 2.19	0.01**	6.75 ± 1.96	6.33 ± 1.87	0.60
PPV (%)	8.91 ± 2.06	6.92 ± 1.93	0.02**	5.67 ± 1.23	5.08 ± 1.16	0.25
CO (L/min)	4.85 ± 1.10	6.10 ± 0.95	0.007*	5.79 ± 1.23	6.03 ± 1.32	0.65
CI (L/min/m^2)	2.82 ± 0.53	3.61 ± 0.51	0.001*	3.30 ± 0.57	3.42 ± 0.59	0.63
SVI (mL/m^2)	38.00 ± 7.56	49.08 ± 8.99	0.004*	48.17 ± 8.39	50.17 ± 9.08	0.58
P_{MAX} (cmH_2O)	25.75 ± 1.71	25.58 ± 1.72	0.82	26.08 ± 2.50	26.00 ± 2.45	0.94
$P_{ET}CO_2$ (mmHg)	35.08 ± 1.93	35.33 ± 1.23	0.71	35.67 ± 1.97	35.58 ± 1.78	0.91

MAP: mean arterial pressure; HR: heart rate; SVV: stroke volume variation; PPV: pulse pressure variation; CO: cardiac output; CI: cardiac index; SVI: stroke volume index; P_{MAX}: maximum airway pressure; * $p < 0.01$, ** $p < 0.05$.

Table 3. Comparison of hemodynamic parameters and relevant variables before and after fluid loading during conventional OLV ($\overline{\chi} \pm s$)

Items	Responders (n = 10)			Non-Responders (n = 11)		
	Before	After	p value	Before	After	p value
MAP (mmHg)	80.50 ± 3.34	85.00 ± 2.58	0.003*	77.18 ± 5.09	79.73 ± 3.07	0.17
HR (beat/min)	71.70 ± 5.64	69.70 ± 6.06	0.46	71.91 ± 7.50	69.82 ± 6.19	0.48
SVV (%)	9.90 ± 1.52	6.90 ± 2.02	0.001*	7.64 ± 1.57	6.73 ± 2.05	0.26
PPV (%)	9.50 ± 1.43	6.20 ± 2.20	0.001*	6.63 ± 1.69	6.01 ± 2.07	0.51
CO (L/min)	4.99 ± 1.24	6.30 ± 1.34	0.036**	5.52 ± 1.18	5.66 ± 1.26	0.78
CI (L/min/m^2)	2.89 ± 0.54	3.57 ± 0.57	0.013**	3.20 ± 0.56	3.28 ± 0.62	0.75
SVI (mL/m^2)	40.60 ± 6.72	53.10 ± 7.65	0.001*	44.91 ± 6.44	46.00 ± 7.96	0.72
P_{MAX} (cmH_2O)	25.50 ± 2.17	25.40 ± 2.79	0.93	25.73 ± 2.28	26.18 ± 2.13	0.64
$P_{ET}CO_2$ (mmHg)	34.90 ± 2.23	34.20 ± 2.15	0.48	35.09 ± 1.37	36.18 ± 1.94	0.14

MAP: mean arterial pressure; HR: heart rate; SVV: stroke volume variation; PPV: pulse pressure variation; CO: cardiac output; CI: cardiac index; SVI: stroke volume index; P_{MAX}: maximum airway pressure; * $p < 0.01$, ** $p < 0.05$.

MAP and HR. As for non-responders, no significant changes were observed in CO, CI, and SVI after fluid loading, either in SVV or PPV (Tables 2 and 3).

3.3. *Correlations analysis*

No correlations were found between pre-fluid loading SVV/ΔSVI in responders of Group P (correlation coefficient r = 0.412, p = 0.184; r = 0.256, p = 0.422, respectively). As for responders in Group C, correlations were observed between pre-fluid loading SVV/PPV and ΔSVI (r = 0.697, p = 0.025; r = 0.637, p = 0.047, respectively) (Figure 2).

3.4. *ROC analysis*

The threshold values of SVV and PPV used to discriminate between responders and non-responders were determined using ROC analysis of hemodynamic parameters of responders in both groups. For Group P, the threshold of SVV was 8.5%. The ROC-area under the curve (AUC) for SVV was 0.767 (sensitivity, 66.7%; specificity, 50%). The threshold of PPV was 8.5% with AUC of 0.778 (sensitivity, 75%; specificity, 83.3%). For group C, the threshold of SVV was 8.5% with AUC of 0.885 (sensitivity, 80%; specificity, 70%). The threshold of PPV was 7.5% with AUC of 0.890 (sensitivity, 90%; specificity, 80%) (Figure 3).

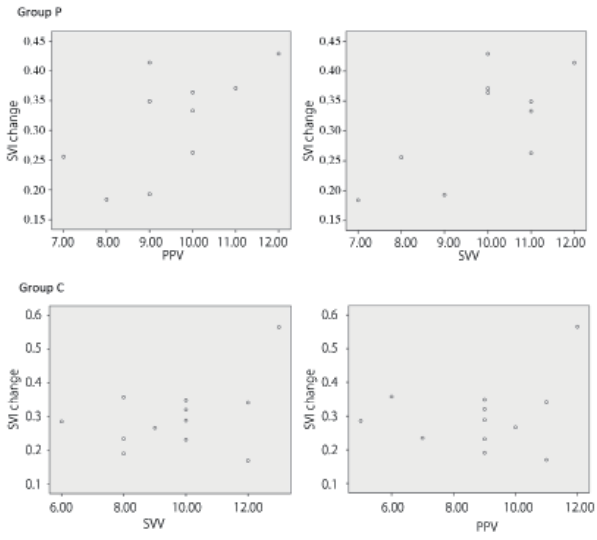

Figure 2. Correlation analysis of the relationship between pre-fluid loading SVV/PPV and ΔSVI in Group P and Group C patients.

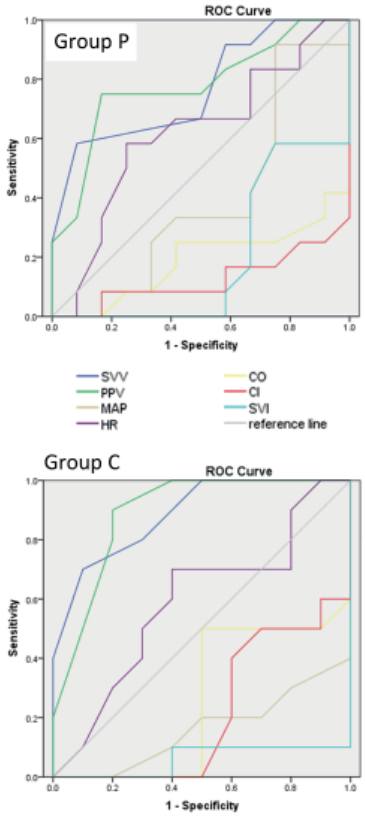

Figure 3. ROC analysis of hemodynamic variables of Responders

4. Discussion

Measurement of SVV by the FloTrac-Vigileo system is derived from variations in venous return blood volume, which is caused by changes in intrathoracic pressure through positive pressure ventilation. Thus, the accuracy of the SVV value depends on the integrity of the pleural cavity, which will be damaged during thoracic surgery and limit the use of SVV monitoring in this kind of procedure. Previous studies have evaluated the predictive value of SVV and other related parameters in open-chest or thoracoscopic surgery and obtained inconsistent results. One study showed that SVV and other dynamic parameters do not necessarily have more predictive potential than static parameters such as central venous pressure (CVP) during OLV (*14*). However, another study supported the monitoring of these dynamic parameters during thoracoscopic surgery (*15*). Alternatively, another report demonstrated the limited value of these parameters during open-chest surgery (*16*) and other volume monitoring strategies were recommended (*17,18*).

Some studies have suggested that the tidal volume was at least 8 mL/kg during ventilation while using these dynamic parameters as predictors of fluid responsiveness (*19,20*). However, in an effort to reduce the risk of lung injury, OLV with low tidal volume and proper PEEP protective mode is gradually becoming the mainstream strategy (*1-3,21*). Some studies have explored the predictive value of hemodynamic parameters in protective ventilation mode. For instance, Lee *et al*. compared protective ventilation (tidal volume: 6 mL/kg, FiO_2: 50%, PEEP: 5 cmH_2O) with conventional ventilation (tidal volume: 10 mL/kg, FiO_2:100%, no PEEP) in patients undergoing thoracotomy. PPV obtained by transesophageal echocardiography was employed as the predictor of fluid responsiveness. The results showed that PPV could predict fluid responsiveness but only in protective ventilation mode (*22*). Despite the conflicting results of this study with those of previous studies, the issue of whether or not the PPV calculated directly from echographic imaging findings is more accurate and reliable requires further study.

The FloTrac-Vigileo system obtains the pressure wave signal from any standard peripheral arterial line and automatically adjusts actual vascular compliance based on patient demographic characteristics (age, gender, height and body weight) to obtain the relevant stroke volume. During OLV intervention, the pleura on the operated side is damaged whereas the pleura on the non-operated side remains intact. Mechanical ventilation-induced cyclic changes in intrathoracic pressure can still, to some extent, transmit to pulmonary vessels and the right atrium, thereby affecting cardiac output (*23*), which is a possible reason for the positive results observed in some studies. Ventilation with a lower tidal volume leads to insufficient cyclic pressure, which definitely influences the accuracy of dynamic parameters. One study has demonstrated that sternotomy, OLV and lateral patient positioning alone can affect the values of dynamic parameters (*24*), which is the reason for the requirement of a minimum tidal volume of > 8 mL/kg. However, when implementing protective ventilation strategy, increased intrathoracic pressure through persistent PEEP support might, to a certain extent, compensate for the insufficiency of low tidal volume, which explains the result of this study demonstrating that SVV and PPV still predicted fluid responsiveness in patients of Group P, but with poorer sensitivity and specificity than those of Group C.

OLV-induced hypoxic pulmonary vasoconstriction and intrapulmonary shunt can partially affect changes in airway pressure (*25*), which is the reason for employing P_{MAX} in this study. However, no significant differences were observed in P_{MAX} between patients in Group P and Group C, which is likely a consequence of the specific surgical procedure of combined laparoscopy and thoracoscopy, the specific model of the double-lumen endotracheal tube and male-dominated subjects. More studies are needed to resolve this issue.

There are several limitations of this study. First, the sample size may be insufficient. This is especially important in correlation studies, where sample size might influence the correlation coefficient. Second, esophageal surgery requires more enhanced visualization of the surgical field than pulmonary surgery. Intraoperative

traction used in other operations might cause a variation in the values of detected parameters, thereby affecting the accuracy of the results. Third, the settings of protective ventilation may lack of individualization, which can be resolved by using a dynamic pressure-volume curve to determine the appropriate tidal volume and PEEP value, thus achieving individualized protective OLV (26,27).

In summary, hemodynamic parameters including SVV and PPV can predict fluid responsiveness in patients on protective OLV during radical esophagectomy using a combined laparoscopic and thoracoscopic approach. However, the predictive values of these parameters were not superior to those values detected in conventional OLV mode in terms of sensitivity, specificity and correlation with cardiac output. Their application in clinical practice is still controversial and further studies are required.

Acknowledgements

Dr. Qiang Fu was supported by a Japan-China Sasagawa medical research fellowship. Thanks to Dr. Junko Kouhei and Prof. Makoto Ozaki (Tokyo Women's Medical University) for their kind guidance and help.

References

1. Serpa Neto A, Cardoso SO, Manetta JA, Pereira VG, Espósito DC, Pasqualucci MdeO, Damasceno MC, Schultz MJ. Association between use of lung-protective ventilation with lower tidal volumes and clinical outcomes among patients without acute respiratory distress syndrome: A meta-analysis. JAMA. 2012; 308:1651-1659.
2. Severgnini P, Selmo G, Lanza C, Chiesa A, Frigerio A, Bacuzzi A, Dionigi G, Novario R, Gregoretti C, de Abreu MG, Schultz MJ, Jaber S, Futier E, Chiaranda M, Pelosi P. Protective mechanical ventilation during general anesthesia for open abdominal surgery improves postoperative pulmonary function. Anesthesiology. 2013; 118:1307-1321.
3. Wolthuis EK, Choi G, Dessing MC, Bresser P, Lutter R, Dzoljic M, van der Poll T, Vroom MB, Hollmann M, Schultz MJ. Mechanical ventilation with lower tidal volumes and positive end-expiratory pressure prevents pulmonary inflammation in patients without preexisting lung injury. Anesthesiology. 2008; 108:46-54.
4. Schwann NM, Hillel Z, Hoeft A, Barash P, Möhnle P, Miao Y, Mangano DT. Lack of effectiveness of the pulmonary artery catheter in cardiac surgery. Anesth Analg. 2011; 113:994-1002.
5. Davies SJ, Minhas S, Wilson RJ, Yates D, Howell SJ. Comparison of stroke volume and fluid responsiveness measurements in commonly used technologies for goal-directed therapy. J Clin Anesth. 2013; 25:466-474.
6. Zhang Z, Lu B, Sheng X, Jin N. Accuracy of stroke volume variation in predicting fluid responsiveness: A systematic review and meta-analysis. J Anesth. 2011; 25:904-916.
7. Kim KM, Gwak MS, Choi SJ, Kim MH, Park MH, Heo BY. Pulse pressure variation and stroke volume variation to predict fluid responsiveness in patients undergoing carotid endarterectomy. Korean J Anesthesiol. 2013; 65:237-243.
8. Cannesson M, Musard H, Desebbe O, Boucau C, Simon R, Hénaine R, Lehot JJ. The ability of stroke volume variations obtained with Vigileo/FloTrac system to monitor fluid responsiveness in mechanically ventilated patients. Anesth Analg. 2009; 108:513-517.
9. Marik PE, Cavallazzi R, Vasu T, Hirani A. Dynamic changes in arterial waveform derived variables and fluid responsiveness in mechanically ventilated patients: A systematic review of the literature. Crit Care Med. 2009; 37:2642-2647.
10. Kang WS, Kim SH, Kim SY, Oh CS, Lee SA, Kim JS. The influence of positive end-expiratory pressure on stroke volume variation in patients undergoing cardiac surgery: An observational study. J Thorac Cardiovasc Surg. 2014; 148:3139-3145.
11. Reuter DA, Bayerlein J, Goepfert MS, Weis FC, Kilger E, Lamm P, Goetz AE. Influence of tidal volume on left ventricular stroke volume variation measured by pulse contour analysis in mechanically ventilated patients. Intensive Care Med. 2003; 29:476-480.
12. Oliveira RH, Azevedo LC, Park M, Schettino GP. Influence of ventilatory settings on static and functional haemodynamic parameters during experimental hypovolaemia. Eur J Anaesthesiol. 2009; 26:66-72.
13. Muller L, Louart G, Bousquet PJ, Candela D, Zoric L, de La Coussaye JE, Jaber S, Lefrant JY. The influence of the airway driving pressure on pulsed pressure variation as a predictor of fluid responsiveness. Intensive Care Med. 2010; 36:496-503.
14. Trepte CJ, Haas SA, Nitzschke R, Salzwedel C, Goetz AE, Reuter DA. Prediction of volume-responsiveness during one-lung ventilation: A comparison of static, volumetric, and dynamic parameters of cardiac preload. J Cardiothorac Vasc Anesth. 2013; 27:1094-1100.
15. Suehiro K, Okutani R. Stroke volume variation as a predictor of fluid responsiveness in patients undergoing one-lung ventilation. J Cardiothorac Vasc Anesth. 2010; 24:772-775.
16. de Waal EE, Rex S, Kruitwagen CL, Kalkman CJ, Buhre WF. Dynamic preload indicators fail to predict fluid responsiveness in open-chest conditions. Crit Care Med. 2009; 37:510-515.
17. Sander M, Spies CD, Berger K, Grubitzsch H, Foer A, Krämer M, Carl M, vonHeymann C. Prediction of volume response under open-chest conditions during coronary artery bypass surgery. Crit Care. 2007; 11:R121.
18. Rex S, Brose S, Metzelder S, Hüneke R, Schälte G, Autschbach R, Rossaint R, Buhre W. Prediction of fluid responsiveness in patients during cardiac surgery. Br J Anaesth. 2004; 93:782-788.
19. Suehiro K, Okutani R.Influence of tidal volume for stroke volume variation to predict fluid responsiveness in patients undergoing one-lung ventilation. J Anesth. 2011; 25:777-780.
20. De Backer D, Heenen S, Piagnerelli M, Koch M, Vincent JL. Pulse pressure variations to predict fluid responsiveness: Influence of tidal volume. Intensive Care Med. 2005; 31:517-523.
21. Ishikawa S, Lohser J. One-lung ventilation and arterial oxygenation. Curr Opin Anaesthesiol. 2011; 24:24-31.
22. Lee JH, Jeon Y, Bahk JH, Gil NS, Hong DM, Kim JH,

Kim HJ. Pulse pressure variation as a predictor of fluid responsiveness during one-lung ventilation for lung surgery using thoracotomy: Randomised controlled study. Eur J Anaesthesiol. 2011; 28:39-44.
23. Pinsky MR. Heart lung interactions during mechanical ventilation. Curr Opin Crit Care. 2012; 18:256-260.
24. De Blasi RA, Palmisani S, Cigognetti L, Iasenzaniro M, Arcioni R, Mercieri M, Pinto G. Effects of sternotomy on heart-lung interaction in patients undergoing cardiac surgery receiving pressure-controlled mechanical ventilation. Acta Anaesthesiol Scand. 2007; 51:441-446.
25. Slinger PD, Campos JH. Anesthesia for thoracic surgery. In: Miller's Anesthesia 7th ed., Elsevier Churchill Livingstone, Philadelphia, USA, 2009; pp. 1819-1887.
26. Harris RS. Pressure-volume curves of the respiratory system. Respir Care. 2005; 50:78-98; discussion 98-99.
27. Jeon K, Jeon IS, Suh GY, Chung MP, Koh WJ, Kim H, Kwon OJ, Han DH, Chung MJ, Lee KS. Two methods of setting positive end-expiratory pressure in acute lung injury: An experimental computed tomography volumetric study. J Korean Med Sci. 2007; 22:476-483.

(Received July 15, 2015; Revised August 16, 2015; Accepted August 25, 2015)

Original Article

DOI: 10.5582/ddt.2015.01053

Fabrication of porous ethyl cellulose microspheres based on the acetone-glycerin-water ternary system: Controlling porosity *via* the solvent-removal mode

Masahiro Murakami*, Akihiro Matsumoto, Chie Watanabe, Yu Kurumado, Masashi Takama

Laboratory of Pharmaceutics, Faculty of Pharmacy, Osaka Ohtani University, Osaka, Japan.

Summary **Porous ethyl cellulose (EC) microspheres were prepared from the acetone-glycerin-water ternary system using an oil/water (O/W)-type emulsion solvent extraction method. The O/W type emulsion was prepared using acetone dissolved ethyl cellulose as an oil phase and aqueous glycerin as a water phase. The effects of the different solvent extraction modes on the porosity of the microspheres were investigated. The specific surface area of the porous EC microspheres was estimated by the gas adsorption method. When the solvent was extracted rapidly by mixing the emulsion with water instantaneously, porous EC microspheres with a maximum specific surface area of 40.7 ± 2.1 m^2/g were obtained. On the other hand, when water was added gradually to the emulsion, the specific surface area of the fabricated microspheres decreased rapidly with an increase in the infusion period, with the area being 25-45% of the maximum value. The results of an analysis of the ternary phase diagram of the system suggested that the penetration of water and glycerin from the continuous phase to the dispersed phase before solidification affected the porosity of the fabricated EC microspheres.**

Keywords: Porous microspheres, ethyl cellulose, acetone-glycerin-water ternary system, phase separation, solvent extraction

1. Introduction

Polymeric microspheres have been investigated widely for use as drug delivery systems. For instance, they can be used for the oral (*1-5*) and pulmonary delivery of drugs (*6*) and as injectable carriers for long-term drug release (*7*). Among the various types of polymeric microspheres being studied, porous microspheres are attracting the greatest attention with respect to pulmonary drug delivery. Owing to their high porosity, porous microspheres exhibit aerodynamic diameters smaller than their geometric ones. The relationship between their aerodynamic and geometric diameters can be expressed as follows:

$$D_{aero} = D_{geo} (P/P_{ref} \cdot R)^{1/2}$$

where D_{aero} is the aerodynamic diameter, D_{geo} is the geometric diameter, R is the shape factor (R is 1 for truly spherical particles), P is the particle density, and P_{ref} is the reference (water) density. The aerodynamic diameter of inhaled particles is one of the primary factors determining the distribution of the particles in the lung. Hence, microspheres with controlled porosity can be delivered readily to the target area in the lung, because the aerodynamic diameter of microspheres can be controlled by varying their porosity.

Researchers have proposed a number of methods for fabricating porous polymeric microspheres. Chai and coworkers have reviewed that most preparation methods are one of the following types: the solvent evaporation method, the polymerization method, the seed-swelling method, the synthesis method, the sintering method, the phase-separation method, and the spray-drying method (*8*). Of these, the solvent evaporation method based on the use of multiple emulsions and, in particular, water-in-oil-in-water (W/O/W) emulsions, is used commonly for fabricating porous microspheres. During the W/O/W-type emulsion solvent evaporation method, pores are formed when water migrates from the internal water phase to the external water phase of

**Address correspondence to:*
Dr. Masahiro Murakami, Osaka Ohtani University, 3-11-1 Nishikori-kita, Tondabayashi, Osaka 584-0854, Japan.
E-mail: murakam@osaka-ohtani.ac.jp

the emulsion. Porogens, which are pore-forming agents, are often added to the dispersed phase for controlling the porosity. Previous studied have used ammonium bicarbonate, sodium chloride, gelatin, paraffin, canola oil, and glycerol monooleate as porogens (*9-11*).

We had previously proposed a new method for fabricating polymeric microspheres without using halogenated solvents (*12*). The method was based on the phase separation of acetone and glycerin; the dispersed and continuous phases used were poly(lactide-co-glycolide) in acetone and aqueous glycerin, respectively. We had demonstrated that the encapsulation efficiency and drug release profile of vitamin-B_{12}-loaded microspheres fabricated using this method were similar to those of microspheres produced by the conventional method using methylene chloride. We had also found that the water content of the continuous phase affected the formation of the microspheres. Although the biphasic area in the low-water-content section of the triangular diagram of the acetone-glycerin-water ternary system was small, we had found that microspheres formed in and near the biphasic area. In contrast, microspheres did not form in the high-water-content area (*i.e*., the monophasic area). However, even though we had demonstrated the phenomenon of emulsification in the ternary system, the process of removal of the solvents from the resultant emulsion was not fully examined.

During the solvent-extraction process, the migration of the porogens can directly lead to the formation of pores. Further, the water and glycerin in the continuous phase can probably act as porogens for porous ethyl cellulose (EC) microspheres, because these materials are poor solvents of EC. Therefore, the flux of water and glycerin between the dispersed and continuous phases probably plays a key role in determining the porosity of the fabricated EC microspheres. Based on this hypothesis, we propose that the porosity of EC microspheres fabricated using the acetone-glycerin-water ternary system can be controlled by varying the mode by which the emulsion and water flow into each other during the solvent-extraction process. Thus, in the present study, we investigated the effects of the solvent-extraction process on the formation of pores on the surfaces of the EC microspheres fabricated from the acetone-glycerin-water ternary system.

2. Materials and Methods

2.1. *Materials*

The EC sample (7 cps) used in this study was donated by Nisshin kasei Co., Ltd (Osaka, Japan). All the other chemicals used were of reagent grade.

2.2. *Fabrication of EC microspheres*

i) *Fabrication without using halogenated solvents* The method for fabricating EC microspheres without using halogenated solvents is illustrated in Figure 1. First EC (2.0 g) was dissolved in acetone (16 g) to obtain the dispersed phase. The dispersed phase was emulsified in a 5% aqueous solution of polyvinyl alcohol (PVA, Kuraray Co., Ltd., Osaka, Japan) (7.5 g)-glycerin (17.5 g) by mixing using a propeller mixer (HEIDON Three-one moter BL1200, Shinto Scientific Co., Ltd., Tokyo, Japan) for 1 min at 300 rpm at room temperature. The resultant emulsion was mixed with 500 mL of water in two modes: (a) the resultant emulsion was mixed in 500 mL of water instantaneously (mode 1 in Figure 1) or (b) 500 mL of water was added slowly to the resultant emulsion and mixed at 400 rpm for a certain period (mode 2). The resulting EC microspheres, which were hard, were washed with deionized water. Next, the aggregated EC microspheres were removed by filtration using 75-μm and 53-μm sieves, and the nonaggregated ones were collected by filtration with a 20-μm sieve. The EC microspheres were the redispersed in deionized water and lyophilized.

ii) *Fabrication by the conventional O/W-type emulsion solvent evaporation method using a halogenated solvent* First, EC (1.0 g) was dissolved in dichloromethane (14 mL) to obtain an oil phase. The oil phase was emulsified in a 0.5% PVA solution (20 mL) using a homogenizer (Polytron®PT3100, Kinematica Ag, Luzern, Switzerland) for 5 min at 4,000 rpm at room temperature. The resultant emulsion was added to 400 mL of water all at once and stirred at 400 rpm at room temperature for 3 h, in order to remove the dichloromethane. The obtained hardened EC microspheres were washed with deionized water. Finally, the aggregated EC microspheres were removed by filtration using 75-μm and 53-μm sieves, and the nonaggregated ones were collected by filtration with a 20-μm sieve. The EC microspheres were then redispersed in

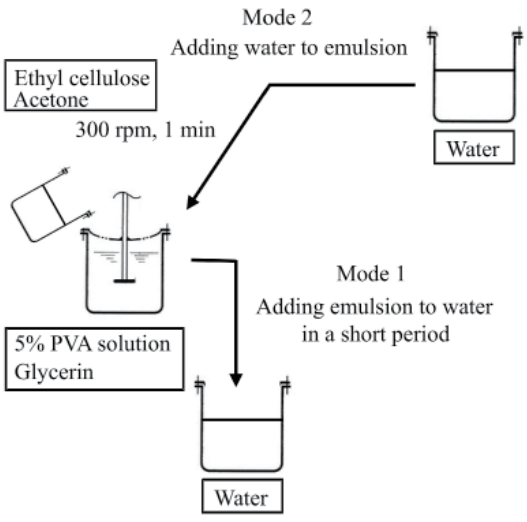

Figure 1. Illustration of the proposed method for preparing EC microspheres. In mode 1, the emulsion is added to water instantaneously. In mode 2, water is added to the emulsion for 1 min, 3 min, 5 min, 10 min, or 20 min.

deionized water and lyophilized.

iii) *Fabrication by the conventional W/O/W-type emulsion solvent evaporation method using a halogenated solvent*
First, EC (1.0 g) was dissolved in dichloromethane (14 mL) to obtain an oil phase. Then, a 0.5% PVA solution (1 mL) was emulsified into the oil phase using a homogenizer (T18 Digital ULTRA-TURRAX®, IKA Works GmbH & Co. KG, Staufen im Breisgau, Germany) for 30 s at 25,000 rpm at room temperature. The obtained W/O emulsion was mixed in a 0.5% PVA solution (20 mL) using the homogenizer for 5 min at 4,000 rpm at room temperature. The resultant emulsion was added to 400 mL of water all at once and stirred at 400 rpm at room temperature for 3 h, in order to remove the dichloromethane. The hardened EC microspheres were washed. Next, the aggregated EC microspheres were removed by filtration using 75-µm and 53-µm sieves and the nonaggregated ones were collected by filtration with a 20-µm sieve. Finally, the EC microspheres were redispersed in deionized water and lyophilized.

2.3. *Microscopy observations*

The fabricated EC microspheres were observed using a scanning electron microscopy (SEM) system (JSM-5500LV, JOEL Ltd., Tokyo, Japan). For the SEM observations, samples of the EC microspheres were prepared by depositing gold-palladium at 15 mA for 3 min (Quick Auto Coater JFC-1500, JOEL Ltd.).

2.4. *Determination of sizes of EC microspheres*

The sizes of the fabricated EC microspheres were determined using a laser diffraction particle size analyzer (SALD-2200, Shimadzu Co. Ltd., Kyoto, Japan).

2.5. *Determination of specific surface areas of EC microspheres*

The specific surface areas of the fabricated EC microspheres were determined by the gas adsorption method (FlowSorb 2310, Shimadzu Co., Ltd.).

2.6. *Analysis of triangular diagram*

The triangular diagram for the acetone-glycerin-water ternary system was taken from the literature. We determined the ratio of the upper phase (*i.e.*, the acetone-rich phase) to the lower phase (*i.e.*, the glycerin-rich phase) (w/w) and the composition of the upper phase in the phase-separated solution of the acetone-glycerin-water ternary system. The glycerin content was considered to be the residual constant weight after drying in vacuum. The water content was determined by the Karl Fisher method; a volume titrator (AQV-300, Hiranuma Sangyo, Co., Ltd., Ibaragi, Japan) was employed for the purpose.

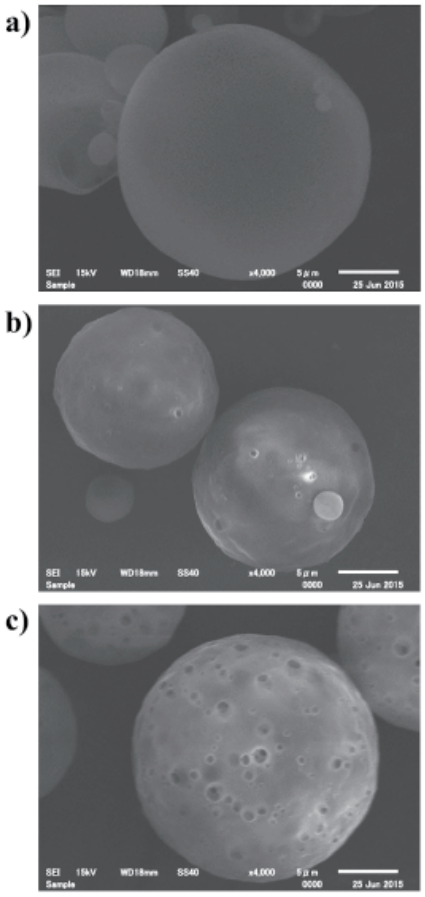

Figure 2. Scanning electron micrographs of the fabricated EC microspheres. The EC microspheres shown were prepared by **(a)** the proposed method (mode 1), **(b)** the conventional O/W-type emulsion solvent evaporation method, and **(c)** the conventional W/O/W-type emulsion solvent evaporation method. The bars represent 5 µm.

3. Results

3.1. *Morphological properties and particle sizes of fabricated EC microspheres*

Micrographs of the fabricated EC microspheres are shown in Figure 2. No micron-sized pores were observed on the surfaces of the EC microspheres fabricated using the new method. On the other hand, a large number of micron- and submicron-sized pores were observed on the surfaces of the EC microspheres fabricated by the conventional W/O/W-type emulsion solvent evaporation method. It should be noted that the EC microspheres fabricated using the conventional O/W-type emulsion solvent evaporation method also had micron- and submicron-sized pores on their surfaces; however, these were fewer in number.

The size distributions of the EC microspheres obtained using the three different methods are shown in Figure 3. The EC microspheres fabricated by the new

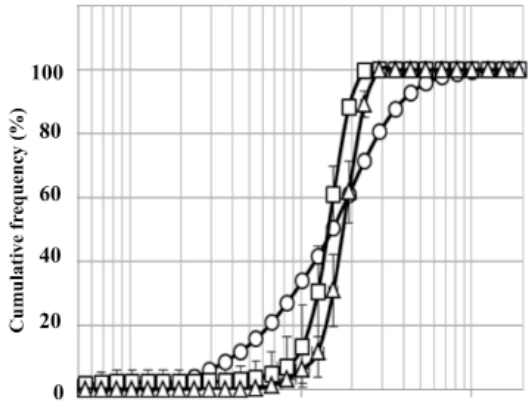

Figure 3. Weight and size distributions of the fabricated EC microspheres. ○: proposed method (mode 1), □: conventional O/W-type emulsion solvent evaporation method, Δ: conventional W/O/W-type emulsion solvent evaporation method. The data shown represent the mean ± standard deviation (SD) (n = 3 batches).

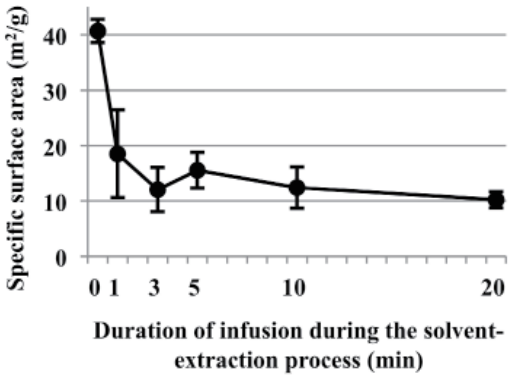

Figure 4. Effects of the infusion period during the solvent-extraction process on the specific surface area of the microspheres. The point at time 0 indicates the specific surface area of the EC microspheres prepared in mode 1. The points at other times indicate the specific surface areas of the EC microspheres prepared in mode 2. The data shown represent the mean ± SD (n = 3 batches).

Table 1. The specific surface area of microspheres prepared by the new and conventional methods

Method	Specific surface area (m^2/g)
New method	
mode 1	40.7 ± 2.10
Conventional method	
O/W-type solvent evaporation	3.12 ± 0.19
W/O/W-type solvent evaporation	5.73 ± 0.63

The data represent the means ± SD (n = 3 batches).

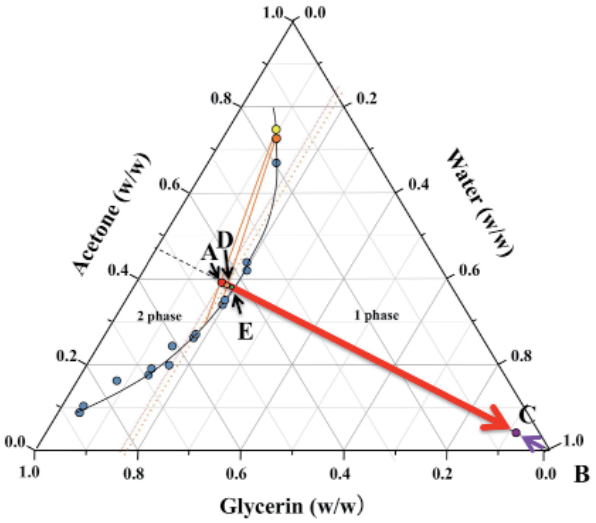

Figure 5. Triangular diagram of the acetone-glycerin-water ternary system. The data corresponding to the border line between phases 1 and 2 were taken from the literature (*12*). The concentrations of acetone, glycerin, and water for the various points were as follows: point A (acetone/glycerin/water = 0.399:0.424:0.178), point D (acetone/glycerin/ water = 0.388:0.424:0.188), and point E (acetone/glycerin/water = 0.386:0.422:0.193).

method had a broader particle-size distribution than did those produced using the two conventional method. The mean particle sizes of the EC microspheres fabricated by the new method, the conventional O/W-type emulsion solvent evaporation method, and the conventional W/O/W-type emulsion solvent evaporation method were 13.7 ± 0.5, 13.3 ± 2.6, and 17.2 ± 1.5 μm, respectively (mean ± standard deviation for 3 batches). In the case of the EC microspheres fabricated by the new method, there were no significant changes in the mean particle size or the size distribution with changes in the solvent-infusion mode and the duration of infusion during the solvent-extraction process.

3.2. *Specific surface areas of fabricated EC microspheres*

As shown in Table 1, the specific surface areas of the EC microspheres fabricated using the three methods could be arranged in the following order: the new method (mode 1) > the conventional W/O/W-type emulsion solvent evaporation method > the conventional O/W-type emulsion solvent evaporation method. In the case of the new method, the mode of solvent extraction had an effect on the specific surface area of the obtained EC microspheres (Figure 4.). Mode 1 resulted in the highest specific surface area, which was 40.7 m^2/g. In contrast, mode 2 resulted in specific surface areas of 10.2-18.5 m^2/g; further, in this case, the specific surface area decreased with an increase in the infusion period.

3.3. *Analysis of triangular diagram*

The triangular diagram of the acetone-glycerin-water ternary system is shown in Figure 5. Point A represents the status of the emulsion formed after the completion of the emulsification stage in the new method. Point C represents the status of emulsion at the end of the solvent-extraction process. The purple and red arrows represent the transitions during the solvent-

Table 2. Phase ratio and composition of the acetone-rich phase at each point in Figure 5

Items	Ratio of acetone-rich phase	Composition of acetone-rich phase (w/w %)		
		Water content	Glycerin content	Acetone content
Point A	0.110	10.5	14.8	74.7
Point D	0.033	11.5	15.7	72.8
Point E			miscible	

Composition: point A (acetone/glycerin/water = 0.399:0.424:0.178), point D (acetone/glycerin/water = 0.388:0.424:0.188), point E (acetone/glycerin/water = 0.386:0.422:0.193).

extraction process. For the case where the solvent was extracted rapidly by mixing the emulsion with water instantaneously, the status of emulsion is represented as the jump from point A to B and the transition from point B to C on the purple arrow (mode 1). The purple arrow is in the monophasic area. For the case where water was added gradually to the emulsion, the status is represented as the transition from point A to C through points D and E on the red arrow (mode 2). The amount ratios (w/w) and compositions of the acetone-rich phase for points A, D, and E of the triangular diagram are listed in Table 2. The amount ratio of the acetone-rich phase at point D in the ternary system was 30% of that at point A, even though only a small amount of water was added. On the other hand, the water and glycerin contents of the acetone-rich phase for the two points were similar. At point E, the ternary system transitioned into the monophasic area.

4. Discussion

In a previous report, we had introduced a new method for fabricating sustained-release microspheres using nonhalogenated solvents. This method was based on the phase separation of acetone and aqueous glycerin (*12*). In this study, we evaluated the feasibility of using this method for fabricating porous EC microspheres. For the purposes of evaluation, we selected the morphological properties and the specific surface area of the fabricated EC microspheres, which is an indicator of their porosity, as the evaluation parameters. Elucidating the morphological properties of porous microspheres is essential for determining their applicability in various fields. Similarly, being able to control the porosity of the microspheres is crucial for adjusting their target profile, that is, for adjusting their release profile with respect to oral and pulmonary drug delivery.

First, we determined the morphological properties and specific surface areas of the fabricated EC microspheres and compared them with those of the microspheres fabricated by the two conventional methods. SEM observations revealed that the surface morphologies of the EC microspheres fabricated by the new method and those of the microspheres produced by the conventional O/W-type emulsion solvent evaporation method were similar. The fabricated EC microspheres had smooth surfaces; this was in keeping with previously obtained results (*12*). On the other hand, the specific surface areas of the EC microspheres prepared by the new and conventional methods were different. The EC microspheres fabricated by the new method (mode 1) had a specific surface area that was approximately 13.0 times than of the microspheres produced by the conventional O/W-type emulsion solvent evaporation method. Further, the specific surface area of the microspheres produced by the new method was 7.1 times than of the microspheres produced by the conventional W/O/W-type emulsion solvent evaporation method; in the latter case, the microspheres had pores on their surfaces. These differences cannot be explained merely by the differences in the particle-size distribution of the EC microspheres, because the microspheres prepared by the new and conventional methods had similar mean sizes.

The formation of pores on the EC microspheres prepared by the conventional methods can be explained as follows. It is known that water exhibits low solubility in dichloromethane, which is used commonly as a solvent for the oil phase in the conventional preparation methods. This means that water cannot penetrate into the oil phase from the external water phase in the case of the conventional methods. Therefore, pore formation is suppressed in the case of the conventional O/W-type emulsion solvent evaporation method. Moreover, in the case of the conventional O/W-type emulsion solvent evaporation method, the amount of porogens in the oil phase was low. Hence, the resulting microspheres had a lower specific surface area. On the other hand, in the case of the conventional W/O/W-type emulsion solvent evaporation method, the inner water phase played the role of a porogen, resulting in the fabrication of porous EC microspheres. Hence, the conventional W/O/W-type emulsion solvent evaporation method resulted in microspheres with a specific surface area twice that of the microspheres produced using the conventional O/W-type emulsion solvent evaporation method.

In the case of the new method, the solvents for the dispersed and external phases were acetone and aqueous glycerin, respectively. The mutual solubility of acetone and aqueous glycerin depends on the concentrations in which these three components, namely, acetone, glycerin, and water, are present in the system. Because aqueous glycerin is a poor solvent of

ethyl cellulose, it can act as a porogen for the synthesis of porous EC microspheres. In the condition of high mutual solubility of acetone and aqueous glycerin, such solvents penetrated in the dispersed phase from the continuous phase result in the formation of pores in EC microspheres when removed during the solvent-extraction process. Hence, the resultant microspheres had a high specific surface area.

Next, we investigated whether it was possible to control the specific surface area on the basis of the flux of glycerin and water into the dispersed phase. It was found that the mode of infusion during the solvent-extraction process determined the specific surface area of the fabricated porous EC microspheres. This phenomenon can be explained on the basis of the triangular diagram of the acetone-glycerin-water ternary system (Figure 5). In the emulsification stage, the ternary system is at point A. When the solvent is extracted rapidly by adding the emulsion to water instantaneously (mode 1), the ternary system jumps from point A to point B and then from point B to point C. From point B to point C, the ternary system is in the monophasic area. Thus, acetone, water, and glycerin are assumed to dissolve mutually in the dispersed phase, before the solidification of the EC microspheres. Therefore, EC microspheres with a high specific surface area could be formed using the new method.

On the other hand, the specific surface area of the obtained EC microspheres decreased when water was added gradually to the emulsion (mode 2). This phenomenon can be explained on the basis of the change in the amount of porogens in the dispersed phase as follows. During the emulsification process, the concentrations of water and glycerin in the dispersed phase reached 10.5% and 14.8% (point A), respectively. Further, the concentrations of water and glycerin in the acetone-rich phase remained almost constant as water was added (A→D transition). The same phenomenon probably also occurred during the D→E transition. However, the volume of the acetone-rich phase decreased markedly (A→D→E transition). This indicated that the solvents in the dispersed phase were extracted into the continuous phase without there being an increase in the amounts of the porogens (water and glycerin) before the solidification of the EC microspheres. Thereafter, the porogens were unable to penetrate into the EC microspheres even when more water was added in the monophasic region (E→C) because the EC microspheres had already solidified. Hence, the formation of additional pores was suppressed.

The above-mentioned results confirmed that the proposed method based on the acetone-glycerin-water ternary system was suitable for fabricating porous EC microspheres. Next, we discuss the potential uses of the porous EC microspheres prepared using the new method. Porous materials can be classified on the basis of their pore size, and the applicability of porous microspheres depends on their pore size. Microspheres with micrometer-sized pores are being explored for use in tissue engineering, because such microspheres can be used as scaffolds for cell growth (*10,13*). On the other hand, mesoporous (2-50 nm) microspheres are being investigated for use for controlled drug release, owing to their larger specific surface area (*1-3,5*). Since we did not measure the sizes of the pores of the fabricated EC microspheres in this study, it is not possible to comment on their use. However, it is likely that the microspheres fabricated using the new method were mesoporous, judging from their electron micrographs and their specific surface area, which was measured using the gas adsorption method. Microspheres with large specific surface areas, such as the ones fabricated using the new method, can be used for the controlled release of drugs. Further, such microspheres can be used as carriers for pulmonary drug delivery, owing to their large specific surface area. Various uses for the microspheres fabricated using the new method are being explored in our laboratory.

Acknowledgements

The authors thank Ms. Kayoko Murakami and Mr. Kohsuke Horita for their technical assistance. We would like to thank Editage (*www.editage.jp*) for English language editing.

References

1. Vaghani S, Vasan ti S, Chaturvedi K, Satish CS, Jivani NP. Stomach-specific drug delivery of 5-Fluorouracil using ethyl cellulose floating microspheres. Pharm Devel Tech. 2010; 15:154-161.
2. Tozuka Y, Sugiyama E, Takeuchi H. Release profile of insulin entrapped on mesoporous materials by freeze-thaw method. Int J Pharm. 2010; 386:172-177.
3. Zhang Y, Zhi Z, Jiang T, Zhang J, Wang Z, Wang S. Spherical mesoporous silica nanoparticles for loading and release of the poorly water-soluble drug telmisartan. J Cont Rel. 2010; 145:257-263.
4. Bhise SB, More AB, Malayandi R. Formulation and in vitro evaluation of rifampicin loaded porous microspheres. Sci Pharm. 2010; 78:291-302.
5. Kapoor S, Hegde R, Bhattacharyya AJ. Influence of surface chemistry of mesoporous alumina with wide pore distribution on controlled drug release. J Cont Rel. 2009; 140:34-39.
6. Arnold MA, Gorman EM, Schieber LJ, Munson EJ, Berland C. NanoCipro encapsulation in monodisperse large porous PLGA microparticles. J Cont Rel. 2007; 121:100-109.
7. Ogawa Y, Yamoto M, Takada S, Okada H, Shimamoto T. Controlled-release of leuprolide acetate from polylactic acid or copoly(lactic/glycolic) acid microcapsules: Influence of molecular weight and copolymer ratio of polymer. Chem Pharm Bull. 1988; 36:1502-1507.

8. Cai Y, Chen Y, Hong X, Liu Z, Yuan W. Porous microsphere and its applications. Int J Nanomed. 2013; 8:1111-1120.
9. Kim TK, Yoon JJ, Lee DS, Park TG. Gas foamed open porous biodegradable polymeric microspheres. Biomaterials. 2006; 27:152-159.
10. Draghi L, Resta S, Pirozzolo MG, Tanzi MC. Microspheres leaching for scaffold porosity control. J Mater Sci Mater Med. 2005; 16:1093-1097.
11. Ahmed AR, Bodmeier R. Preparation of preformed porous PLGA microparticles and antisense oligonucleotides loading. Eur J Pharm Biopharm. 2009; 71:264-270.
12. Matsumoto A, Kitazawa T, Murata J, Horikiri Y, Yamahara H. A novel preparation method for PLGA microspheres using non-halogenated solvents. J Cont Rel. 2008; 129:223-227.
13. Keskar V, Marion NW, Mao JJ, Gemeinhart RA. In vitro evaluation of microporous hydrogels to facilitate stem cell infiltration, growth and mineralization. Tissue Eng. 2009; 15:1695-1707.

(Received August 10, 2015; Revised August 25, 2015; Accepted August 26, 2015)

DD&T
Drug Discoveries & Therapeutics

Guide for Authors

1. Scope of Articles

Drug Discoveries & Therapeutics welcomes contributions in all fields of pharmaceutical and therapeutic research such as medicinal chemistry, pharmacology, pharmaceutical analysis, pharmaceutics, pharmaceutical administration, and experimental and clinical studies of effects, mechanisms, or uses of various treatments. Studies in drug-related fields such as biology, biochemistry, physiology, microbiology, and immunology are also within the scope of this journal.

2. Submission Types

Original Articles should be well-documented, novel, and significant to the field as a whole. An Original Article should be arranged into the following sections: Title page, Abstract, Introduction, Materials and Methods, Results, Discussion, Acknowledgments, and References. Original articles should not exceed 5,000 words in length (excluding references) and should be limited to a maximum of 50 references. Articles may contain a maximum of 10 figures and/or tables.

Brief Reports definitively documenting either experimental results or informative clinical observations will be considered for publication in this category. Brief Reports are not intended for publication of incomplete or preliminary findings. Brief Reports should not exceed 3,000 words in length (excluding references) and should be limited to a maximum of 4 figures and/or tables and 30 references. A Brief Report contains the same sections as an Original Article, but the Results and Discussion sections should be combined.

Reviews should present a full and up-to-date account of recent developments within an area of research. Normally, reviews should not exceed 8,000 words in length (excluding references) and should be limited to a maximum of 100 references. Mini reviews are also accepted.

Policy Forum articles discuss research and policy issues in areas related to life science such as public health, the medical care system, and social science and may address governmental issues at district, national, and international levels of discourse. Policy Forum articles should not exceed 2,000 words in length (excluding references).

Case Reports should be detailed reports of the symptoms, signs, diagnosis, treatment, and follow-up of an individual patient. Case reports may contain a demographic profile of the patient but usually describe an unusual or novel occurrence. Unreported or unusual side effects or adverse interactions involving medications will also be considered. Case Reports should not exceed 3,000 words in length (excluding references).

News articles should report the latest events in health sciences and medical research from around the world. News should not exceed 500 words in length.

Letters should present considered opinions in response to articles published in Drug Discoveries & Therapeutics in the last 6 months or issues of general interest. Letters should not exceed 800 words in length and may contain a maximum of 10 references.

3. Editorial Policies

Ethics: Drug Discoveries & Therapeutics requires that authors of reports of investigations in humans or animals indicate that those studies were formally approved by a relevant ethics committee or review board.

Conflict of Interest: All authors are required to disclose any actual or potential conflict of interest including financial interests or relationships with other people or organizations that might raise questions of bias in the work reported. If no conflict of interest exists for each author, please state "There is no conflict of interest to disclose".

Submission Declaration: When a manuscript is considered for submission to Drug Discoveries & Therapeutics, the authors should confirm that 1) no part of this manuscript is currently under consideration for publication elsewhere; 2) this manuscript does not contain the same information in whole or in part as manuscripts that have been published, accepted, or are under review elsewhere, except in the form of an abstract, a letter to the editor, or part of a published lecture or academic thesis; 3) authorization for publication has been obtained from the authors' employer or institution; and 4) all contributing authors have agreed to submit this manuscript.

Cover Letter: The manuscript must be accompanied by a cover letter signed by the corresponding author on behalf of all authors. The letter should indicate the basic findings of the work and their significance. The letter should also include a statement affirming that all authors concur with the submission and that the material submitted for publication has not been published previously or is not under consideration for publication elsewhere. The cover letter should be submitted in PDF format. For example of Cover Letter, please visit http://www.ddtjournal.com/downcentre.php (Download Centre).

Copyright: A signed JOURNAL PUBLISHING AGREEMENT (JPA) must be provided by post, fax, or as a scanned file before acceptance of the article. Only forms with a hand-written signature are accepted. This copyright will ensure the widest possible dissemination of information. A form facilitating transfer of copyright can be downloaded by clicking the appropriate link and can be returned to the e-mail address or fax number noted on the form (Please visit Download Centre). Please note that your manuscript will not proceed to the next step in publication until the JPA form is received. In addition, if excerpts from other copyrighted works are included, the author(s) must obtain written permission from the copyright owners and credit the source(s) in the article.

Suggested Reviewers: A list of up to 3 reviewers who are qualified to assess the scientific merit of the study is welcomed. Reviewer information including names, affiliations, addresses, and e-mail should be provided at the same time the manuscript is submitted online. Please do not suggest reviewers with known conflicts of interest, including participants or anyone with a stake in the proposed research; anyone from the same institution; former students, advisors, or research collaborators (within the last three years); or close personal contacts. Please note that the Editor-in-Chief may accept one or more of the proposed reviewers or may request a review by other qualified persons.

Language Editing: Manuscripts prepared by authors whose native language is not English should have their work proofread by a native English speaker before submission. If not, this might delay the publication of your manuscript in Drug Discoveries & Therapeutics.

The Editing Support Organization can provide English proofreading, Japanese-English translation, and Chinese-English translation services to authors who want to publish in Drug Discoveries & Therapeutics and need assistance before submitting a manuscript. Authors can visit this organization directly at http://www.iacmhr.com/iac-eso/support.php?lang=en. IAC-ESO was established to facilitate manuscript preparation by researchers whose native language is not English and to help edit works intended for international academic journals.

4. Manuscript Preparation

Manuscripts should be written in clear, grammatically correct English and submitted as a Microsoft Word file in a single-column format. Manuscripts must be paginated and typed in 12-point Times New Roman font with 24-point line spacing. Please do not embed figures in the text. Abbreviations should be used as little as possible and should be explained at first mention unless the term is a well-known abbreviation (*e.g.* DNA). Single words should not be abbreviated.

Title page: The title page must include 1) the title of the paper (Please note the title should be short, informative, and contain the major key words); 2) full name(s) and affiliation(s) of the author(s), 3) abbreviated names of the author(s), 4) full name, mailing address, telephone/fax numbers, and e-mail address of the corresponding author; and 5) conflicts of interest (if you have an actual or potential conflict of interest to disclose, it must be included as a footnote on the title page of the manuscript; if no conflict of interest exists for each author, please state "There is no conflict of interest to disclose"). Please visit Download Centre and refer to the title page of the manuscript sample.

Abstract: The abstract should briefly state the purpose of the study, methods, main findings, and conclusions. For article types including Original Article, Brief Report, Review, Policy Forum, and Case Report, a one-paragraph abstract consisting of no more than 250 words must be included in the manuscript. For News and Letters, a brief summary of main content in 150 words or fewer should be included in the manuscript. Abbreviations must be kept to a minimum and non-standard abbreviations explained in brackets at first mention. References should be avoided in the abstract. Key words or phrases that do not occur in the title should be included in the Abstract page.

Introduction: The introduction should be a concise statement of the basis for the study and its scientific context.

Materials and Methods: The description should be brief but with sufficient detail to enable others to reproduce the experiments. Procedures that have been published previously should not be described in detail but appropriate references should simply be cited. Only new and significant modifications of previously published procedures require complete description. Names of products and manufacturers with their locations (city and state/country) should be given and sources of animals and cell lines should always be indicated. All clinical investigations must have been conducted in accordance with Declaration of Helsinki principles. All human and animal studies must have been approved by the appropriate institutional review board(s) and a specific declaration of approval must be made within this section.

Results: The description of the experimental results should be succinct but in sufficient detail to allow the experiments to be analyzed and interpreted by an independent reader. If necessary, subheadings may be used for an orderly presentation. All figures and tables must be referred to in the text.

Discussion: The data should be interpreted concisely without repeating material already presented in the Results section. Speculation is permissible, but it must be well-founded, and discussion of the wider implications of the findings is encouraged. Conclusions derived from the study should be included in this section.

Acknowledgments: All funding sources should be credited in the Acknowledgments section. In addition, people who contributed to the work but who do not meet the criteria for authors should be listed along with their contributions.

References: References should be numbered in the order in which they appear in the text. Citing of unpublished results, personal communications, conference abstracts, and theses in the reference list is not recommended but these sources may be mentioned in the text. In the reference list, cite the names of all authors when there are fifteen or fewer authors; if there are sixteen or more authors, list the first three followed by *et al*. Names of journals should be abbreviated in the style used in PubMed. Authors are responsible for the accuracy of the references. Examples are given below:

Example 1 (Sample journal reference):
Nakata M, Tang W. Japan-China Joint Medical Workshop on Drug Discoveries and Therapeutics 2008: The need of Asian pharmaceutical researchers' cooperation. Drug Discov Ther. 2008; 2:262-263.

Example 2 (Sample journal reference with more than 15 authors):
Darby S, Hill D, Auvinen A, *et al*. Radon in homes and risk of lung cancer: Collaborative analysis of individual data from 13 European case-control studies. BMJ. 2005; 330:223.

Example 3 (Sample book reference):
Shalev AY. Post-traumatic stress disorder: Diagnosis, history and life course. In: Post-traumatic Stress Disorder, Diagnosis, Management and Treatment (Nutt DJ, Davidson JR, Zohar J, eds.). Martin Dunitz, London, UK, 2000; pp. 1-15.

Example 4 (Sample web page reference):
World Health Organization. The World Health Report 2008 – primary health care: Now more than ever. *http://www.who.int/whr/2008/whr08_en.pdf* (accessed September 23, 2010).

Tables: All tables should be prepared in Microsoft Word or Excel and should be arranged at the end of the manuscript after the References section. Please note that tables should not in image format. All tables should have a concise title and should be numbered consecutively with Arabic numerals. If necessary, additional information should be given below the table.

Figure Legend: The figure legend should be typed on a separate page of the main manuscript and should include a short title and explanation. The legend should be concise but comprehensive and should be understood without referring to the text. Symbols used in figures must be explained.

Figure Preparation: All figures should be clear and cited in numerical order in the text. Figures must fit a one- or two-column format on the journal page: 8.3 cm (3.3 in.) wide for a single column, 17.3 cm (6.8 in.) wide for a double column; maximum height: 24.0 cm (9.5 in.). Please make sure that artwork files are in an acceptable format (TIFF or JPEG) at minimum resolution (600 dpi for illustrations, graphs, and annotated artwork, and 300 dpi for micrographs and photographs). Please provide all figures as separate files. Please note that low-resolution images are one of the leading causes of article resubmission and schedule delays. All color figures will be reproduced in full color in the online edition of the journal at no cost to authors.

Units and Symbols: Units and symbols conforming to the International System of Units (SI) should be used for physicochemical quantities. Solidus notation (*e.g.* mg/kg, mg/mL, mol/mm^2/min) should be used. Please refer to the SI Guide www.bipm.org/en/si/ for standard units.

Supplemental data: Supplemental data might be useful for supporting and enhancing your scientific research and Drug Discoveries & Therapeutics accepts the submission of these materials which will be only published online alongside the electronic version of your article. Supplemental files (figures, tables, and other text materials) should be prepared according to the above guidelines, numbered in Arabic numerals (*e.g.*, Figure S1, Figure S2, and Table S1, Table S2) and referred to in the text. All figures and tables should have titles and legends. All figure legends, tables and supplemental text materials should be placed at the end of the paper. Please note all of these supplemental data should be provided at the time of initial submission and note that the editors reserve the right to limit the size and length of Supplemental Data.

5. Submission Checklist

The Submission Checklist will be useful during the final checking of a manuscript prior to sending it to Drug Discoveries & Therapeutics for review. Please visit Download Centre and download the Submission Checklist file.

6. Online submission

Manuscripts should be submitted to Drug Discoveries & Therapeutics online at http://www.ddtjournal.com. The manuscript file should be smaller than 5 MB in size. If for any reason you are unable to submit a file online, please contact the Editorial Office by e-mail at office@ddtjournal.com

7. Accepted manuscripts

Proofs: Galley proofs in PDF format will be sent to the corresponding author *via* e-mail. Corrections must be returned to the editor (proof-editing@ddtjournal.com) within 3 working days.

Offprints: Authors will be provided with electronic offprints of their article. Paper offprints can be ordered at prices quoted on the order form that accompanies the proofs.

Page Charge: A page charge of $140 will be assessed for each printed page of an accepted manuscript. The charge for printing color figures is $340 for each page. Under exceptional circumstances, the author(s) may apply to the editorial office for a waiver of the publication charges at the time of submission.

(Revised February 2013)

Editorial and Head Office:

Pearl City Koishikawa 603
2-4-5 Kasuga, Bunkyo-ku
Tokyo 112-0003
Japan
Tel: +81-3-5840-9697
Fax: +81-3-5840-9698
E-mail: office@ddtjournal.com

DD&T
Drug Discoveries & Therapeutics

JOURNAL PUBLISHING AGREEMENT (JPA)

Manuscript No.:

Title:

Corresponding author:

The International Advancement Center for Medicine & Health Research Co., Ltd. (IACMHR Co., Ltd.) is pleased to accept the above article for publication in Drug Discoveries & Therapeutics. The International Research and Cooperation Association for Bio & Socio-Sciences Advancement (IRCA-BSSA) reserves all rights to the published article. Your written acceptance of this JOURNAL PUBLISHING AGREEMENT is required before the article can be published. Please read this form carefully and sign it if you agree to its terms. The signed JOURNAL PUBLISHING AGREEMENT should be sent to the Drug Discoveries & Therapeutics office (Pearl City Koishikawa 603, 2-4-5 Kasuga, Bunkyo-ku, Tokyo 112-0003, Japan; E-mail: office@ddtjournal.com; Tel: +81-3-5840-9697; Fax: +81-3-5840-9698).

1. Authorship Criteria

As the corresponding author, I certify on behalf of all of the authors that:

1) The article is an original work and does not involve fraud, fabrication, or plagiarism.
2) The article has not been published previously and is not currently under consideration for publication elsewhere. If accepted by Drug Discoveries & Therapeutics, the article will not be submitted for publication to any other journal.
3) The article contains no libelous or other unlawful statements and does not contain any materials that infringes upon individual privacy or proprietary rights or any statutory copyright.
4) I have obtained written permission from copyright owners for any excerpts from copyrighted works that are included and have credited the sources in my article.
5) All authors have made significant contributions to the study including the conception and design of this work, the analysis of the data, and the writing of the manuscript.
6) All authors have reviewed this manuscript and take responsibility for its content and approve its publication.
7) I have informed all of the authors of the terms of this publishing agreement and I am signing on their behalf as their agent.

2. Copyright Transfer Agreement

I hereby assign and transfer to IACMHR Co., Ltd. all exclusive rights of copyright ownership to the above work in the journal Drug Discoveries & Therapeutics, including but not limited to the right 1) to publish, republish, derivate, distribute, transmit, sell, and otherwise use the work and other related material worldwide, in whole or in part, in all languages, in electronic, printed, or any other forms of media now known or hereafter developed and the right 2) to authorize or license third parties to do any of the above.

I understand that these exclusive rights will become the property of IACMHR Co., Ltd., from the date the article is accepted for publication in the journal Drug Discoveries & Therapeutics. I also understand that IACMHR Co., Ltd. as a copyright owner has sole authority to license and permit reproductions of the article.

I understand that except for copyright, other proprietary rights related to the Work (*e.g.* patent or other rights to any process or procedure) shall be retained by the authors. To reproduce any text, figures, tables, or illustrations from this Work in future works of their own, the authors must obtain written permission from IACMHR Co., Ltd.; such permission cannot be unreasonably withheld by IACMHR Co., Ltd.

3. Conflict of Interest Disclosure

I confirm that all funding sources supporting the work and all institutions or people who contributed to the work but who do not meet the criteria for authors are acknowledged. I also confirm that all commercial affiliations, stock ownership, equity interests, or patent-licensing arrangements that could be considered to pose a financial conflict of interest in connection with the article have been disclosed.

Corresponding Author's Name (Signature):

Date: